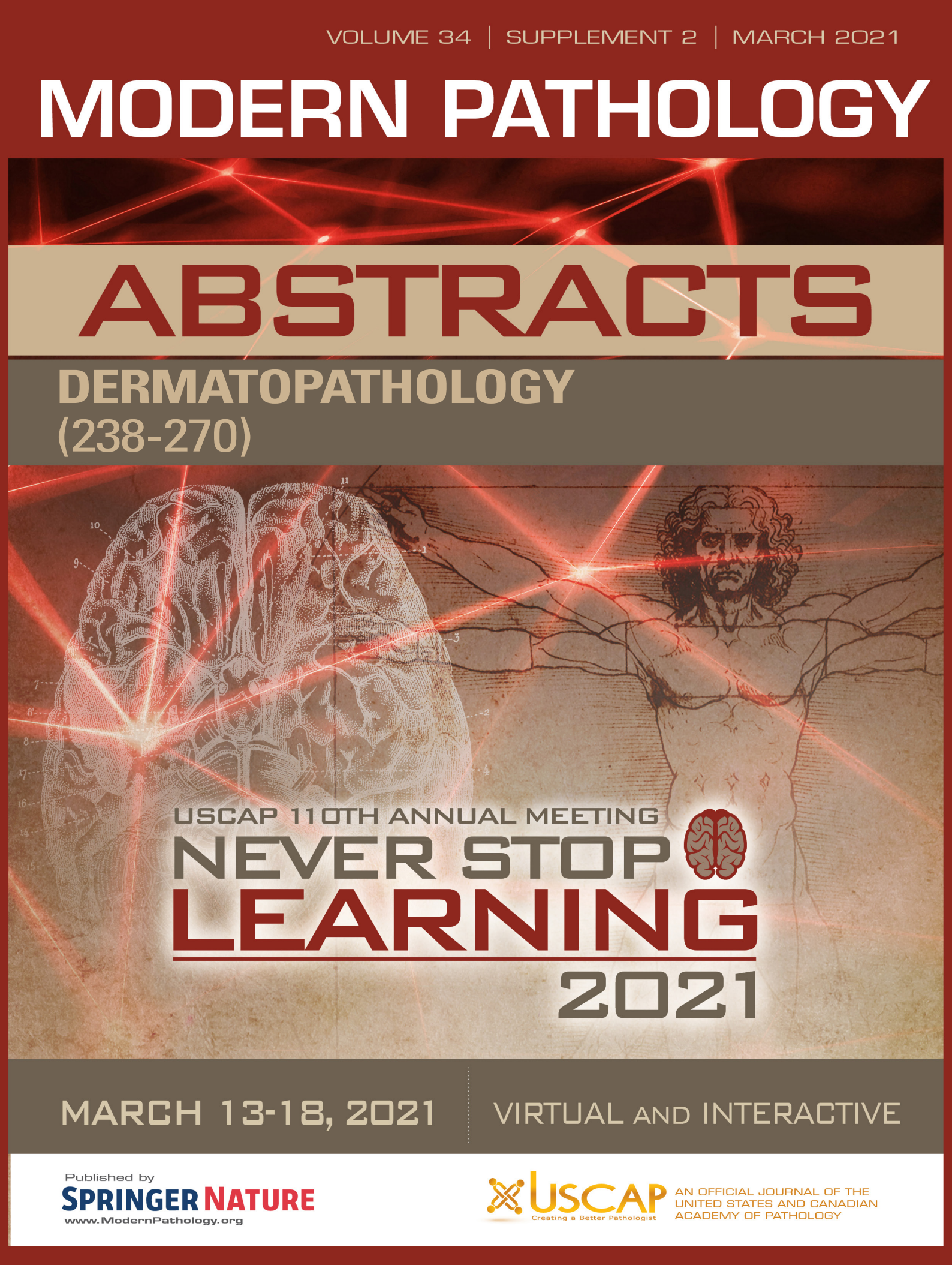


MODERN PATHOLOGY

ABSTRACTS

BREAST PATHOLOGY
(66-147)



USCAP 110TH ANNUAL MEETING
NEVER STOP
LEARNING
2021

MARCH 13-18, 2021

VIRTUAL AND INTERACTIVE

Published by
SPRINGER NATURE
www.ModernPathology.org

 **USCAP** AN OFFICIAL JOURNAL OF THE
UNITED STATES AND CANADIAN
ACADEMY OF PATHOLOGY
Creating a Better Pathologist

EDUCATION COMMITTEE

Jason L. Hornick
Chair

Rhonda K. Yantiss, Chair
Abstract Review Board and Assignment Committee

Kristin C. Jensen
Chair, CME Subcommittee

Laura C. Collins
Interactive Microscopy Subcommittee

Raja R. Seethala
Short Course Coordinator

Ilan Weinreb
Subcommittee for Unique Live Course Offerings

David B. Kaminsky
(Ex-Officio)
Zubair W. Baloch
Daniel J. Brat
Sarah M. Dry
William C. Faquin
Yuri Fedoriw
Karen Fritchie
Jennifer B. Gordetsky
Melinda Lerwill
Anna Marie Mulligan

Liron Pantanowitz
David Papke,
Pathologist-in-Training
Carlos Parra-Herran
Rajiv M. Patel
Deepa T. Patil
Charles Matthew Quick
Lynette M. Sholl
Olga K. Weinberg
Maria Westerhoff
Nicholas A. Zoumberos,
Pathologist-in-Training

ABSTRACT REVIEW BOARD

Benjamin Adam
Rouba Ali-Fehmi
Daniela Allende
Ghassan Allo
Isabel Alvarado-Cabrero
Catalina Amador
Tatjana Antic
Roberto Barrios
Rohit Bhargava
Luiz Blanco
Jennifer Boland
Alain Borczuk
Elena Brachtel
Marilyn Bui
Eric Burks
Shelley Caltharp
Wenqing (Wendy) Cao
Barbara Centeno
Joanna Chan
Jennifer Chapman
Yunn-Yi Chen
Hui Chen
Wei Chen
Sarah Chiang
Nicole Cipriani
Beth Clark
Alejandro Contreras
Claudiu Cotta
Jennifer Cotter
Sonika Dahiya
Farbod Darvishian
Jessica Davis
Heather Dawson
Elizabeth Demicco
Katie Dennis
Anand Dighe
Suzanne Dintzis
Michelle Downes

Charles Eberhart
Andrew Evans
Julie Fanburg-Smith
Michael Feely
Dennis Firchau
Gregory Fishbein
Andrew Folpe
Larissa Furtado
Billie Fyfe-Kirschner
Giovanna Giannico
Christopher Giffith
Anthony Gill
Paula Ginter
Tamar Giorgadze
Purva Gopal
Abha Goyal
Rondell Graham
Alejandro Gru
Nilesh Gupta
Mamta Gupta
Gillian Hale
Suntrea Hammer
Malini Harigopal
Douglas Hartman
Kammi Henriksen
John Higgins
Mai Hoang
Aaron Huber
Doina Ivan
Wei Jiang
Vickie Jo
Dan Jones
Kirk Jones
Neerja Kambham
Dipti Karamchandani
Nora Katabi
Darcy Kerr
Francesca Khani

Joseph Khoury
Rebecca King
Veronica Klepeis
Christian Kunder
Steven Lagana
Keith Lai
Michael Lee
Cheng-Han Lee
Madelyn Lew
Faqian Li
Ying Li
Haiyan Liu
Xiuli Liu
Lesley Lomo
Tamara Lotan
Sebastian Lucas
Anthony Magliocco
Kruti Maniar
Brock Martin
Emily Mason
David McClintock
Anne Mills
Richard Mitchell
Neda Moatamed
Sara Monaco
Atis Muehlenbachs
Bitu Naini
Dianna Ng
Tony Ng
Michiya Nishino
Scott Owens
Jacqueline Parai
Avani Pendse
Peter Pytel
Stephen Raab
Stanley Radio
Emad Rakha
Robyn Reed

Michelle Reid
Natasha Rekhman
Jordan Reynolds
Andres Roma
Lisa Rooper
Avi Rosenberg
Esther (Diana) Rossi
Souzan Sanati
Gabriel Sica
Alexa Siddon
Deepika Sirohi
Kalliopi Siziopikou
Maxwell Smith
Adrian Suarez
Sara Szabo
Julie Teruya-Feldstein
Khin Thway
Rashmi Tondon
Jose Torrealba
Gary Tozbikian
Andrew Turk
Evi Vakiani
Christopher VandenBussche
Paul VanderLaan
Hannah Wen
Sara Wobker
Kristy Wolniak
Shaofeng Yan
Huihui Ye
Yunshin Yeh
Anjana Yeldandi
Gloria Young
Lei Zhao
Minghao Zhong
Yaolin Zhou
Hongfa Zhu

To cite abstracts in this publication, please use the following format: **Author A, Author B, Author C, et al. Abstract title (abs#). In "File Title." *Modern Pathology* 2021; 34 (suppl 2): page#**

66 Prognostic Significance of Coexistent Ductal Carcinoma in Situ (DCIS) with Metaplastic Breast Carcinoma: A Tertiary Academic Institution's Experience

Evi Abada¹, Vishakha Pardeshi², Kingsley Ebare³, Eman Abdulfatah, Omar Fehmi⁴, Omar Effendi⁵, Rouba Ali¹, Sudeshna Bandyopadhyay¹

¹Wayne State University, Detroit, MI, ²Detroit Medical Center/Wayne State University, Detroit, MI, ³Staten Island University Hospital/Northwell Health, Baylor College of Medicine, TX, ⁴University of Michigan, Ann Arbor, MI, ⁵Michigan State University, East Lansing, MI

Disclosures: Evi Abada: None; Vishakha Pardeshi: None; Kingsley Ebare: None; Eman Abdulfatah: None; Omar Fehmi: None; Omar Effendi: None; Rouba Ali: None; Sudeshna Bandyopadhyay: None

Background: Metaplastic breast carcinoma (MBC) is a histologically diverse group of malignancies defined by the presence of non-glandular epithelial (squamous) or mesenchymal (spindle or matrix producing) elements associated with ductal carcinoma in situ (DCIS) or conventional mammary type invasive carcinoma. We aimed to study the clinicopathologic characteristics and prognostic differences between MBC with coexistent DCIS and MBC without DCIS in our patient population.

Design: A retrospective review of MBC was conducted (n = 125). Histologic slides were reviewed for variables including tumor morphology and hormonal status. Additional clinical data were obtained from electronic medical records. Bayesian Cox Proportional model method was used to determine the association between survival and several clinicopathologic variables.

Results: Of the 125 patients diagnosed with MBC, 47 (37.6%) had coexistent DCIS and 78 (62.4%) were not associated with DCIS. High grade, solid DCIS was the most common pattern (83%) identified in the group with DCIS. Squamous differentiation (36.2%) was the metaplastic component most common in the group with DCIS. Heterologous differentiation (32.1%) was the metaplastic component most common in the group without DCIS. The group with DCIS had a smaller mean tumor size (3 cm) compared with the group without DCIS (5 cm) [P = 0.0048]. The group with DCIS also presented at a lower clinical-stage compared with the group without DCIS [P <0.0001]. The group with DCIS were more likely to be obese compared to the group without DCIS [P = 0.006], however, this effect had no impact on overall survival. MBC with coexistent DCIS had a longer mean overall survival (62.2 months) compared with MBC without DCIS (44.4 months), however, this finding was not statistically significant. Patient clinicopathologic characteristics and outcomes are summarized in Table 1.

Table 1: Patient Characteristics and Prognosis of Metaplastic Breast Carcinoma with Coexistent DCIS and Metaplastic Breast Carcinoma without DCIS

Patient Characteristics	Metaplastic Breast Carcinoma with Coexistent DCIS n = 47; (%)	Metaplastic Breast Carcinoma without DCIS n = 78; (%)	P-value; NS = Not Significant
Demographics			
Age, mean (range)	59.6 (38-88)	56.4 (27 – 92)	NS
Race			
Caucasian	13 (27.7)	30 (38.5)	
African American	30 (63.8)	41 (52.5)	
Others	4 (8.5)	7 (9)	
Histopathologic descriptors			
Tumor size, mean (range) cm	3 (0.6 – 18)	5 (0.5 – 21.5)	0.0048
Lymphovascular invasion	15 (32)	18 (23.1)	NS
Lymph node metastasis	12 (25.5)	23 (29.5)	NS
Triple-negative tumors	31 (66)	62 (79.5)	NS
Tumor components			
Squamous only	17 (36.2)	19 (24.4)	
Spindle cells only	12 (25.5)	20 (25.6)	
Heterologous elements	13 (27.7)	25 (32.1)	
Mixed MBC	5 (10.6)	14 (17.9)	
DCIS Tumor Grade			
Low	3 (6.4)	Not applicable	
Intermediate	5 (10.6)	Not applicable	
High	39 (83)	Not applicable	
Invasive Carcinoma tumor grade			
Low	1 (2.1)	2 (2.6)	NS
Intermediate	3 (6.4)	4 (5.1)	
High	43 (91.5)	72 (92.3)	
AJCC Tumor Stage			
Stage 1	13 (27.7)	16 (20.5)	
Stage 2	29 (61.7)	31 (39.7)	
Stage 3	4 (8.5)	16 (20.5)	
Stage 4	1 (2.1)	15 (19.3)	
Comorbidities			
Obesity	35 (74.5)	40 (51.3)	0.006
Smoking	16 (34)	37 (47.4)	NS
Disease Outcome			
Overall survival, mean (range) months	62.2 (1 – 221)	44.2 (1 – 181)	
Reported deaths (n, %)	3 (6.4)	10 (12.8)	

Conclusions: Metaplastic breast carcinoma is a rare and heterogeneous disease and results from our patient population suggest that squamous differentiation is the metaplastic component most commonly seen in MBC with coexistent DCIS. In addition, MBC with coexistent DCIS appears to present at a lower clinical-stage compared with MBC without DCIS. Additional research in this area is needed to further elucidate the clinical implications of this finding.

67 Long Term Outcomes in Encapsulated and Solid Papillary Carcinoma of the Breast, High Risk of Local Recurrence with Close and Positive MarginsDhuha Al-Sajee¹, Phillip Williams²¹Hamilton Health Science McMaster Hospital, Hamilton, Canada, ²Mount Sinai Hospital, University of Toronto, Toronto, Canada**Disclosures:** Dhuha Al-Sajee: None; Phillip Williams: None**Background:** Encapsulated papillary carcinoma (EPC) and solid papillary carcinoma (SPC) of the breast without concurrent invasive carcinoma are favorable lesions in the breast with behavior similar to an in-situ lesion. Yet, it is hard to predict patient outcome. Conservative surgical excision is the standard treatment, with some patients receiving sentinel lymph node biopsy, endocrine therapy, or radiation. The focus of our study is to investigate the overall long-term outcomes in relation to histological characteristics of EPC and SPC.**Design:** We retrospectively examined the long-term outcomes of EPC and SPC cases from January 1, 2005, to January 31, 2020. Resection specimens coded as a breast mastectomy or lumpectomy with the words “solid”, “papillary”, “intracystic”, or “encapsulated” in the diagnosis or comment field were identified in the electronic medical records. All pathology reports meeting these criteria were reviewed, and cases with a concurrent invasive carcinoma excluded. An anonymized unique study identification number was assigned to each case. The histological, clinical, and follow-up information, as well as outcome, were recorded; these data included age at diagnosis, site of the lesion, size of the lesion, lymph node status, margin status, local recurrence, metastatic disease, and death.**Results:** We identified 11 EPC and 8 SPC cases with follow-up available. All patients were females and the mean age at diagnosis was 66.5 years, range: 46-88 years. All cases of EPC/SPC were associated with DCIS. EPC and SPC had a reported mean size of 29.8 mm and 29.5 mm respectively. Follow-up time ranged from 1 month to 20 years with a mean follow-up of 4.6 years. No cases of SPC had a local or distant recurrence. Three cases of EPC developed local recurrence for a recurrence rate of 27% (3/11). All EPC cases with local recurrence had either close or positive margins: DCIS 1mm to posterior margin (1/3), DCIS present at the posterior margin with superior and anterior margins close at 1mm (1/3), and EPC <1mm to lateral margin t (1/3). No EPC cases developed distant metastatic disease or death from the disease.**Conclusions:** Based on the sampled cases of EPC, we observed that positive or close margins (1mm or less) were at a higher risk of local recurrence. Re-excision of close margins should be considered in these cases and close follow-up is needed. Among EPC cases, including those with local recurrence, none developed distant metastatic disease or death from the disease.**68 Peritumoral CD8+/FOXP3+ Cell Ratio Has Prognostic Value in Triple Negative Breast Cancer (TNBC)**Rana Aldrees¹, Tiansheng Shen², Gene Siegal¹, Shi Wei¹¹The University of Alabama at Birmingham, Birmingham, AL, ²The Ohio State University Wexner Medical Center, Columbus, OH**Disclosures:** Rana Aldrees: None; Tiansheng Shen: None; Gene Siegal: None; Shi Wei: None**Background:** There has been compelling evidence published demonstrating the prognostic significance of Tumor-infiltrating Lymphocytes (TILs) in various solid cancers, including BC. A high level of TILs is reportedly associated with a favorable prognosis in TNBC, a subtype generally associated with a poor clinical outcome but highly heterogeneous. There have been limited studies investigating the importance of subsets of T-cells in TILs. Moreover, the significance of intratumoral vs. peritumoral TILs remains controversial. In this study, we sought to explore the prognostic relevance of tumor-associated CD8⁺ cytotoxic T cells and FOXP3⁺ regulatory T cells in TNBC.**Design:** Consecutive excisional TNBC cases prior to chemotherapy in the authors' institution were retrieved between 2001 and 2015. Those with de novo metastatic BC, bilateral BC, a second malignancy, patients not receiving systemic chemotherapy and cases without a tumor-host interface in the tissue sections were excluded.

This resulted in a total of 35 cases meeting the inclusion criteria. Intratumoral TILs were characterized as stromal TILs within the borders of the invasive tumor, while peritumoral TILs were defined as TILs within one high power field (HPF; 0.5 mm) of the invasive front. The CD8⁺ and FOXP3⁺ cell count (expressed as per HPF on average of 10 HPFs) and their ratios were dichotomized on the basis of the median value. The median follow up time was 7 years.

Results: There was a wide range of CD8⁺ and FOXP3⁺ T-cells within the peritumoral (27-410 and 1-38, respectively) and intratumoral stroma (1-105 and 0-24, respectively). Both CD8⁺ and FOXP3⁺ TILs were significantly higher at the former location than the latter (157 vs. 25, P<0.0001 and 10 vs. 5, P=0.003). The numbers of CD8⁺ and FOXP3⁺ T-cells, either within peritumoral or intratumoral stroma, were not significantly associated with distant relapse-free or disease-specific survival (RFS/DSS), probably attributed to their wide-ranging distribution. However, the peritumoral CD8⁺/FOXP3⁺ ratio of TILs was significantly associated with a prolonged RFS (hazard ratio [HR] 0.3, P=0.04) and DSS (HR 0.2, P=0.02). This association was not observed with the CD8⁺/FOXP3⁺ ratio of intratumoral TILs. As expected, pathologic tumor and nodal stages were both significantly associated with survival outcomes.

Conclusions: While the numbers of CD8⁺ and FOXP3⁺ T cells were not associated with prognostic outcomes, the peritumoral CD8⁺/FOXP3⁺ ratio showed a significant positive correlation with RFS and DSS in TNBC. These observations suggest that the immunological balance in the tumor microenvironment might determine antitumor immunity. Further, the peritumoral TILs appear to play a more important role in the progression of TNBC when compared to the intratumoral TILs, thus reaffirming the necessity of revisiting the method for assessment of TILs in the pursuit of precision medicine.

69 The Survival Benefit of Endocrine Therapy in Low Estrogen Receptor Positive/HER2 Negative Invasive Breast Cancer

Mohamed Alhamar¹, Bassam Alkamachi¹, Harshita Mehrotra¹, Hovsep Ohan¹, Haythem Ali¹, Nilesh Gupta¹, Oudai Hassan¹, Dhananjay Chitale², Daniel Schultz¹, Ghassan Allo², Wamidh Alkhoory¹
¹Henry Ford Health System, Detroit, MI, ²Henry Ford Hospital, Detroit, MI

Disclosures: Mohamed Alhamar: None; Bassam Alkamachi: None; Harshita Mehrotra: None; Hovsep Ohan: None; Haythem Ali: *Consultant*, Genentech Roche; Nilesh Gupta: None; Oudai Hassan: None; Dhananjay Chitale: None; Daniel Schultz: None; Ghassan Allo: *Employee*, Tempus Labs; Wamidh Alkhoory: None

Background: In 2020, American Society of Clinical Oncology/College of American Pathologists (ASCO/CAP) released new recommendations to consider Invasive Breast Cancer (IBC) with 1-10% Estrogen Receptor (ER) positivity by immunohistochemistry (IHC) as low ER+ with a comment to reflect the limited data on the overall benefit of Endocrine Therapy (ET) in such patients. We studied the benefit of ET in low ER+/HER2- IBC patients & compared their survival to triple negative (TN-) IBC patients.

Design: All IBC patients with low ER+/HER2- from 2010-2018 were identified (n=67). ER was interpreted using IHC based on ASCO/CAP guidelines at the time of reporting. These cases were compared to a control group of similar pT stage TN- IBC cases (n=67). We retrospectively retrieved clinical data (age, ET, chemo & radiotherapy) & histopathologic features (Tumor type, grade, pT stage, highest ER IHC %). Outcomes studied were recurrence, metastasis, Disease Free Survival (DFS) & Overall Survival (OS). Kaplan-Meier curves were generated & compared using log-rank test. Multivariate analysis was performed using Cox hazards models.

Results: Low ER+ patients showed a median age of 59 years (range 31-89). The median ER IHC was 3% (1-10%) & the median tumor grade was 3. Tumor types included: Ductal-No special type (54/67), Lobular (5/67), mixed (2/67), & special ductal (6/67).

ET was given to 33/67 (49%) patients [Anastrozole (Arimidex) in 18/33], 9/33 (27%) patients had ET related side effects (hot flashes x3, arthralgia x2, other x4). Table shows clinical & histopathologic features of cases; no significant relationship was observed between the variables.

The median follow-up was 1219 days (range 71-3697). Two of the low ER+ patients were alive with disease, 9 patients died due to IBC, & 3 died due to other causes. Figure 1 shows no statistically significant difference in OS

(p=0.188) & DFS (p=0.233) for those received ET vs. No ET. In addition, no statistically significant difference in OS (p=0.359) & DFS (p=0.442) is observed between low ER+ & TN- IBC (Figure 2).

Multivariate analysis showed that pT stage was the only independent predictor for OS in the low ER+ cohort.

	Low ER (1-10%)			ER Negative	P-value
	Received Endocrine Therapy (n=33)	Endocrine Therapy Not given (n=34)	Combined (Endocrine & No Endocrine Therapy) (n= 67)	(n=67)	
Median Age	60	59	59	60	0.965
pT Stage					0.678
pTmic	0	1	1	2	
pT1	17	14	31	30	
pT2	7	4	11	10	
pT3	1	3	4	6	
pT4	1	1	2	0	
ypT0-ypT1	4	6	10	11	
ypT2-ypT4	0	4	4	4	
Not available	3	1	4	4	
Median Tumor Grade	3	3	3	3	0.601
Median ER expression by IHC (%)	5%	2%	3%	0%	0.067
Neoadjuvant Chemotherapy	5	11	16	17	0.235
Adjuvant Chemotherapy	24	22	46	48	0.319
Radiotherapy	21	29	50	50	0.267
Developed Metastasis	4	6	10	15	0.691
Developed Local Recurrence	0	1	1	7	0.507

Figure 1 - 69

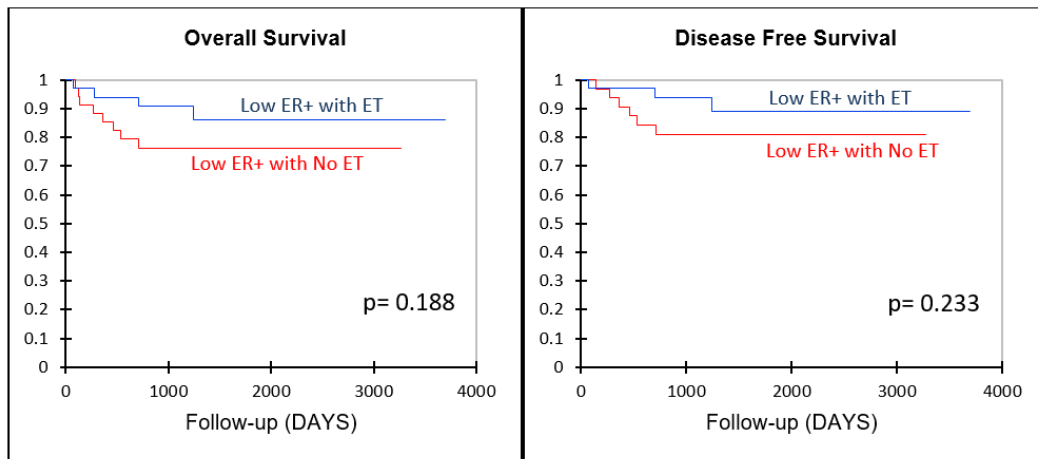
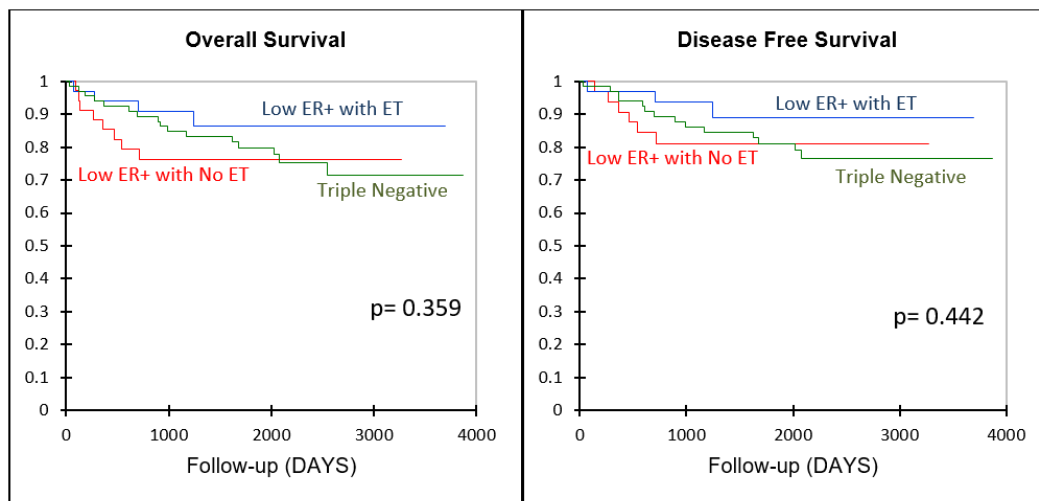


Figure 2 - 69



Conclusions: Our study shows no survival benefit with ET in low ER+ IBC patients & outcome that is similar to TN-IBC patients. Therefore, our findings support the current ASCO/CAP guidelines in considering ER cases with 1-10% staining on IHC as low ER+ separating them from the rest of ER+ IBC. Larger, prospective longitudinal studies are needed to validate these findings.

70 Histopathologic Features and the Effects of Androgen Therapy in Breast Tissue of Female-to-Male Transgender Individuals

Emily Anderson¹, Kim Rabe¹, Lianne Siegel¹, Jessica Butts¹, Molly Klein¹
¹University of Minnesota, Minneapolis, MN

Disclosures: Emily Anderson: None; Kim Rabe: None; Lianne Siegel: None; Jessica Butts: None; Molly Klein: None

Background: Few studies have described the histopathologic features in gender affirming mastectomy specimens from female-to-male transgender men (TM), and even fewer have specifically addressed the effects of exogenous androgen therapy (AT). This is the largest study to describe the histopathologic features in breast specimens from TM with and without a history of AT, and to compare them to a control group of elective breast reduction specimens from cisgender women.

Design: Data from chart review and blinded slide review was collected for 289 TM undergoing gender-affirming bilateral mastectomy (237 were on AT and 52 were not). These 2 groups were then compared to 63 cisgender women undergoing bilateral elective breast reduction using Fisher’s Exact and Kruskal-Wallis tests.

Results: Results from 289 TM subjects (median age 24, range:14-59), of which 237 were on AT and 52 were not, and 63 cisgender women subjects (median age 33, range: 15-68) were analyzed. Four tissue cassettes were submitted per subject (median). In breast tissue from TM on AT, lobules occupy 5% of the examined area (median), and 70% of the lobules show intralobular atrophy (median). Longer exogenous AT use among TM was associated with a lower median percentage of lobules by area ($p < 0.001$). TM on AT and without AT both had a significantly higher median percentage of intralobular atrophy compared to the cisgender women ($p = 0.001$). For TM on AT, the mastectomy specimens showed some degree of inflammation in 20.3%, duct ectasia in 16.0%, apocrine cysts in 12.2%, non-apocrine cysts in 11.8%, fibroadenomatoid change in 10.2%, luminal calcifications in 5.1%, usual ductal hyperplasia in 4.2%, fibroadenomas in 3.4%, columnar cell change in 2.1% and atypia in 0.8%. The atypia in specimens from TM included 2 cases of atypical lobular hyperplasia (ALH) and 1 case of flat epithelial atypia (FEA). In the control group showed atypia in 3.2% (one case with atypical ductal hyperplasia and one case with ALH and FEA). There were no cases of invasive carcinoma or carcinoma in situ across groups.

Conclusions: Histologic findings observed in TM on AT include increased intralobular atrophy compared to cisgender breast reductions and a reduction in percentage lobules by area with increased length of AT. The prevalence of atypia was low among all subjects and did not differ significantly across groups. With an even larger number of cases (obtained by extending the time frame for inclusion), we will further analyze the results, controlling for age and BMI.

71 M2 Tumor Associated Macrophages are Associated with Decreased Response to Neoadjuvant Chemotherapy in Triple Negative Breast Carcinoma

Vidya Arole¹, Hiro Nitta², Lai Wei¹, Anil Parwani¹, Zaibo Li³

¹The Ohio State University, Columbus, OH, ²Roche Tissue Diagnostics, Tucson, AZ, ³The Ohio State University Wexner Medical Center, Columbus, OH

Disclosures: Vidya Arole: None; Hiro Nitta: *Employee*, Roche Tissue Diagnostics; Anil Parwani: None; Zaibo Li: None

Background: Two types of macrophages are present in tumor microenvironment. M1 macrophages exhibit potent anti-tumor properties, while M2 macrophages play the pro-tumoral roles. The presence of M2 macrophages is associated with worsened overall survival in triple negative breast carcinoma (TNBC) patients. However, the relationship between M2 macrophages and response to neoadjuvant chemotherapy (NAC) is unknown.

Design: M2 macrophages were investigated on biopsy whole sections from 66 TNBCs treated with NAC by CD163 together with other immune checkpoint markers (PD1, PD-L1 and CD8) using a multi-color immunohistochemical multiplex assay.

Results: Incomplete response was significantly associated with older age, lower PD-L1 expression (tumor and stroma), lower levels of CD8-positive TILs in stroma, but higher level of CD163-positive macrophages, with the level of CD163-positive macrophages in peritumoral area as the strongest factor. (Table 1)

Table 1. Univariate and multivariate analysis of factors associated with response to neoadjuvant chemotherapy in 66 triple negative breast carcinomas

Variable	Level	Incomplete response (n=38)	Complete response (n=28)	Univariate analysis p-value	Multivariable analysis p-value
Age	Mean (min, max)	53.2 (31, 74)	47 (26, 72.9)	0.041	0.226
Histology type	Ductal	36 (95%)	28 (100%)	0.504	Not included
	Metaplastic	2 (5%)	0 (0%)		
Nottingham grade	2	7 (18%)	3 (11%)	0.498	Not included
	3	31 (82%)	25 (89%)		
Tubule formation	2	1 (3%)	0 (0%)	1	Not included
	3	37 (97%)	28 (100%)		
Nuclear pleomorphism	2	6 (16%)	3 (11%)	0.722	Not included
	3	32 (84%)	25 (89%)		
Mitotic activity	1	3 (8%)	1(4%)	0.078	0.031
	2	25 (66%)	12 (43%)		
	3	10 (26%)	15 (54%)		
LN metastasis (0-no, 1-yes)	Missing	36 (95%)	16 (57%)	0.506*	Not included
	0	0 (0%)	5 (18%)		
	1	2 (5%)	7 (25%)		
PD-L1-tumor	Mean	2.6%	7.8%	0.004	0.340
	(min, max)	(0,30%)	(0,60%)		
PDL1-stroma	Mean	1.90%	7.30%	0.007	0.005
	(min, max)	(0,15%)	(0,50%)		

CD8-tumoral	Mean	7.40%	11%	0.004	0.138
	(min, max)	(0,50%)	(0,40%)		
CD8-peritumoral	Mean	8.7%	15%	0.001	0.125
	(min, max)	(0,40%)	(0,50%)		
CD163-tumoral	Mean	35.9%	22.8%	0.003	0.694
	(min, max)	(0,80%)	(5%, 50%)		
CD163-peritumoral	Mean	39.2%	24.8%	0.003	<0.001
	(min, max)	(10%, 80%)	(5%, 50%)		

Conclusions: Our data have demonstrated that the level of CD163-positive macrophages was significantly higher in TNBC patients with incomplete response than patients with complete response, suggesting M2 macrophages' important role in predicting TNBC patients' response to NAC.

72 Evaluating Mismatch Repair Status in Clinically Advanced Breast Carcinoma

Vidya Arole¹, Tiansheng Shen², Anil Parwani¹, Zaibo Li²

¹The Ohio State University, Columbus, OH, ²The Ohio State University Wexner Medical Center, Columbus, OH

Disclosures: Vidya Arole: None; Tiansheng Shen: None; Anil Parwani: None; Zaibo Li: None

Background: Very few studies have investigated mismatch repair (MMR) deficiency in breast carcinoma (BC). Given the recent FDA approval of Pembrolizumab for unresectable solid tumors with dMMR, we aimed to examine MMR status in clinically advanced breast carcinoma.

Design: Immunohistochemistry (IHC) with anti-MLH1, anti-PMS2, anti-MSH2 or anti-MSH6 was performed on metastatic triple negative breast carcinoma (TNBC) specimens routinely or other BC specimens by clinician's request to evaluate MMR status in our institution since 2017 after FDA approval of Pembrolizumab for solid tumors with dMMR. In addition, next generation sequencing (NGS) approach (FoundationOne® CDx, Foundation Medicine) to detect microsatellite instability was also performed.

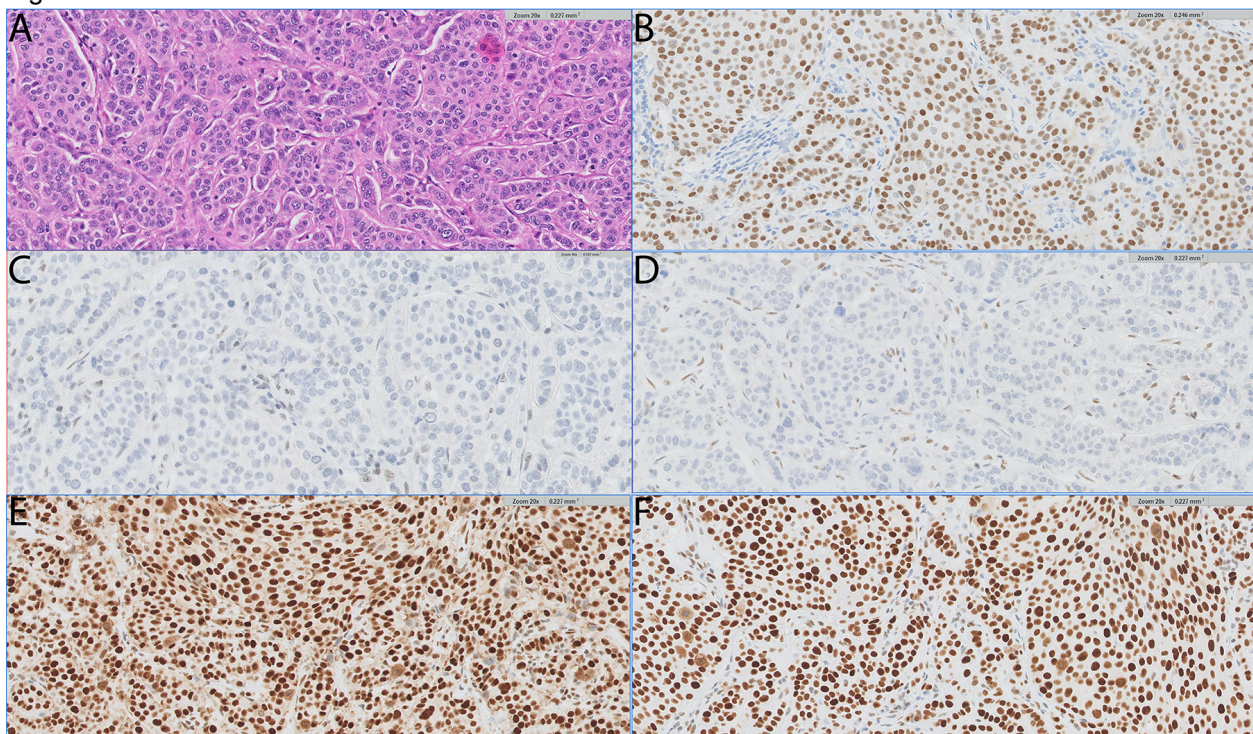
Results: Current cohort contained 127 clinical advanced BCs, including 4 primary, 14 locally recurrent and 109 metastatic BCs. Twenty-four were ER-positive/HER2-negative, 16 were HER2+, and 87 were TNBCs. MMR status was evaluated by IHCs in 95 cases and by NGS in 32 cases. Among all 127 cases, only one case (0.8%) showed MMR deficiency. (Table 1) The case with MMR deficiency showed loss of MLH1 and PMS2 proteins, but no hypermethylation of MLH1 promoter on MLH1 promoter methylation study. Sequencing analysis revealed *MLH1* genetic alteration with a splice site mutation (208-1G>A), which results in disruption of the N-terminal ATPase-containing domain (amino acids 25-336) and inactivation of MLH1 protein.

Table 1. Clinicopathologic features and mismatch repair status in 127 advanced breast carcinomas.

		#	% (range)
Total case #		127	
Age (years) (median, range)		54.7	28-92
Specimen	Biopsy	99	78.0%
	resection	28	22.0%
Location	Primary	4	3.1%
	Local recurrent	14	11.0%
	Metastatic	109	85.8%
Metastatic site	Bone	18	14.2%
	Lung	9	7.1%

Metastatic site	Brain	18	14.2%
	Liver	38	29.9%
	Lymph node	13	10.2%
	other	13	10.2%
Biomarkers	ER+/HER2-	24	18.9%
	HER2+	16	12.6%
	TNBC	87	68.5%
MMR testing	IHC	95	74.8%
	NGS	32	25.2%
MMR status	Preserved	126	99.2%
	Deficient	1	0.8%

Figure 1 - 72



Conclusions: MMR deficiency exists in an extremely low percentage of advanced BCs including metastatic TNBCs, suggesting a routine MMR testing may not be cost effective.

73 Pathologic Characterization of Non-Malignant Breast Lesions Detected by 3D-Digital Breast Tomosynthesis (DBT) Versus 2D-Digital Mammography (DM)

Jasmeet Assi¹, Ira Bleiweiss², Anupma Nayak¹

¹Perelman School of Medicine at the University of Pennsylvania, Philadelphia, PA, ²Hospital of the University of Pennsylvania, Philadelphia, PA

Disclosures: Jasmeet Assi: None; Ira Bleiweiss: None; Anupma Nayak: None

Background: Breast cancer screening using 3D-DBT has resulted in increased detection of small cancers and a reduction in recall rates across all age and breast density groups compared with 2D-DM. Little is known about its effect on detection of high risk lesions of the breast. In this study, we explore whether the range and frequency of

non-malignant diagnoses has changed with the implementation of 3D-DBT or if it yields core biopsies with nonspecific histology in greater numbers.

Design: At our institution, 3D-DBT was adopted as the frontline breast cancer screening modality in September 2011. In this retrospective analysis, we compared the pathologic diagnoses of non-malignant core biopsies diagnosed at our institution during two consecutive 2 year periods, the 2 years before and the 2 years after the change from 2D-DM to 3D-DBT. We also compared the frequency of specific radiologic findings during these two periods. The percent change was calculated between the 2 periods of time as well as the *p* value (Fisher's exact test).

Results: A total of 512 cases were diagnosed as non-malignant, including 230 detected by 2D-DM (pre 3D-DBT period) and 282 detected by 3D-DBT (post 3D-DBT implementation). The change in modality accounted for a 18% increase in core biopsies. With respect to non-malignant pathologic findings, radial scar, papilloma, ADH, lobular neoplasia, duct ectasia, nonspecific benign changes, and PASH all had an increase (percent change), most notable being radial scar (362.2%), intraductal papilloma (75.7%) and PASH (715.6%). Fibrocystic changes, fibroadenoma, lymph node, miscellaneous benign tumors, and fat necrosis all had decreases (percent change), most prominent being lymph node (-30.1%) and fibrocystic changes (-27.4%). The lesions that did change statistically significantly with the introduction of 3D-DBT were radial scar (*p*=0.003), fibrocystic changes (*p*=0.017), and PASH (*p*=0.009). With regards to radiologic findings, there was an increase in architectural distortion, asymmetry, mass, and dilated ducts; and a decrease in calcifications and cysts. However, only change in architectural distortion showed statistical significance (*p*=0.009). See table 1 for complete data.

Table 1 - Comparison of pathologic and radiologic findings before and after 3D-DBT

Pathologic Findings	Before 3D-DBT (n)	Before 3D-DBT (%)	After 3D-DBT (n)	After 3D-DBT (%)	Percent Change (%)	p value
Total (n=512)	230		282		18.4%	
Radial Scar	3	1.30%	17	6.03%	362.2%	0.003
Intraductal Papilloma	13	5.65%	28	9.93%	75.7%	0.068
Fibrocystic changes	82	35.65%	73	25.89%	-27.4%	0.017
Fibroadenoma	70	30.43%	78	27.66%	-9.1%	0.492
Lymph node	14	6.09%	12	4.26%	-30.1%	0.356
Duct ectasia	4	1.74%	5	1.77%	2.0%	0.997
ADH	3	1.30%	4	1.42%	8.7%	0.912
Lipoma	0	0.00%	2	0.71%	-	0.156
Lobular neoplasia	5	2.17%	7	2.48%	14.2%	0.817
Micellaneous Benign Tumors	4	1.74%	4	1.42%	-18.4%	0.773
Non specific benign changes	22	9.57%	34	12.06%	26.0%	0.364
PASH	1	0.43%	10	3.55%	715.6%	0.009
Fat necrosis	8	3.48%	8	2.84%	-18.4%	0.681
Diabetic Mastopathy	1	0.43%	0	0.00%	-	0.316
Radiologic Findings						
Architectural distortion	1	0.43%	10	3.55%	715.6%	0.009
Asymmetry	8	3.48%	10	3.55%	2.0%	0.967
Calcifications	83	36.09%	78	27.66%	-23.4%	0.053

Cyst	11	4.78%	10	3.55%	-25.9%	0.489
Mass	126	54.78%	169	59.93%	9.4%	0.241
Dilated duct	1	0.43%	5	1.77%	307.8%	0.241

Conclusions: 3D-DBT detected more benign risk-associated pathologic lesions, including radial scar and intraductal papilloma and detected architectural distortion at a greater frequency. However, there was also an increase in detection of non-specific findings such as PASH with the implementation of 3D-DBT.

74 Pathologic Lesions Correlating with Mammographic Architectural Distortion: A Study of 557 Core Needle Biopsies

Emily Bachert¹, Aaron Jen², Denison Christine², Sona Chikarmane², Jane Karimova², Dylan Kwait², Susan Lester²

¹Brigham and Women's Hospital, Harvard Medical School, Boston, MA, ²Brigham and Women's Hospital, Boston, MA

Disclosures: Emily Bachert: None; Aaron Jen: None; Denison Christine: None; Sona Chikarmane: None; Dylan Kwait: None; Susan Lester: None

Background: Architectural distortion (AD) is a localized alteration in the uniform texture of the breast characterized by lines radiating from a central point, without a definite mass. This finding has become more common due to the increased ability of tomosynthesis to detect these subtle findings. Radiologic/pathologic correlation is more difficult in this setting because the types of lesions producing AD are not as well defined as the more common findings of masses or calcifications and, thus, what signifies a discordant finding requiring excision is unclear. There is also only limited data about the types of benign lesions on core needle biopsy (CNB) that are predictive of carcinoma on excision.

Design: The objective was to determine the types of lesions on CNBs performed for AD and the likelihood of malignancy on excision. Pathology reports for CNBs and subsequent excisions from 01/01/2015 to 08/01/2020 were identified.

Results: 557 CNBs met inclusion criteria (Table 1). The most common lesion was invasive cancer (29%). Lobular (31%) and cancers with lobular features (17%) comprised 48% of cases, whereas 42% of the cancers were ductal. 93% were grade 1 or 2, 98% were ER-positive, and 98% were HER2-negative. Ductal carcinoma in situ was found in an additional 21 cases (4%).

The second most common type of lesion (29%) included those with sclerosis (complex or radial sclerosing lesions and sclerosing adenosis). If no atypia was present, only 1 case (2%) was found to have malignancy on excision. In this case, DCIS was present adjacent to the sclerosing lesion.

There were 39 cases of ADH or cases described as “atypical”. Of these, 12 of 34 undergoing excision (35%) showed malignancy. There were 33 cases of ALH/LCIS, and 4 of 20 undergoing excision (20%) showed malignancy. An associated sclerosing lesion did not increase the risk of malignancy.

The remaining 181 cases had a variety of benign findings that did not clearly correlate with AD. Of the 63 cases undergoing excision, 8% showed malignancy.

Table 1. Pathologic Correlates of Mammographic Architectural Distortion

Pathologic Lesion	No. of Cases (%)	No. Excised	No. Malignant (%)
Invasive carcinoma	162 (29%)	150	150 (100%)*
DCIS	21 (4%)	20	20 (100%)
Atypical ductal hyperplasia**	10 (2%)	9	4 (44%)
Other types of atypia**	8 (1%)	7	2 (29%)
ALH/LCIS**	16 (3%)	8	2 (25%)
Sclerosing lesions***	159 (29%)	96	9 (9%)
• Without atypia	• 121	• 66	• 1 (2%)
• With atypia (other than ALH)	• 21	• 18	• 6 (33%)
• With ALH/LCIS	• 17	• 12	• 2 (17%)
Other benign lesions (not including ALH, ADH, or LCIS)	181 (32%)	63	5 (8%)
TOTAL	557 (100%)	353	193 (55%)

* One small invasive carcinoma was completely removed by the core needle biopsy.

** These categories do not include cases in which a sclerosing lesion was also present. These cases are reported separately.

*** Includes sclerosing adenosis, radial sclerosing lesion (radial scar), and complex sclerosing lesion.

Conclusions: 29% of lesions causing AD were due to invasive carcinomas that were likely to be grade 1 or 2 and have lobular features. 29% were associated with sclerosing lesions. If no atypia was present, the likelihood of malignancy on excision was very low (2%). 32% of CNBs showed non-specific benign findings, making a determination of radiology correlation challenging. However, only 8% of cases undergoing excision showed malignancy. Both atypical ductal and lobular lesions were predictive of malignancy on excision regardless of the presence of a sclerosing lesion. This is in contrast to incidental ALH/LCIS associated with other types of lesions (such as masses or calcifications), for which the likelihood of malignancy is <5%. Although the number of cases is low, ALH/LCIS may be a predictor of malignancy in the setting of AD, perhaps due to the higher association of invasive carcinomas with lobular features with AD.

75 Clinicopathological Features of Microinvasive Carcinomas of the Breast: An Institutional Experience

Deyze Badarane¹, Farnaz Hasteh², Oluwole Fadare³, Somaye Zare²

¹University of California, San Diego, San Diego, CA, ²University of California, San Diego, La Jolla, CA, ³UC San Diego School of Medicine, La Jolla, CA

Disclosures: Deyze Badarane: None; Farnaz Hasteh: None; Oluwole Fadare: None; Somaye Zare: None

Background: The widespread use and improved sensitivity of screening methods have led to increased early detection of in situ and microinvasive carcinomas of the breast. Microinvasive carcinomas (MIC) are relatively uncommon, and the prognosis and clinical management of patients that are diagnosed with MIC remain controversial. The current study is a comprehensive evaluation of clinicopathologic characteristics, including patient outcomes, in an institutional cohort of MIC.

Design: The study cohort consisted of all patients with a final pathologic stage of pT1mi in a breast excision specimen over a 20-year period. Clinicopathologic data were collected and analyzed. For comparative analyses

regarding the frequency of lymph node (LN) metastases, two additional cohorts of pTis [DCIS] and pT1a [invasive] cancers that were diagnosed over a shorter timeframe, were used.

Results: Excisions from a total of 87 patients, median age of 57 y (range 29-84) were identified. MIC was diagnosed in the preceding biopsy in only 33% of cases. The background in situ carcinoma was most frequently intermediate and high grade DCIS (93.1%); the remainder were LCIS (4.6%) and low grade DCIS (2.2%). LN involvement was identified in 5 cases (5.7%: 1 macroscopic, 3 microscopic and 1 isolated tumor cells). In comparison, LN metastasis was detected in 1.1% and 7.2% of separate DCIS and pT1a cohorts respectively. MIC was multifocal in 16 cases (18.4%). The presence of multifocal disease was significantly associated with larger extent of in situ disease ($p = .001$) and no hormone receptor expression ($p = .017$), but not LN metastasis, patient age or recurrence rates. HER2/neu overexpression was detected in 35 (40.2%) of tumors. HER2/neu overexpression was significantly associated with high grade DCIS ($p = .001$) and negative hormone receptor status ($p < .001$), but not LN metastasis, extent of the disease, patient age or recurrence rates. Overall, after an average follow up duration of 50.4 months, only 1 patient (1.1%) experienced a recurrence in ipsilateral breast.

Conclusions: The rate of LN involvement in MIC -5.7%- is higher than DCIS, which highlights the significance of the finding. Multifocality of the microinvasion was not of any prognostic significance in our cohort. MIC are commonly HER2/neu-positive (approximately 40%), which is probably a function of the background high grade DCIS from which they arise. However, in contrast to invasive carcinomas, HER2/neu overexpression in MIC is not associated with LN metastases or higher recurrence rates.

76 Can Sentinel Lymph Node Biopsy Be Spared in High Nuclear Grade, Extensive Size and/or HER2+ DCIS with Upstage on Excision

Mara Banks¹, Evgeny Yakirevich², Li Juan Wang³, Yihong Wang⁴

¹Brown University, Rhode Island Hospital, Lifespan, Providence, RI, ²Rhode Island Hospital, Providence, RI, ³Alpert Medical School of Brown University, Providence, RI, ⁴Brown University, Rhode Island Hospital, Providence, RI

Disclosures: Mara Banks: None; Evgeny Yakirevich: None; Li Juan Wang: None; Yihong Wang: None

Background: Microinvasive breast cancer is defined by the presence of 1mm or less invasive cancer and is considered a subset of T1 disease (T1mi) by AJCC and associated with a background of ductal carcinoma in situ (DCIS) in most cases. Studies have investigated the histopathological characteristics and clinical outcomes of microinvasive DCIS; however, impact factors such as the DCIS size, nuclear grade, presence of comedo necrosis, and/or HER2 status on decision marking for sentinel lymph node biopsy (SLNB) have not been well addressed. The current literature suggests lack of a consensus in the surgical management of this disease. Since patients can occasionally develop metastatic disease, SLNB is often considered during surgery.

Design: A retrospective review of consecutive cases diagnosed preoperatively with DCIS or DCIS suspicious for microinvasion on core needle biopsy (CNB) was performed at our institution from 2009 to 2019. Forty-eight cases were identified with the inclusion criteria of upstage on excision and available clinical follow up information. Slides were reviewed and pathological parameters, biomarkers and relevant clinical information were recorded.

Results: All 48 patients were females with mean age of 63 (range 34-98 years). Eighty-eight percent (42/48) of the cases were T1mi and 12.5% (6/48) were upstaged to T1a on excision. SLNB was performed on 50% (24/48) of the cases. The histological features on CNB of the 48 DCIS included 69% with nuclear grade 3, 89% with comedo necrosis, 27% with extensive DCIS size (≥ 40 mm) and 42% with HER2 positivity. Of the 24 cases that underwent SLNB, the percentage of those histological parameters increased to 79% for nuclear grade 3, 100% for presence of comedo necrosis, 42% for extensive size and 75% for HER2 positivity. One case underwent SLNB revealed a positive SLN (4.2%, 1/24). This patient had a 52mm extensive DCIS, nuclear grade 3 with comedo necrosis and HER2 positivity. All patients were alive and disease free without recurrence with a mean follow up of 57.6 months.

Conclusions: CNB DCIS with upstage on excision rarely involves SLN even in DCIS with extensive size, high nuclear grade, and presence of comedo necrosis and/or HER2 positivity. The overall prognosis and long term survival is excellent. We propose that evaluation of SLNB should not be indicated in patients with DCIS who are managed by local control lumpectomy.

77 Angiomyxoma of the Breast: Clinicopathologic Analysis of 43 Cases

Esther Baranov¹, Erin Alston¹, Susan Lester¹, Christopher Fletcher¹, Leona Doyle¹

¹Brigham and Women's Hospital, Boston, MA

Disclosures: Esther Baranov: None; Erin Alston: None; Susan Lester: None; Christopher Fletcher: None; Leona Doyle: None

Background: Superficial angiomyxoma (SAM) is a benign neoplasm typically involving dermis and subcutis and composed of bland spindle cells and prominent small vessels in a myxoid stroma. A subset of cases (especially of breast or external ear canal) are associated with Carney complex, but mutations in *PRKAR1A* are found in both sporadic and syndromic cases. Approximately 20% recur when incompletely excised. SAM of breast may arise subcutaneously in the nipple-areolar complex (NAC) or within parenchyma; however, these lesions are not well-recognized, may mimic myxoid fibroepithelial lesions or reactive proliferations, and have been described in the literature by other names (e.g. 'myxoma', 'nodular mucinosis'). This study characterizes the clinical and histologic features of angiomyxoma of breast.

Design: 43 cases were identified from surgical pathology and consultation files. Clinical demographics and histologic features were reviewed. Immunohistochemistry for *PRKAR1A* was performed on 33 cases; data for CD34, S-100, smooth muscle actin (SMA), desmin, p63 and pan-keratin were available for a subset.

Results: 25 patients were female and 18 male; median age was 41 years (range 14 - 72). Most cases (58%) presented as slow-growing parenchymal masses, 21% as subcutaneous NAC masses, and 21% as subcutaneous masses outside the NAC. 44% were thought to represent other entities, including low-grade sarcomas, based on submitting differential diagnoses. All showed classic features of SAM at other locations: bland spindle/stellate fibroblasts in a myxoid stroma, elongated thin-walled vasculature, and a neutrophilic infiltrate in 70%. Mitotic rate was low overall (<1 per 10 hpf). Most tumors were hypocellular, poorly circumscribed and lobulated; 10 showed prominent infiltrative growth, and tumors of the NAC often infiltrated through areolar muscle. 53% involved breast parenchyma histologically with adjacent or entrapped benign breast lobules. Additional features included pseudocystic change (35%), mild degenerative nuclear atypia (28%) and mast cell infiltrates (72%). Unusual features were increased cellularity in 6 parenchymal tumors, 4 of which had increased mitoses (up to 6 per 10 hpf). Tumor cells showed loss of *PRKAR1A* expression in 58% of cases. CD34 expression was seen in 57% and SMA in 40%; S-100, desmin, p63 and pan-keratin were consistently negative. One tumor recurred multiple (5) times. No patient had a known history of Carney complex.

Conclusions: Angiomyxomas of the breast may arise in subcutaneous or parenchymal locations and are under-recognized, particularly when parenchymal. Histologic features are identical to those of SAM at other sites, but parenchymal tumors may show greater cellularity, entrapped breast lobules and infiltrative growth, making diagnosis more difficult. Recognition of classic features, absence of a fibroepithelial lesion, and loss of *PRKAR1A* expression are helpful diagnostic clues.

78 Prediction of Homologous Recombination Deficiency of Breast Carcinomas on Digitalized HE Slides Using Machine and Deep Learning Approaches

Guillaume Bataillon¹, Anne Vincent-Salomon¹, Thomas Walter¹, Marc-Henri Stern¹, Peter Naylor¹, Youlia Kirova¹, Tristan Lazard¹, Etienne Decenciere², François Clément Bidard¹, Dominique Stoppa-Lyonnet¹

¹Institut Curie, Paris, France, ²Paris, France

Disclosures: Guillaume Bataillon: None; Anne Vincent-Salomon: None; Thomas Walter: None; Marc-Henri Stern: *Primary Investigator*, Myriad Genetics; Peter Naylor: None; Youlia Kirova: None; Tristan Lazard: None; Etienne Decenciere: None; François Clément Bidard: None; Dominique Stoppa-Lyonnet: None

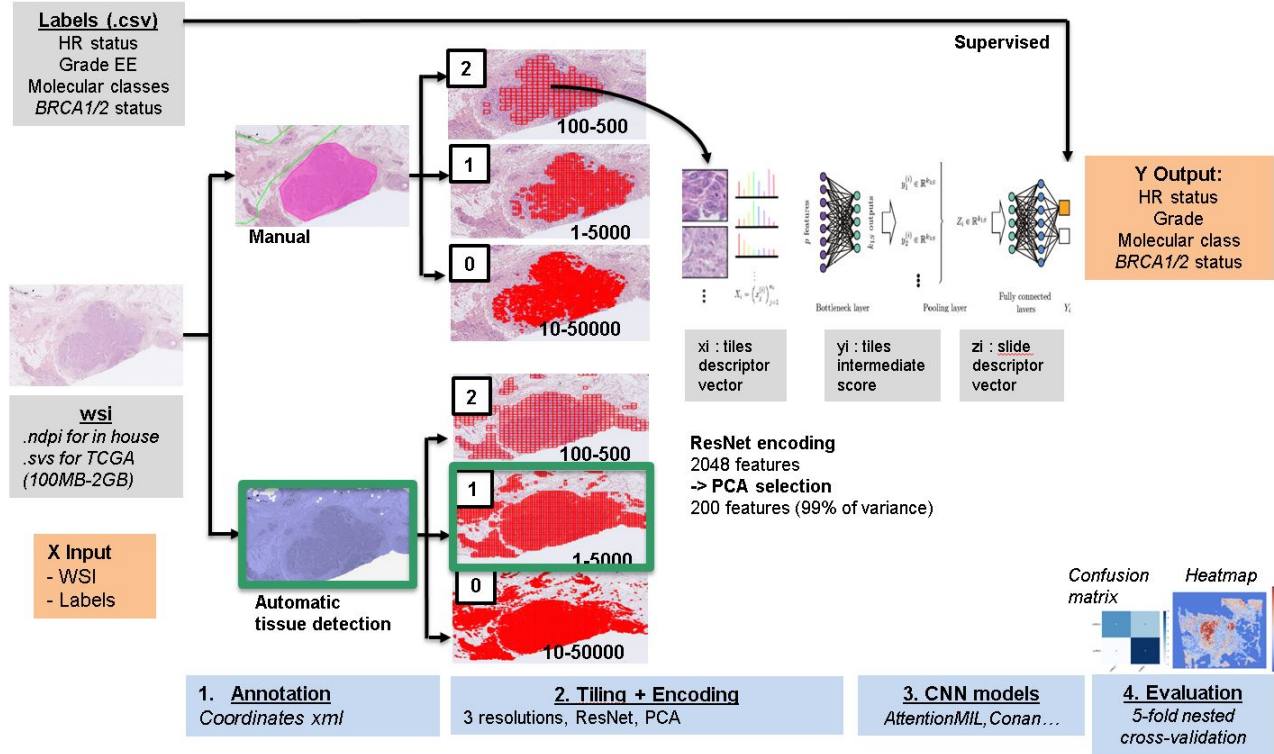
Background: In breast cancer (BC), neither a specific phenotype nor a morphological pattern is known to reliably assess the presence of homologous recombination deficiency (HRD) at the genomic level. Identifying HRD in triple negative (TN) and luminal B (LB) could help to better select the target group for platinum salts and PARP inhibitors (PARPi). However, systematic assessment of HRD by screening for *BRCA1/2* mutations for all LB and TNBC representing 35% and 15 % of all BC respectively does not seem a feasible strategy today. We hypothesized that

image analysis could be a cost-effective tool to associate complex features of tissue organization with genomic alterations. In this study, we present an image-based approach to predict HR status, grade, molecular class of BC from Hematoxylin Eosin (HE) slides using deep learning.

Design: We use stratified K-fold (K = 5) nested cross-validation using a total of n=1628 whole slide images (WSI) HE stained with molecular associated data from two independent datasets (In-house, n=813 patients; and The Cancer Genome Atlas (TCGA), n=815 patients). These two datasets encompass annotations of HRD status, set by LST signature of Popova *et al* (998 LST low and 630 LST “high”), molecular class (1178 luminal; 450 TN) and germline *BRCA* (*gBRCA*) status (236 *gBRCA1*; 216 *gBRCA2*). After splitting the WSI into tiles and encoding them with ResNet50 trained on ImageNet, we use several convolutional neural networks approaches: AttentionMIL (Isle *et al*), CHOWDER (Courtiol *et al*), Self-attention mechanism (Li *et al*) and CONAN (in house model) to predict the labels (Figure1).

Results: We first assessed the prediction of HR status. On Luminal AFA-fixed tumors subgroup of in-house dataset, the accuracy was $0,68 \pm 0,06$ with an area under the curve (AUC) of $0,78 \pm 0,05$. In TCGA cohort the results were not significantly different from random. Conversely, our network was able to predict molecular class with an accuracy of $0,70 \pm 0,05$ and an AUC of $0,76 \pm 0,07$ on TCGA and an accuracy of $0,8 \pm 0,04$ with an AUC of $0,89 \pm 0,05$ on in-house cohorts. Furthermore, on in-house cohort, the identification of *gBRCA1/2* mutations demonstrated an accuracy of $0,68 \pm 0,03$ and an AUC of $0,73 \pm 0,06$ and separated grade 1 and 3 with an accuracy of $0,81 \pm 0,09$ and an AUC of

Figure 1 - 78



Conclusions: Our results show that there is a clear link between tissue phenotype and HR status. HR status may be assessed from tissue data, albeit with an accuracy that would need to be improved to be used in clinical practice. The discrepancy between results obtained between TCGA and in-house datasets demonstrates that for complicated prediction tasks going beyond a pure automatization of a pathologist’s assessment, it is essential to use curated data where the effect of potential confounders can be controlled. Larger cohorts will improve these encouraging results, paving the way to a simple, cheap and reliable biological stratification for breast cancers to undergo genomic analysis.

79 Clinical Usefulness of 3-Tiered WHO Classification of Phyllodes Tumor Versus SGH Nomogram

Davsheen Bedi¹, Beth Clark², Gloria Carter², Jing Yu³, Jeffrey Fine³, Tatiana Villatoro¹, Rohit Bhargava²
¹University of Pittsburgh Medical Center, Pittsburgh, PA, ²UPMC Magee-Womens Hospital, Pittsburgh, PA, ³University of Pittsburgh, Pittsburgh, PA

Disclosures: Davsheen Bedi: None; Beth Clark: None; Gloria Carter: None; Jing Yu: None; Jeffrey Fine: *Stock Ownership*, SplIntellx, Inc.; Tatiana Villatoro: None; Rohit Bhargava: *Advisory Board Member*, Eli Lilly & Company

Background: Phyllodes tumors (PT) are categorized by World Health Organization (WHO) classification of tumors as benign, borderline, and malignant. A study conducted at the Singapore General Hospital (SGH) by Tan et al developed a recurrence risk assessment tool, which calculates a nomogram score based on three histological criteria (cytological Atypia, Mitosis and stromal Overgrowth) and the Surgical margin status (AMOS criteria). This score helps predict recurrence free survival in patients with diagnosis of PT. We aimed to compare the clinical usefulness of SGH nomogram with the WHO classification.

Design: We identified 270 cases of PT (15 year period) with available information to calculate the nomogram score. The data was extracted from pathology reports. Slides were reviewed for cases with missing information for calculation of nomogram scores. Recurrence data was obtained from electronic medical records. Average nomogram scores for each of the WHO classes with respect to surgical margin status were compared. Recurrence rate for WHO classes is reported. The PTs with and without recurrence were compared for each of the nomogram components, age, and tumor size.

Results: Of the 270 total cases, 195 (72%) were classified as benign, 49 (18%) as borderline, and 26 (10%) as malignant. Final surgical margin status was positive in 39% of benign, 14% of borderline and 0% of malignant cases. For PTs with negative margins, the average SGH nomogram scores were 4.5 for benign, 14.7 for borderline, and 32.1 for malignant. For PTs with positive margins, the average SGH nomogram scores were 43.8 for benign and 54.3 for borderline. The recurrence rate was 2.3% for benign (average follow up of 49 months), 4.3% for borderline (average follow up of 62 months), and 25% for malignant (average follow up of 44 months). The difference was statistically significant (benign vs malignant p-value: 0.0002). Follow up data was available on 246 cases. Cases that recurred (n=12) and cases without recurrence (n=234) are compared in table 1.

Table 1: Comparison of cases that recurred versus cases without recurrence

	Recurred (n=12)	No recurrence (n=234)	p-value
Atypia			
Mild	6	171	Reference
Moderate	3	47	0.4167
Marked	3	16	0.0448
Mitosis/10 hpf			
Mean	15.7	3.7	<0.0001
Stromal Overgrowth			
Absent	6	206	0.0023
Present	6	28	
Surgical margin			
Negative	11	158	0.1107
Positive	1	76	
Nomogram score, mean			
All cases	23.83	21.25	0.6454
Excluding benign	29.25	23.48	0.3389
Only malignant	36.17	31.17	0.3316
Age in years			
Mean	50	39	0.0201
Tumor size in cm			
Mean	8.5	4.1	0.0009
WHO Classification			
Benign	4	172	Reference
Borderline	2	44	0.6064
Malignant	6	18	0.0002

Conclusions: Despite positive margin status, benign PTs only rarely recur and therefore utility of SGH nomogram is limited in such cases. Other features of nomogram (atypia, mitosis, and overgrowth) are important in determining recurrence but are also used for WHO classification. Older age and larger tumor size are associated with recurrence, but both of these parameters are more commonly observed with malignant PT (data not shown). WHO 3-tiered classification is clinically useful, with SGH nomogram possibly useful in select cases.

80 MYB RNA in situ Hybridization is a Useful Tool to Distinguish Breast Adenoid Cystic Carcinoma From Other Triple Negative Breast Carcinomas

Monica Butcher¹, Lisa Rooper¹, Pete Argani², Marissa White³, Ashley Cimino-Mathews³

¹The Johns Hopkins Hospital, Baltimore, MD, ²Johns Hopkins Hospital, Ellicott City, MD, ³Johns Hopkins University School of Medicine, Baltimore, MD

Disclosures: Monica Butcher: None; Lisa Rooper: None; Pete Argani: None; Marissa White: None; Ashley Cimino-Mathews: None

Background: Breast adenoid cystic carcinoma (AdCC) has overlapping immunophenotypic and histologic features with basal-like triple negative ductal carcinomas (TNBC). However, breast AdCC has a more favorable clinical course, making the distinction critical for patient treatment and prognosis. Similar to salivary gland AdCC, breast AdCC demonstrates recurrent genomic alterations including t(6;9) *MYB-NFIB* gene fusion, *MYB* gene amplification, and *MYBL1* gene rearrangement, which can be confirmed by fluorescence in situ hybridization (FISH). We previously showed that immunohistochemistry (IHC) for *MYB* is a sensitive marker for breast AdCC (Am J Surg Pathol. 2017;41:973-9). A novel assay, chromogenic RNA ISH for *MYB*, has emerged having equivalent sensitivity and superior specificity for salivary gland AdCC compared to *MYB* IHC. Here, we evaluate *MYB* RNA ISH in invasive ductal carcinomas (IDC), with an emphasis on basal-like TNBC.

Design: Recent cases (2019-2020) of breast AdCC in which *MYB* RNA ISH was performed were identified in the pathology archives. *MYB* RNA ISH was performed with a commercially available probe (Advanced Cell Diagnostics, Hayward, CA) on previously-constructed tissue microarrays containing 78 evaluable IDC, including 30 basal-like TNBC (EGFR+ and/or CK5/6+), 19 luminal A (ER+/HER2-), 12 HER2+ (ER-/HER2+), 11 non-basal-like TNBC, and 6 luminal B (ER+/HER2+). Control RNA ISH for the housekeeping gene *PPIB* was performed on all cases. *MYB* RNA ISH overexpression was defined as >3 punctate signals or 1 large clumped signal in the nucleus or cytoplasm of >30% of tumor cells, with rare single signals considered negative. Half (50%, n=15/30) of the basal-like TNBC were previously evaluated by *MYB* IHC and FISH (Am J Surg Pathol. 2017;41:973-9).

Results: *MYB* RNA ISH overexpression was seen in 100% (n=5/5) of breast AdCC and 10% (n=8/78) of IDC (p<0.0001). Specifically, *MYB* RNA ISH overexpression was seen in 37% (n=7/19) of luminal A and 8% (n=1/12) HER2+ IDC, and in no cases of basal-like TNBC, non-basal-like TNBC, or luminal B IDC. *MYB* RNA ISH signals were strong and diffuse in AdCC but focal in IDC. Confirmatory *MYB* FISH was performed as part of the diagnostic evaluation of two AdCC, both of which demonstrated *MYB* gene rearrangement. As previously reported, *MYB* IHC was positive in 60% (n=9/15) of basal-like TNBC, with *MYB* rearrangement detected in 7% (n=1/15).

Figure 1 - 80

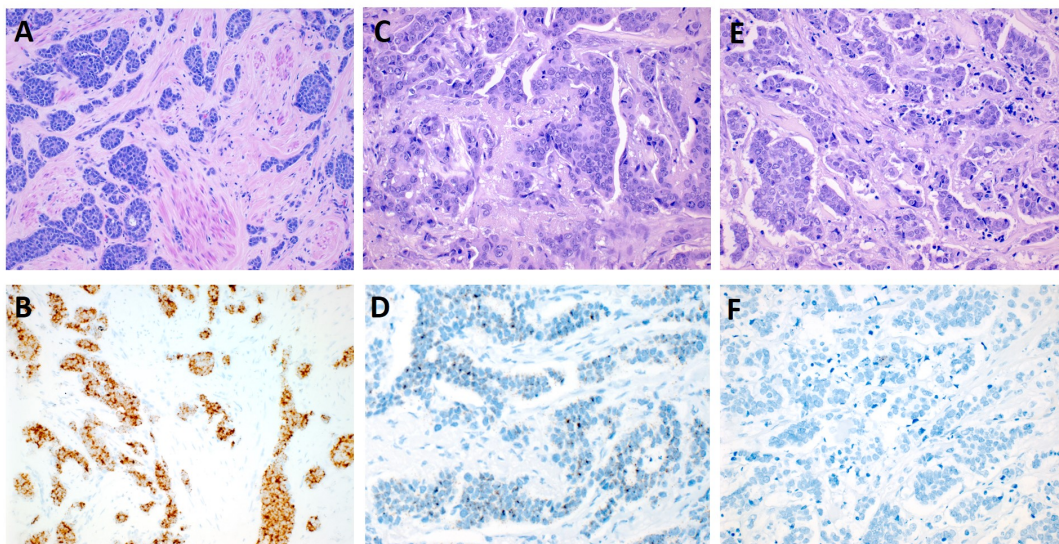


Figure 1: MYB RNA in-situ hybridization (ISH). Overexpression of MYB by RNA ISH was present in all cases of adenoid cystic carcinoma (A & B, H&E and MYB RNA ISH, 64x) and approximately one-third of infiltrating ductal carcinomas with a luminal A phenotype (C & D, H&E and MYB RNA ISH, 100x). No case of basal-like triple negative breast carcinoma showed overexpression (E & F, H&E and MYB RNA ISH, 100x).

Conclusions: MYB RNA ISH is equally sensitive but has superior specificity for breast AdCC compared to MYB IHC and FISH, with MYB RNA ISH labeling seen in a notable subset of luminal A IDC but no basal-like TNBC. The potential significance of MYB RNA ISH labeling in luminal A carcinomas merits further evaluation; interestingly, MYB is postulated to play a role in DNA damage repair in ER+ breast cancer (Oncogene. 2019;38:5239-49). MYB RNA ISH is sensitive and specific for breast AdCC and could be a useful, rapid diagnostic adjunct in the work-up of a TNBC in the breast.

81 Effect of Testosterone Therapy in Transgender Female-to-Male Mastectomies

Manita Chaum¹, Jiaxi Chen¹, Vivian Hu², Edward Ray¹, Ashley Marumoto¹, Stephanie Angarita³, Armando Giuliano¹, Shikha Bose¹

¹Cedars-Sinai Medical Center, West Hollywood, CA, ²David Geffen School of Medicine at UCLA, Los Angeles, CA, ³Cedars-Sinai Medical Center, Los Angeles, CA

Disclosures: Manita Chaum: None; Vivian Hu: None; Edward Ray: None; Ashley Marumoto: None; Stephanie Angarita: None; Shikha Bose: None

Background: Gender assigning surgeries are increasing in number. Testosterone therapy (TT) and bilateral mastectomies are part of the female-to-male reassignment process. Increasing female transgender individuals are initiating testosterone for masculinization before proceeding to mastectomy to affirm their gender identity. To date, the histopathologic effects on breast tissue from exogenous androgen and the interplay with endogenous female hormones in the breast are poorly understood. In this study we document the histopathologic findings in transgender female-to-male mastectomies (FTMM) and also investigate the effects of TT on estrogen receptors (ER) and androgen receptors (AR) in the breast tissue.

Design: After IRB approval, 66 cases of FTMM were retrieved from the department files between the period of 10.26.17 to 5.5.20. All patients had TT prior to FTMM. A control group of age matched 66 women who underwent reduction mastectomies (RM) were also retrieved. Patient demographics and duration of TT was recorded. Pathology slides were reviewed. The histologic findings and number of sections submitted were recorded. In addition immunohistochemistry for AR and ER was performed in 15 cases, 5 each of RM without TT (group 1), FTMM with 12 months TT (group 2) and FTMM with greater than 60 months TT (group 3). The overall positivity rate and receptor intensity were assessed.

Results: In comparison to RM, FTMM revealed dense fibrotic stroma, lobular atrophy, thickened lobular basement membranes, and gynecomastoid changes (Fig. 1). Findings were more marked in group 3. Incidence of atypia or cancer was much lower in the FTMM, in spite of a greater number of sections (2.5x) being examined (Table1).

ER and AR expression were similar in groups 1 and 2 but increased expression was noted in group 3 (Fig. 2). In addition stromal cells in groups 2 and 3 were noted to stain positive for AR (Fig. 2).

	Mean age, years	Average Breast Sections per Case	Number of Cases with Atypia (%)	Number of Cases with Malignancy (%)
Female-to-Male Mastectomy (n=66)	25.6	30	1/66 (1.5)	0/66 (0)
Reduction Mammoplasty (n=66)	25.5	12	3/66 (4.5)	0/66 (0)

Figure 1 - 81

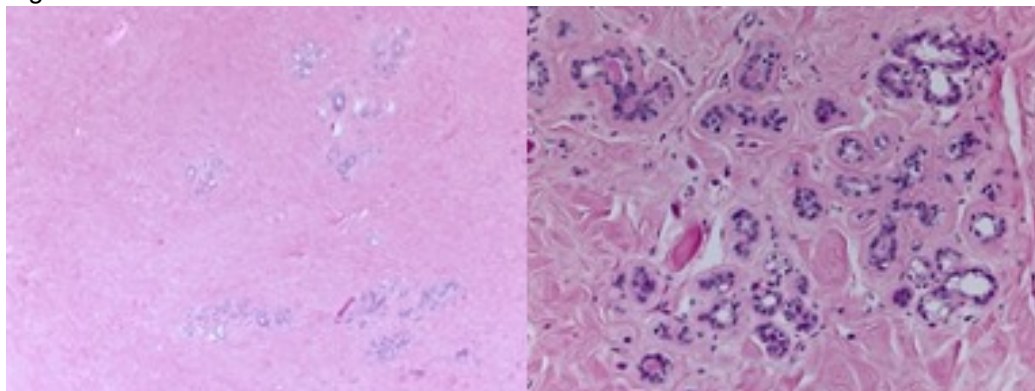
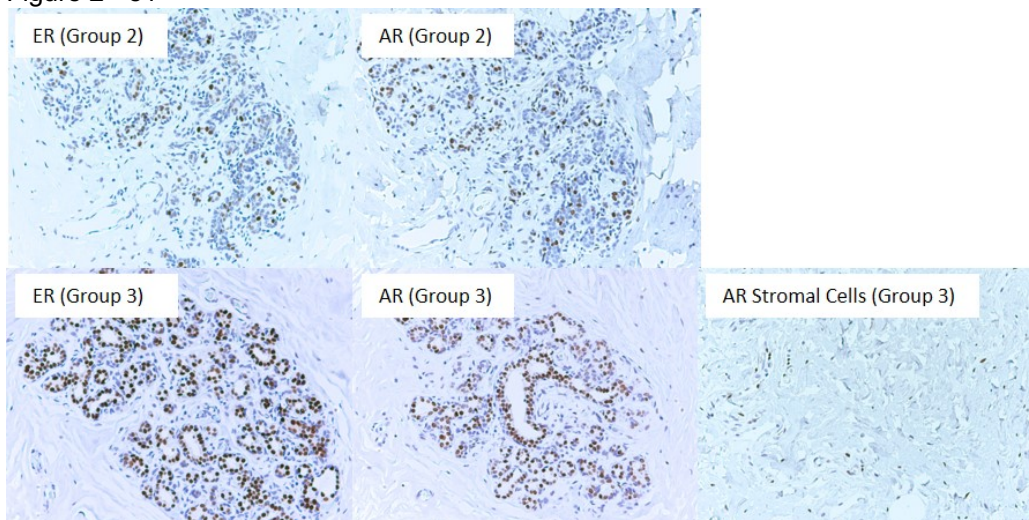


Figure 2 - 81



- Conclusions:**
1. Testosterone causes lobular atrophy and gynecomastoid changes in breast parenchyma
 2. Incidence of atypia/carcinoma is very low. Routine examination of a large number of sections is not required.

3. ER and AR are expressed more strongly in lobular epithelium in patients on prolonged TT. AR positivity is also noted in stromal cells in patients on TT. We postulate that TT induces stromal fibrosis in the breast leading to lobular atrophy. Additional studies are needed to confirm these findings.

82 Computerized Measurements of Nuclear Morphology Features, Mitosis Rate, and Tubule Formation from H&E Images Predicts Recurrence-Free Survival in ER+ & LN- Invasive Breast Cancer: A Multi-Institutional Study

Yuli Chen¹, Haojia Li¹, Andrew Janowczyk², Can Koyuncu¹, Paula Toro², German Corredor², Jon Whitney², Cheng Lu², Shridar Ganesan³, Michael Feldman⁴, Pingfu Fu², Hannah Gilmore⁵, Aparna Harbhajanka⁶, Haley Sechrist⁷, Sangeeta Desai⁸, Vani Parmar⁸, Anant Madabhushi²

¹CCIPD, Case Western Reserve University, Cleveland, OH, ²Case Western Reserve University, Cleveland, OH, ³Rutgers Cancer Institute of New Jersey, New Brunswick, NJ, ⁴University of Pennsylvania, Wilmington, ⁵University Hospitals Case Medical Center, Case Western Reserve University, Cleveland, OH, ⁶Case Western Reserve University/University Hospitals Cleveland Medical Center, Cleveland, OH, ⁷Case Western Reserve University School of Medicine, Cleveland, OH, ⁸Tata Memorial Centre, Mumbai, India

Disclosures: Yuli Chen: None; Haojia Li: None; Andrew Janowczyk: None; Can Koyuncu: None; Paula Toro: None; German Corredor: None; Jon Whitney: None; Cheng Lu: None; Shridar Ganesan: *Consultant, Merck; Consultant, Foundation Medicine; Employee, Merck; Advisory Board Member, Silagene; Consultant, Roche*; Michael Feldman: None; Pingfu Fu: None; Hannah Gilmore: None; Aparna Harbhajanka: None; Haley Sechrist: None; Sangeeta Desai: None; Vani Parmar: None; Anant Madabhushi: *Advisory Board Member, Aiforia Inc; Primary Investigator, Bristol Myers-Squibb; Primary Investigator, Astrazeneca*

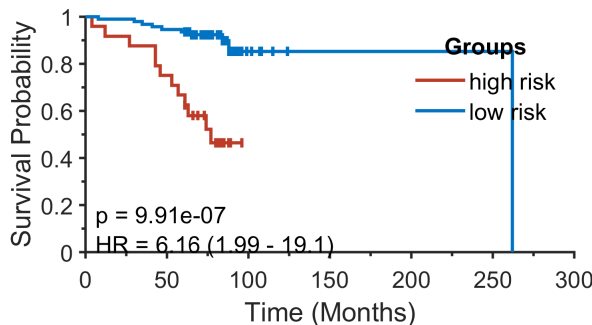
Background: Estrogen receptor-positive (ER+) lymph node negative (LN-) Invasive Breast Cancer (IBC) is the most common subtype of IBC in the United States. Given the significant side effects of adjuvant chemotherapy, it is critical to identify ER+ & LN- breast cancer patients at a lower risk of recurrence, who are unlikely to benefit from chemotherapy. Complying with the modified Bloom–Richardson grading scheme, we computationally extracted quantitative histomorphometric features relating to nuclear morphology, mitotic counts, and tubule formation, and associated them with recurrence-free survival (RFS) in ER+ & LN- IBC.

Design: H&E-stained whole slide images from a cohort of 116 patients (22 recurrences), diagnosed with early-stage ER+ & LN- IBC, and treated at University Hospital Cleveland Medical Center, Cleveland, Ohio, USA, were retrospectively collected and used as training set D1. All censored patients without recurrence have at least ten-year follow-up. 84 ER+ & LN- breast cancer patients (21 recurrences) treated at Indian Tata Memorial Hospital, Mumbai, India constituted an independent testing set D2 (see Table 1). Three different deep learning models were respectively employed to detect nuclei, mitosis, and tubules. Subsequently, features relating to nuclear morphology (e.g. spatial distribution, shape, texture, orientation entropy), mitotic features (e.g. mitosis hotspot, mitotic rates), and tubule formation (e.g. tubular nuclei distribution, tubule rate entropy) were computationally extracted for each individual patient. A lasso regularized Cox regression model (named M_{NMT}) was employed to identify the 12 (~10% of patient number in D1) most predictive features of RFS and generate a continuous risk score. The optimal risk threshold was identified on D1 to dichotomize risk scores into high vs. low risk categories. M_{NMT} was subsequently validated on D2 and a Kaplan-Meier Survival analysis was performed.

Results: The top 12 features employed by M_{NMT} included nuclei morphology, tubule formation, and mitosis counts. Patients identified by M_{NMT} as high risk had significantly worse prognosis in terms of RFS with a Hazard Ratio of 6.16 ($p=9.91e-07$, 95% CI=1.99~19.1) in D1 (Figure 1) and HR=3.2 ($p=0.00464$, 95% CI=1.14~8.95) in D2 (Figure 2) from the log-rank test, respectively.

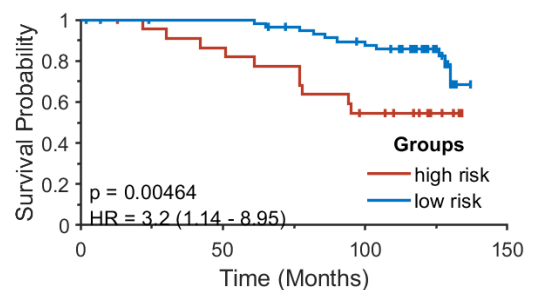
Clinical Variables	Training set D1 (UH)	Validation set D2 (Tata)
	N(%)	N(%)
No. of patients	116	84
Age	59.7±10.4	50.4±10.4
>=50 yrs.	99(85%)	40(48%)
< 50 yrs.	17(15%)	44(52%)
Race		
Caucasian	89(77%)	0(0%)
Africa American	26(22%)	0(0%)
Indian	0(0%)	84(100%)
other	1(1%)	0(0%)
PR status		
Positive	98(84%)	72(86%)
Negative	17(15%)	12(14%)
Unknown	1(1%)	0(0%)
Her2 status		
Positive	1(1%)	0(0%)
Negative	113(97%)	84(100%)
Unknown	2(2%)	0(0%)
Tumor Grade		
Grade 1	26(22%)	1(1%)
Grade 2	72(62%)	30(36%)
Grade 3	18(16%)	53(63%)
unknown	0(0%)	0(0%)
Tumor size		
<=2cm	75(65%)	17(20%)
>2cm	40(34%)	60(72%)
unknown	1(1%)	7(8%)
Chemotherapy		
Yes	32(28%)	57(68%)
No	82(71%)	6(7%)
unknown	2(1%)	21(25%)
Recurrence status		
Recurrent	22(19%)	21(25%)
Non-recurrent	90(78%)	51(61%)
unknown	4(3%)	12(14%)

Figure 1 - 82



high risk	24	18	0	0	0	0	0
low risk	92	87	6	1	1	1	0

Figure 2 - 82



high risk	23	19	11	0
low risk	61	58	49	0

Conclusions: We introduced a prognostic model based on the combined features of nuclear morphology, mitosis count, and tubule formation that can help distinguish patients with early-stage ER+ & LN- IBC at a higher risk of recurrence from those experiencing longer RFS.

83 Nodular Fasciitis of the Breast: Clinicopathologic and Molecular Analysis of 12 Cases with Identification of Novel USP6 Fusion Partners

Jeffrey Cloutier¹, Christian Kunder¹, Gregory Charville¹, Elizabeth Hosfield², Richard Sibley³, Robert West⁴, Megan Troxell³, Kimberly Allison¹, Gregory Bean¹

¹Stanford Medicine/Stanford University, Stanford, CA, ²Permanente Medicine, San Francisco, CA, ³Stanford University Medical Center, Stanford, CA, ⁴Stanford University, Stanford, CA

Disclosures: Jeffrey Cloutier: None; Christian Kunder: None; Gregory Charville: None; Elizabeth Hosfield: None; Richard Sibley: None; Robert West: None; Megan Troxell: None; Kimberly Allison: None; Gregory Bean: None

Background: Nodular fasciitis (NF) is a benign self-limited myofibroblastic neoplasm with the potential to mimic malignancy owing to its rapid growth, cellularity and mitotic activity. Most commonly NF occurs in the subcutaneous tissue of the extremities, trunk, and head and neck; there are only rare reports of involvement of mammary tissue.

Design: As the largest individual series to date, 12 cases of NF involving the breast were collected. Each case was reviewed by at least 2 soft tissue pathologists, and the clinicopathologic features were recorded. Targeted RNA sequencing-based fusion analysis was performed on 11 cases.

Results: All patients were female, with median age at diagnosis of 35 years (range 15-61). The tumors ranged in size from 0.4 to 5.8 cm (median 0.9). Three patients presented with skin retraction, and two occurred near the axilla. One patient reported preceding trauma, and another occurred during pregnancy. All tumors showed characteristic histologic features of NF, including bland myofibroblastic spindle cells, variably myxoid stroma and extravasated erythrocytes. Mitotic figures ranged from 1 to 12 per 10 high-power fields (median 3). Focal infiltration into adipose tissue was common (n=10); in 4 cases, the tumor abutted (n=2) or infiltrated (n=2) breast epithelium. Immunohistochemically, lesional cells expressed SMA (10/10) and were negative for pan-cytokeratin (0/8), p63 (0/8), desmin (0/9), CD34 (0/10), S100 (0/9) and nuclear β -catenin (0/5). RNA fusion analysis on 11 cases revealed *USP6* rearrangements in 7, including the canonical *MYH9-USP6* in 3 cases. Three novel gene fusions were identified, including *NACA-USP6*, *SLFN11-USP6* and *LDHA-USP6*. Another case harbored a previously reported rare alternative fusion, *CTNNB1-USP6*. All fusions juxtaposed the 5' partner's promoter with the entire coding sequence of *USP6*. *USP6* rearrangement was confirmed by FISH in the 12th case. Outcome data were available for 9 patients, with a median duration of 60 months (range 8 to 108). Seven patients underwent surgical excision, and 2 patients received no treatment after diagnosis on core biopsy. No patient developed a recurrence, and no tumors metastasized.

Conclusions: Albeit uncommon, NF should be considered in the differential diagnosis of breast spindle cell lesions. A broad immunohistochemical panel may be required to rule out histologic mimics, including metaplastic carcinoma. Detection of *USP6* rearrangement would support the diagnosis of NF, which has potential therapeutic implications.

84 Does HER2 Affect CDK4/6 Pathway Activity in Breast Cancer?

Xiaoyan Cui¹, William Sinclair²

¹The Ohio State University, Columbus, OH, ²The Ohio State University Wexner Medical Center, Columbus, OH

Disclosures: Xiaoyan Cui: None; William Sinclair: None

Background: Cyclin D1-CDK4/6-pRb is the pathway to promote progression of the cell cycle from G1 to S phase that resulting in cell proliferation. CDK4/6 inhibitors bind to CDK4/6 thus prevent cancer progression. Clinically, they have proven to be beneficial for ER+ breast cancer, especially when combined with anti-estrogen therapies. The relationship of HER2 and cyclin D1-CDK4/6-pRb pathway has not been well characterized. In this study, phosphorylated Rb (pRb) was used as an index for CDK4/6 activation and its expression to HER2 expression as well as gene copy number were studied.

Design: 130 cases of breast biopsies with invasive carcinoma were collected, including 77 cases of HER2+ (39 cases of ER+PR±HER2+ and 38 cases of ER-PR-HER2+) and 53 cases of HER2- (ER-PR-HER2-). Immunostain

of pRb was performed and quantified by H-score (intensity x percentage of positive cells), with the intensity scored as 0, 1, 2 and 3 (no stain, weak, moderate and strong, respectively).

Results: For all cases, the H-score ranges from 3 to 270 (Table 1). The average H-score for the ER-PR-HER2-, ER-PR-HER2+, and ER+PR±HER2+ groups was 61.5 ± 18.1 , 115.82 ± 25.0 , and 93.1 ± 22.2 , respectively. For all HER2+ cases, the average score was 104.5 ± 16.7 , which is significantly higher than HER2- cases ($p=0.001$). There is no significant difference between the two HER2+ subgroups (Figure 1). When evaluating the HER2 gene copy numbers with their corresponding H-scores, there was a trend of positive correlation, i.e. higher HER2 copy number with higher H-score, although not statistically significant ($r=0.2$, $p=0.09$) (Figure 2).

H-score	1-100	101-200	201-300	Total case number
ER-PR-HER2+	20 (52.6%)	12 (31.6%)	6 (15.8%)	38
ER+PR±HER2+	22 (56.4%)	15 (38.5%)	2 (5.1%)	39
ER-PR-HER2-	42 (79.2%)	8 (15.1%)	3 (5.7%)	53

Figure 1 - 84

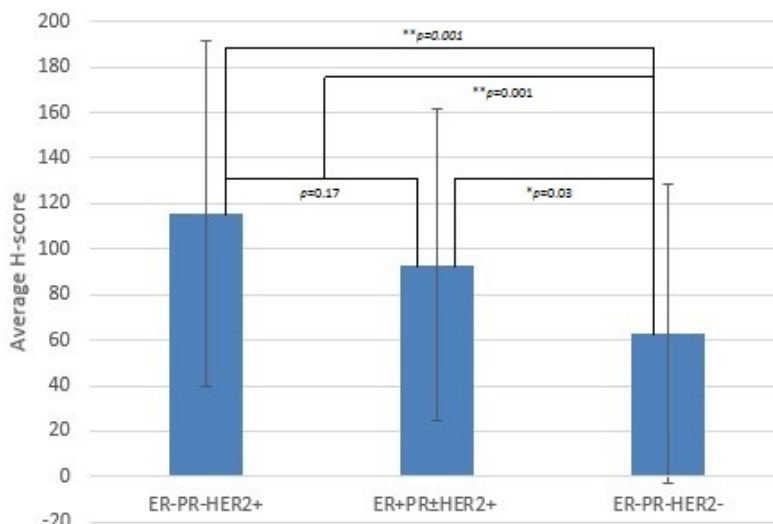
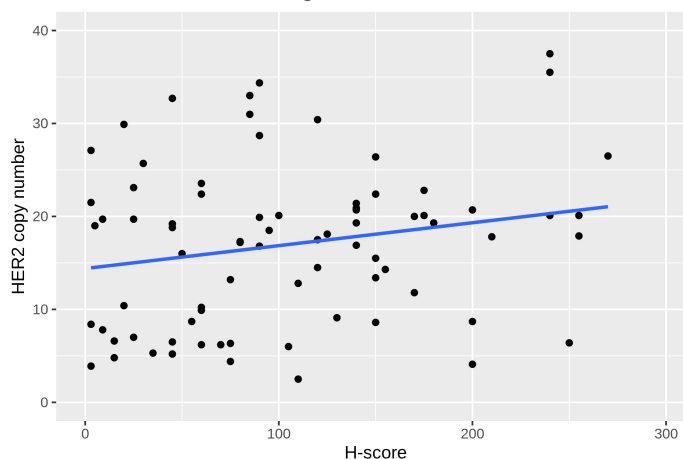


Figure 2 - 84



Conclusions: The significant higher levels of pRb expression in HER2+ group suggests that increased HER2 expression may lead to CDK4/6 pathway activation. The trend of positive correlation between HER2 gene copy number and pRb expression provides further evidence. This indicates the potential effects of CDK4/6 inhibitors in treating HER2+ breast cancer as well as the possible synergistic effects of HER2-targeted therapy and CDK4/6 inhibitors. Future study of pRb expression in relation to response to CDK4/6 inhibitors may be important to confirm if pRb can be used as a predicative biomarker to CDK4/6 inhibitors treatment. Of interest, few ER-PR-HER2- cases also have higher H-scores (7.5%, H-score \geq 200). If confirmed, these patients may also respond to CDK4/6 inhibitors.

85 Measurement of Tumour Nuclear Area by Artificial Intelligence is Associated with Residual Cancer Burden Index After Neoadjuvant Chemotherapy in Estrogen Receptor Positive Breast Cancer

David Dodington¹, Andrew Lagree², Sami Tabbarah², Majidreza Mohebpour², Ali Sadeghi-Naini³, William Tran⁴, Fang-I Lu⁴

¹University of Toronto, Toronto, Canada, ²Sunnybrook Research Institute, Toronto, Canada, ³Sunnybrook Health Sciences Centre, Toronto, Canada, ⁴Sunnybrook Health Sciences Centre, University of Toronto, Toronto, Canada

Disclosures: David Dodington: None; Andrew Lagree: None; Sami Tabbarah: None; Majidreza Mohebpour: None; Ali Sadeghi-Naini: None; William Tran: None; Fang-I Lu: None

Background: Neoadjuvant chemotherapy (NAC) is commonly used to treat patients with high risk or locally advanced breast cancer. Despite advances in treatment, predicting how a patient will respond to NAC remains a significant clinical challenge. While some patients experience a pathological complete response (defined as complete eradication of tumour), many will have residual disease, which can be quantified using the residual cancer burden (RCB) index. RCB index has also been shown to predict long-term survival after NAC in all molecular subtypes of breast cancer. The objective of this study was to determine if tumour nuclear features in pre-treatment biopsies were associated with RCB index after NAC.

Design: From a retrospective cohort of breast cancer patients, H&E-stained breast core biopsies were selected from 36 patients who had residual disease after NAC. Multiple deep convolutional neural networks were developed to automate tumor bed detection and nuclear segmentation. Nuclear count and morphological nuclear features including nuclear area and circularity were computed. Image-based first and second-order features including mean pixel intensity and grey level co-occurrence matrix (GLCM) features were determined.

Results: The cohort consisted of ER-positive tumours (n = 26) and ER-negative tumours (n = 10). RCB index ranged from 0.64 to 3.88 (RCB Class 1: n = 11, RCB Class II: n = 18, RCB Class III: n = 7). Clinicopathological variables including age, menopausal status, tumour size/extent, lymph node involvement, histologic grade, and HER2 status were not associated with the RCB index. For ER-positive tumours, nuclear area was strongly and inversely correlated with the RCB index (R = - 0.57, R² = 0.33, p = 0.002). Nuclear count, circularity, intensity and GLCM texture features were not significantly associated with RCB index. Among ER-negative tumours, none of the AI-determined nuclear features, including nuclear area, were associated with the RCB index.

Conclusions: Tumour nuclear area in pre-treatment biopsies is inversely associated with the RCB index in ER-positive breast cancer. Assessment of nuclear features using AI is a promising tool for predicting the response to NAC in order to better guide clinical decision-making.

86 RANK Expression is Associated with Better Overall Survival in Triple-Negative Breast Carcinoma

Darin Dolezal¹, Kamaljeet Singh², Wael Ibrahim³, Lori Charette³, Marguerite Pinto⁴, Malini Harigopal¹

¹Yale School of Medicine, New Haven, CT, ²Women and Infants Hospital, Providence, RI, ³Yale New Haven Hospital, New Haven, CT, ⁴Yale University, New Haven, CT

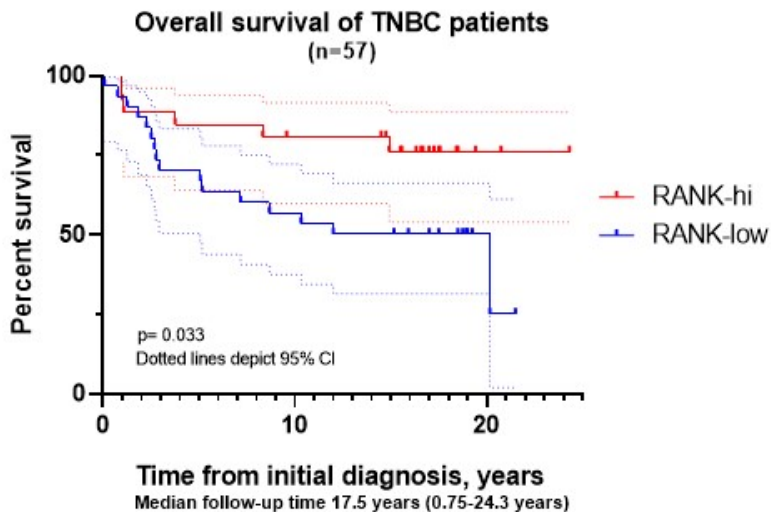
Disclosures: Darin Dolezal: None; Kamaljeet Singh: None; Wael Ibrahim: None; Lori Charette: None; Marguerite Pinto: None; Malini Harigopal: None

Background: The use of the RANK-L-inhibitor denosumab in the adjuvant setting for early-stage breast cancer remains uncertain. Although RANK expression has been observed in poorly differentiated and triple negative breast carcinoma (TNBC), the roles of RANK and RANK-L in TNBC have been largely unexplored. We assessed the possible associations between RANK/RANK-L upregulation in TNBC and overall patient survival (OS).

Design: RANK and RANK-L expression by IHC was assessed in 71 primary breast carcinomas using a tissue microarray (TMA) enriched for TNBC (n=57). Histologic subtypes of TNBCs included IDC (non-specific type NST, n=45), metaplastic breast carcinoma (adenosquamous carcinoma (ASC), n=4; MBC with matrix production, n=1), and carcinoma with medullary features (CMF, n=7). For comparison we assessed expression in 14 cases of Luminal A or B IDC-NST. RANK and RANK-L were evaluated by H-score (score range=0-300). RANK-L expression was not detected in tumor cells from any TNBC case; faint RANK-L expression could be seen in the blood vessels only. OS rate was assessed by Kaplan-Meier test; median follow-up time was 17.5 years.

Results: RANK expression was detected in 53 of 57 (93%) TNBC cases (H avg: 108, range: 0-270) and was significantly higher than that seen in Luminal A/B Ca (detected in 10/14, 72%, H avg. 46, range: 0-100; p<.01). RANK expression was significantly higher in poorly-differentiated (PD) TNBC (n=41, H avg: 126, range: 0-270) compared to TNBC with moderately-differentiated (MD) histology (n=16, H avg: 62, range: 0-220; p<.01). TNBC displaying high RANK expression (H>100, n=26; H avg 188) had a significantly better overall survival compared to those displaying low RANK (H≤100, n=31; H avg 41); patients with RANK-hi TNBC had an undefined median OS with median follow-up of 17 years whereas patients with RANK-low TNBC had a median OS of 10.3 years (p=.033)(Figure 1). In special TNBC histologic subtypes, RANK expression was high in all cases of ASC (H avg 173, range 120-220, n=4) and CMF (H avg 210, range 170-270, n=7). Patients with RANK-hi ASC and RANK-hi CMF had favorable outcomes, with no disease recurrences and only one patient death in a median follow-up time of 16.3 years (all patients presented with Stage I or II disease).

Figure 1 - 86



Conclusions: Our results suggest that RANK is significantly upregulated in PD-TNBC relative to MD-TNBC, implying a biological role for RANK in the progression of disease. Robust RANK expression was seen in special types of TNBCs that had favorable outcomes.

87 PD-L1 & Loss of MHC Class I Expression in Breast Cancer: Implications for Immunotherapy

Anna Dusenbery¹, Joseph Maniaci¹, Natalie Hillerson¹, Erik Dill¹, Timothy Bullock¹, Anne Mills¹
¹University of Virginia, Charlottesville, VA

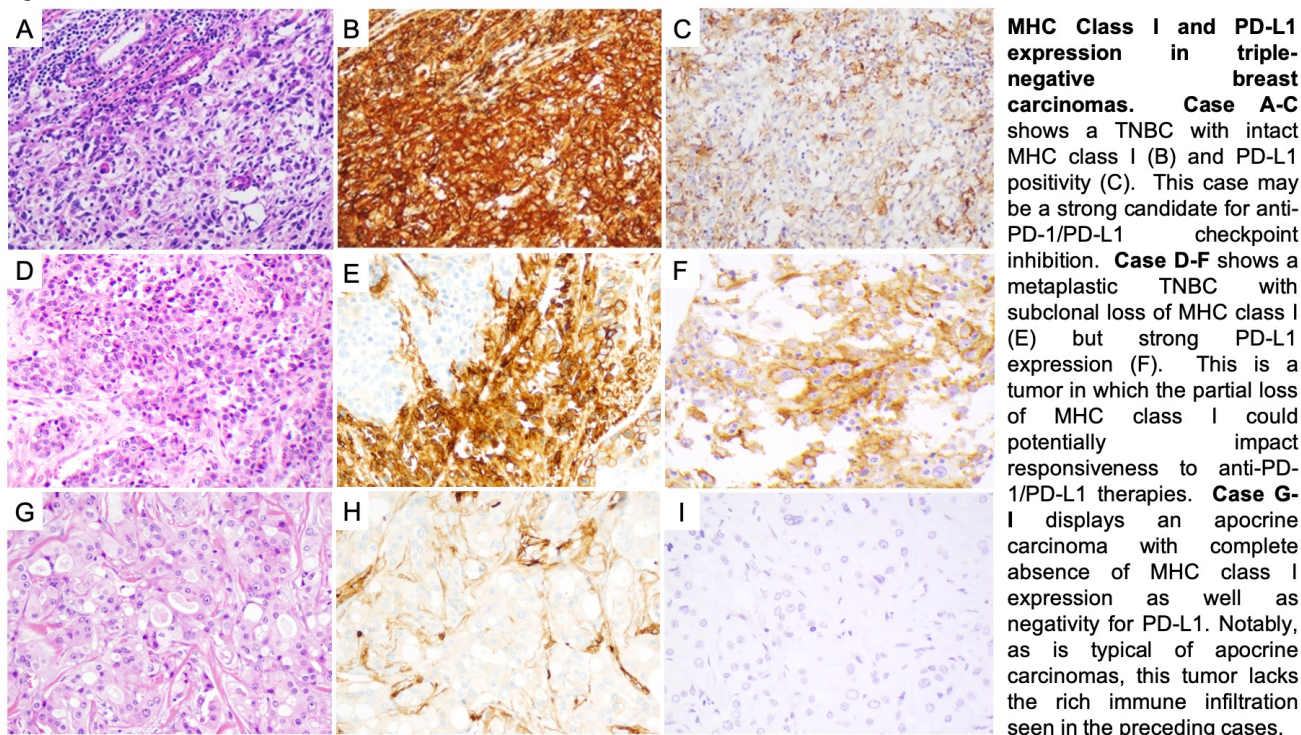
Disclosures: Anna Dusenbery: None; Joseph Maniaci: None; Natalie Hillerson: None; Erik Dill: None; Timothy Bullock: None; Anne Mills: None

Background: Immune modulating drugs such as PD-1/PD-L1 checkpoint inhibitors have promise in a subset of breast cancers, particularly PD-L1-positive triple-negative breast carcinomas (TNBC). However, many PD-L1-positive tumors fail to respond, and additional biomarkers of immunotherapeutic vulnerability are needed. Drugs that enhance the adaptive immune response rely on major histocompatibility complex (MHC) class I for tumor antigen presentation, and its loss has been described in breast cancer. We herein investigate MHC class I expression across a range of breast carcinomas and compare to PD-L1 status.

Design: 117 invasive primary breast carcinomas with a range of histologic subtypes were evaluated on tissue microarrays. Immunohistochemical expression of MHC Class I (clone: EMR8-5) was scored as intact, subclonal loss, or diffuse loss based on the degree of membranous tumoral expression. Results were compared to PD-L1 expression (clone: SP142) using the FDA-approved tumor-infiltrating immune score.

Results: 61% (71/117) of breast cancers demonstrated subclonal or diffuse MHC class I loss, including 49% (23/47) of PD-L1-positive cases and 59% (19/32) of TNBC (Fig 1). Among TNBC, diffuse loss was limited to the apocrine subtype. Diffuse loss was significantly more common in non-TNBC than non-apocrine TNBC [19% (16/85) vs. 0% (0/23)], while subclonal loss was slightly higher in non-apocrine TNBC than non-TNBC [52% (12/23) vs. 42% (36/85)].

Figure 1 - 87



Conclusions: MHC class I loss is common in breast cancers, including nearly half of PD-L1-positive cases, and represents a putative mechanism of immunotherapeutic resistance in this setting. Diffuse loss is more common in immunologically “cold” tumors like non-TNBC and apocrine TNBC, whereas conventional TNBC—which are typically lymphocyte-enriched—most often show subclonal loss. This suggests that the pattern of MHC class I loss

may have significance, with subclonal loss suggesting adaptive evasion of the host immune response and complete loss perhaps indicating a constitutive defect unrelated to the immune microenvironment. Studies evaluating the relationship between MHC class I loss pattern and resistance to anti-PD-1/PD-L1 checkpoint inhibitors will be of interest.

88 Digital Image Analysis of Tumor Immune Microenvironment in Ductal Carcinoma in Situ Reveals Distinct Subsets Based on Presence of CD8 and Foxp 3 Positive Cells and CD8/Foxp3 Ratio

Alexander Filatenkov¹, Cheryl Lewis¹, Sunati Sahoo¹, Yan Peng¹, Yisheng Fang¹, Helena Hwang¹, Venetia Sarode¹

¹UTSouthwestern Medical Center, Dallas, TX

Disclosures: Alexander Filatenkov: None; Sunati Sahoo: None; Yan Peng: None; Yisheng Fang: None; Helena Hwang: None; Venetia Sarode: None

Background: Although it is well established that presence of CD8 positive cells and high CD8/Foxp 3 ratio in invasive carcinoma are associated with better clinical outcome, the prognostic significance of immune infiltrates in ductal carcinoma in situ (DCIS) is not well established. The goals of the study are (1) to develop standardized approach to evaluate CD8 and Foxp3 infiltrates to analyze tumor microenvironment in DCIS, and (2) determine the density of CD8 and Foxp3 infiltrates and CD8/Foxp3 ratio in DCIS.

Design: After institutional review board approval, the tissue microarrays (TMAs) of 107 DCIS were analyzed. TMAs were prepared from formalin fixed paraffin embedded (FFPE) resection specimens. DCIS TMAs associated with invasive carcinoma were excluded. Grade, ER, Her2 and Ki67 status were determined by a pathologist according to standard clinical guidelines. Immunohistochemistry (IHC) was used to detect CD8 and Foxp3 positive cells in DCIS. The Aperio Image Scope software was used to eliminate inter- and intraobserver variation and provide a standardized reproducible approach to evaluate tumor immune microenvironment. TMAs were scanned and membrane algorithm v9 was used to detect CD8 positive cells, and nuclear algorithm v9 was used to detect Foxp3 positive cells. Both intraepithelial and stromal CD8 and Foxp3 positive cells were counted. DCIS that are CD8 infiltrate positive were designated as “hot” tumors whereas DCIS not associated with CD8 infiltrate were designated as “cold” tumors.

Results: 66% of ER-positive, 62% of Her2 positive, and 78.5% of ER/Her2 negative DCIS contained CD8 positive cells (“hot” tumors). There was no significant difference in density of CD8 infiltrate between the groups ($p=0.98$). Ki 67 proliferative index was similar in “hot” and “cold” DCIS. Interestingly, density of CD8 infiltrates in “hot” DCIS was not significantly different in low vs high grade DCIS. There was no significant difference in density of Foxp3 infiltrate between the all three DCIS subsets ($p=0.86$). However, much higher proportion of Her 2 positive DCIS was associated with Foxp3 cells in comparison with ER-positive and ER/Her2-negative (58.2 vs 38.2 and 28% respectively). Remarkably, CD8/Foxp3 ratio was significantly higher in a subset of Her2 positive DCIS in comparison with ER-positive and ER/Her2 negative subsets ($p<0.05$).

Conclusions: The data show that DCIS can be classified as several distinct subsets based on presence of CD8 and Foxp3 cells. ER positive, Her2 positive and ER/Her2 negative DCIS can be divided in “hot” and “cold” subsets. The percentage of “hot” tumors was comparable between the groups with similar density of CD8 infiltrate. However, Her2 positive DCIS were more frequently associated with Foxp3 infiltrate and higher CD8/Foxp3 ratio. Further studies to correlate clinical outcomes in patients with DCIS based on presence of CD8 and Foxp3 infiltrate and CD8/Foxp3 ratio are needed.

89 Expression of β -Catenin and E-Cadherin in Invasive Mammary Carcinomas with Mixed Ductal and Lobular Features

Andrey-Ann Galibois¹, Miralem Mrkonjic², Gulisa Turashvili²

¹Hôpital du Saint-Sacrement, Quebec, Canada, ²Mount Sinai Hospital, University of Toronto, Toronto, Canada

Disclosures: Andrey-Ann Galibois: None; Miralem Mrkonjic: None; Gulisa Turashvili: None

Background: *CDH1* gene encoding E-cadherin, an epithelial cell adhesion molecule, is frequently mutated in lobular carcinomas of the breast. Lack of immunohistochemical (IHC) expression of E-cadherin protein may be used to differentiate lobular and ductal carcinomas, while loss of membranous staining and/or cytoplasmic relocalization of other members of the E-cadherin adhesion complex, such as p120-catenin, α - or β -catenin, have also been described as markers of lobular differentiation. We set out to evaluate the utility of E-cadherin and β -catenin IHC in breast carcinomas with mixed ductal and lobular features (CMDL).

Design: We retrospectively identified patients diagnosed with CMDL, including tubulolobular carcinoma (TLC), at our institution between 2000 and 2020. Microscopic slides were reviewed and IHC studies for E-cadherin and β -catenin were performed in all cases. For both proteins, staining was interpreted as intact (membranous expression), aberrant (absent or markedly reduced expression) or mixed (distinct areas of intact and aberrant expression). Statistical analysis was performed in SPSS 26.0.

Results: A total of 71 tumors were identified and reclassified based on morphology, including 31 CMDLs, 16 invasive ductal carcinomas of no special type (IDC), 21 invasive lobular carcinomas (ILC; 14 classic, 3 solid, 2 alveolar, 2 pleomorphic) and 3 TLCs. The difference between E-cadherin and β -catenin expression was statistically significant ($p < 0.0001$). In 65/71 tumors (91.5%), E-cadherin and β -catenin demonstrated identical staining patterns, including 27 with intact expression, 19 with mixed expression and 19 with aberrant expression. Of the 6 tumors with discordant expression, 3 were morphologically more in keeping with ILC but showed intact E-cadherin and aberrant β -catenin staining (classified as ILC), 2 CMDLs had aberrant E-cadherin and mixed β -catenin expression (reclassified as true mixed carcinoma (MC) with ductal and lobular components), while 1 CMDL had intact E-cadherin but mixed β -catenin expression (reclassified as MC). Overall, based on E-cadherin and β -catenin staining patterns the initial morphologic diagnoses of CMDL were changed to MC in 22 tumors, IDC in 8 tumors and ILC in 1 tumor (Table 1).

Table 1. Summary of morphologic diagnoses and IHC staining patterns of E-cadherin and β -catenin

		Diagnosis prior to IHC				Pearson Chi-Square P-value	Total
		IDC	ILC	CMDL	TLC		
E-cadherin	Intact	16(100%)	3(14.3%)	9(29.0%)	3(100%)	0.0001	31(43.7%)
	Aberrant	0	18(85.7%)	3(9.7%)	0		21(29.6%)
	Mixed	0	0	19(61.3%)	0		19(26.8%)
Beta-catenin	Intact	16(100%)	0	8(25.8%)	3(100%)	0.0001	27(38.0%)
	Aberrant	0	21(100%)	1(3.2%)	0		22(31.0%)
	Mixed	0	0	22(71.0%)	0		22(31.0%)
IHC concordance	Yes	16(100%)	18(85.7%)	28(90.3%)	3(100%)	0.434	65(91.5%)
	No	0	3(14.3%)	3(9.7%)	0		6(8.5%)
Diagnosis post-IHC	IDC	16(100%)	0	8(28.8%)	0	0.0001	24(33.8%)
	ILC	0	21(100%)	1(3.2%)	0		22(31.0%)
	MC	0	0	22(71.0%)	0		22(31.0%)
	TLC	0	0	0	3(100%)		3(4.2%)
Change in diagnosis	Yes	0	0	31(100%)	0	0.0001	31(43.7%)
	No	16(100%)	21(100%)	0	3(100%)		40(56.3%)

Conclusions: Expression of E-cadherin by IHC is similar to that of β -catenin in the majority of breast carcinomas. However, β -catenin staining may be useful in the differential diagnosis of morphologically ambiguous cases of ILC and CMDL.

90 **Non-Mammary Metastases to Breast Parenchyma: A Clinicopathologic Study from a Large Academic Institution**

Toshi Ghosh¹, Malvika Solanki¹
¹Mayo Clinic, Rochester, MN

Disclosures: Toshi Ghosh: None; Malvika Solanki: None

Background: Metastatic disease to the breast, including all metastasis except from within breast (non-mammary breast metastasis, NMBM) poses a unique challenge to patient care. Although rare, they have a significant impact on patient treatment and prognosis. This study evaluates a large cohort of patients with NMBM and adds clinicopathologic and long-term follow-up data to the limited literature.

Design: We identified 89 patients with a pathologic diagnosis of NMBM between 1992 and 2020. Histologic slides were reviewed by two pathologists. Clinicopathologic characteristics and follow-up data were recorded. We excluded 31 patients with breast skin, subcutaneous tissue, or intramammary lymph node metastasis, as they did not involve the breast parenchyma. In the remaining 58 patients (54 F, 4 M) included in our study, parenchymal involvement was confirmed by histopathology or imaging in 53 patients, while 5 patients had cytology samples.

Results: The median age at diagnosis of NMBM was 57 years (range, 33-83 years). The most common metastatic tumor was carcinoma (59%: mostly lung and gastrointestinal (GI), followed by gynecologic, renal, thyroid, thymic, prostate, and salivary gland). This was followed by neuroendocrine tumor/NET (21%: mostly GI), melanoma (17%: mostly cutaneous), and sarcoma (3%: mostly abdominal and uterine leiomyosarcoma). The diagnoses were confirmed by immunohistochemistry in 71% of cases. 60% of NMBM were unifocal, and the median size of the metastatic focus was 16 mm (range, 4-65 mm). Most presented as a palpable mass (47%) or were non-palpable and identified on imaging (40%). NMBM was the first presentation of metastasis in 9% of patients, while it was concurrent with other organ metastases in 19% of patients. Median time to NMBM was 3.1 years (range, 0 days-22.7 years). Median follow-up interval from the date of NMBM to last follow-up was 1.2 years (range, 8 days-13.9 years). Of the patients deceased at last follow-up (72%), median survival since diagnosis of NMBM was 1.1 years (range, 22 days-13 years).

Conclusions: In our cohort of patients with NMBM, the most common tumor type was metastatic carcinoma, followed by metastatic NET, and then melanoma. Distinction of NMBM from primary breast carcinoma can be challenging, especially when NMBM is the initial presentation or has unifocal metastasis. In our study, 28% of patients presented with NMBM as their first presentation with metastatic disease. Careful morphologic assessment, immunohistochemistry, and clinicoradiologic correlation can be very helpful to identify NMBM and provide optimal patient care.

91 **Collagen Fiber Orientation by Image Analysis and Its Clinical Utility**

Akisha Glasgow¹, Haojia Li², Haley Sechrist³, Pingfu Fu⁴, Philip Bomeisl⁵, Hannah Gilmore⁶, Aparna Harbhajanka⁷, Anant Madabhushi⁴

¹University Hospitals Cleveland Medical Center, Case Western Reserve University, Cleveland, OH, ²CCIPD, Case Western Reserve University, Cleveland, OH, ³Case Western Reserve University School of Medicine, Cleveland, OH, ⁴Case Western Reserve University, Cleveland, OH, ⁵University Hospitals Cleveland Medical Center, Cleveland, OH, ⁶University Hospitals Case Medical Center, Case Western Reserve University, Cleveland, OH, ⁷Case Western Reserve University/University Hospitals Cleveland Medical Center, Cleveland, OH

Disclosures: Akisha Glasgow: None; Haojia Li: None; Haley Sechrist: None; Pingfu Fu: None; Philip Bomeisl: *Consultant*, Path AI; Hannah Gilmore: None; Aparna Harbhajanka: None; Anant Madabhushi: *Advisory*

Board Member, Aiforia Inc; Primary Investigator, Bristol Myers-Squibb; Primary Investigator, AstraZeneca; Advisory Board Member, Boehringer-Ingelheim

Background: Stromal collagen is an important structural factor in breast cancer. However, its specific role is not fully understood. The collagen fibers surrounding the tumor may act as a barrier that prevents cancer cell migration. Their alignment may also give some insight into which tumors are more likely to metastasize and therefore, be treated more aggressively. The aim of this study was to assess the association between collagen fiber organization using image analysis and compare these findings with commonly used clinicopathologic findings.

Design: After IRB approval, all newly diagnosed ER+/PR +/-HER2- breast cancer patients with available Oncotype Dx recurrence scores (ODX-RS) between January 2008 and June 2018 were included. The original pathology reports were reviewed, and chart review was performed for information regarding outcome events. Other information obtained included demographic data, tumor size, grade, histologic subtype, and ER, PR, and HER2 status and the Nottingham scores were documented. The available slides were scanned, and an algorithm was applied to automatically detect the orientation of the collagen fibers and assess the disorder degree of the fiber orientations in the tumor-associated stroma. The patients were classified as having organized and disorganized collagen around tumor cells. Statistical tests include a chi-squared test and Kaplan Meier survival curves. A *p*-value of <0.05 was considered statistically significant.

Results: The cohort consisted of 493 cases. The mean age was 60.9 (range: 25-80). The median follow-up was 45 months. Table 1 demonstrates the demographic data. Disorganized collagen was significantly associated with higher tumor grade, increasing nuclear pleomorphism and mitotic count, associated high grade ductal carcinoma in situ (DCIS), invasive ductal subtype, and ODX-RS using TAILORx cutoffs. There were 29 outcome events during the study period: 17 locoregional recurrences, 11 distant recurrences and 1 breast cancer related deaths. Most of the locoregional and distant metastasis and the breast cancer-related deaths had disorganized collagen fiber orientation. There was no significant difference between overall survival, locoregional or distant recurrence-free survival with disorganized and organized collagen (Figure 1 and 2).

Age, n (%)	Disorganized Collagen	Organized Collagen	Total	<i>p</i> -value
≤50	43 (52)	39 (48)	82	0.614
>50	203 (49)	208 (51)	411	
T stage, n (%)				0.181
1	176 (52)	162 (48)	338	
2	66 (45)	81 (55)	147	
3	4 (50)	14 (50)	18	
N stage, n (%)				0.940
N0	202 (50)	206 (50)	408	
N(0)i+	8 (50)	8 (50)	16	
N1mi	13 (50)	13 (50)	26	
N1	13 (43)	17 (57)	30	
Nx	7 (78)	2 (22)	9	
Tumor grade, n (%)				0.0001
1	32 (34)	62 (66)	94	
2	156 (48)	166 (52)	322	
3	54 (75)	18 (25)	72	
Tubule formation, n (%)				0.362
1	13 (38)	21 (62)	34	
2	38 (45)	47 (55)	85	
3	165 (53)	148 (47)	313	

Nuclear pleomorphism, n (%)				<0.0001
1	6 (32)	13 (68)	19	
2	145 (44)	181 (56)	326	
3	65 (75)	22 (25)	87	
Mitotic count, n (%)				<0.0001
1	123 (41)	174 (59)	297	
2	69 (72)	27 (28)	96	
3	23 (62)	14 (38)	37	
Associated DCIS, n (%)				0.028
None reported	70 (43)	92 (57)	162	
Low grade	14 (45)	17 (55)	31	
Intermediate grade	101 (49)	105 (51)	206	
High grade	58 (66)	30 (34)	88	
Histologic Subtype, n (%)				0.021
IDC	184 (53)	166 (47)	350	
ILC	39 (47)	44 (53)	83	
IMC	19 (34)	37 (66)	56	
DCIS	3 (100)	0 (0)	3	
Oncotype Dx risk categories, n (%)				0.003
Low risk (<11)	52 (70)	22 (30)	74	
Intermediate risk (11-25)	132 (43)	176 (57)	308	
High risk (>25)	58 (54)	49 (46)	107	
Low risk (<18)	26 (70)	11 (30)	37	0.149
Intermediate risk (18-30)	86 (47)	96 (53)	182	
High risk (>30)	130 (48)	140 (52)	270	

Figure 1 - 91

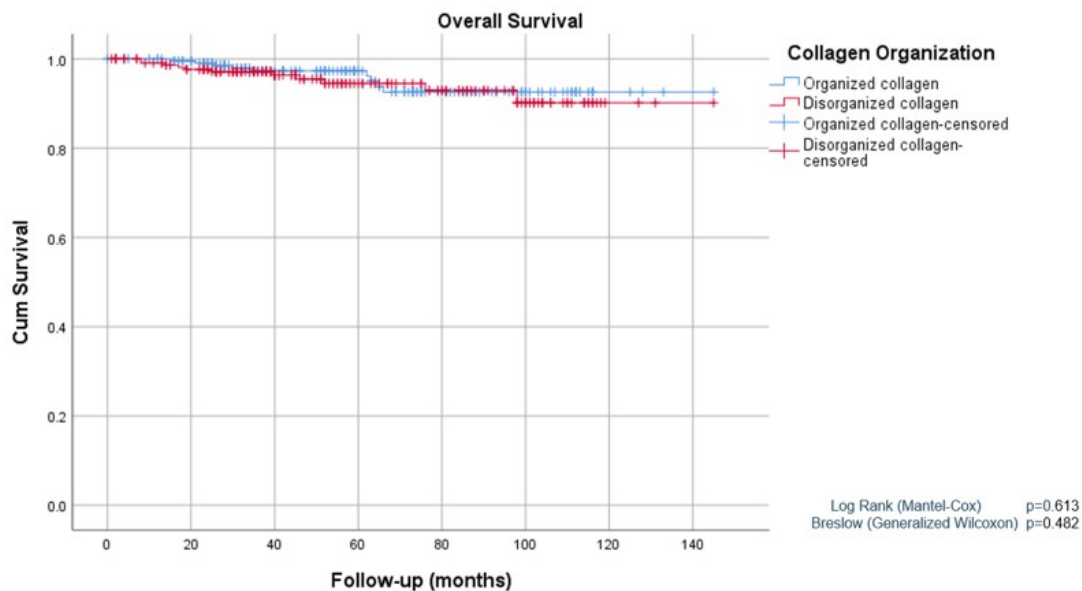
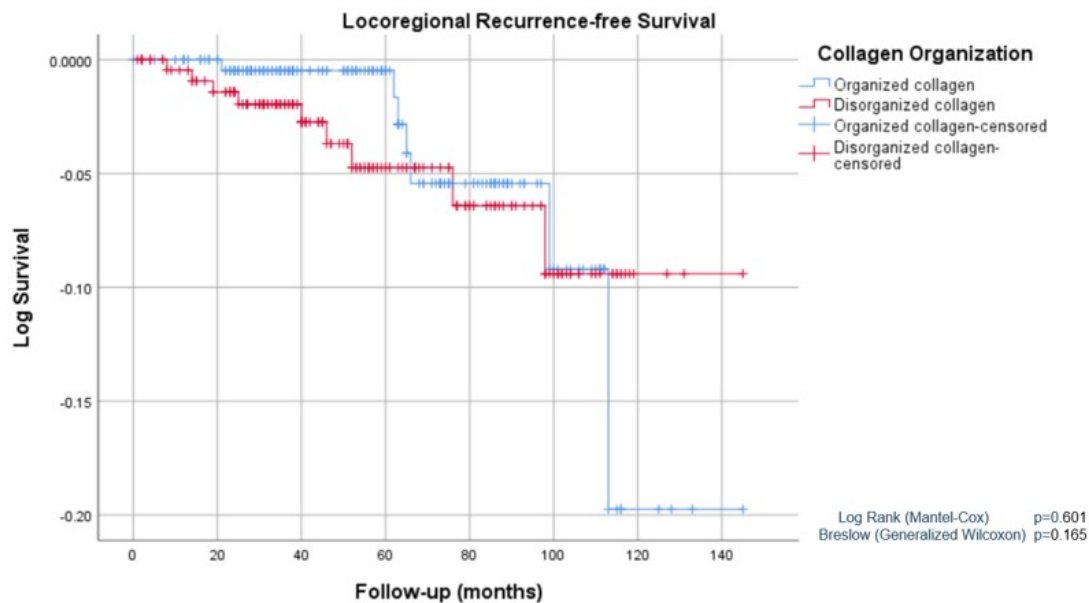


Figure 2 - 91



Conclusions: Collagen fiber orientation was significantly associated with many commonly used clinicopathologic factors and ODX-RS based on TAILORx cutoffs. This technique can potentially be used to identify patients with high risk cancers who may need more aggressive treatment.

92 Patient Outcomes After Non-Compliance With Adjuvant Chemotherapy for Estrogen-Receptor Positive, HER2 Negative, and Lymph Node Negative Invasive Breast Cancer Based on 21-Gene Recurrence Scores

Akisha Glasgow¹, Haley Sechrist², Philip Bomeisl³, Hannah Gilmore⁴, Aparna Harbhajanka⁵
¹University Hospitals Cleveland Medical Center, Case Western Reserve University, Cleveland, OH, ²Case Western Reserve University School of Medicine, Cleveland, OH, ³University Hospitals Cleveland Medical Center, Cleveland, OH, ⁴University Hospitals Case Medical Center, Case Western Reserve University, Cleveland, OH, ⁵Case Western Reserve University/University Hospitals Cleveland Medical Center, Cleveland, OH

Disclosures: Akisha Glasgow: None; Haley Sechrist: None; Philip Bomeisl: *Consultant*, Path AI; Hannah Gilmore: None; Aparna Harbhajanka: None

Background: Most invasive breast cancer cases are early-stage, hormone receptor positive, HER-2 negative and lymph node-negative. Oncotype (ODX) assists clinicians in chemotherapy recommendations based on defined recurrence scores (RS). Literature is limited regarding the outcome of this subset of patients who refuse chemotherapy based on ODX-RS. The aim of this study is to assess the outcome of patients who were offered adjuvant therapy and refuse.

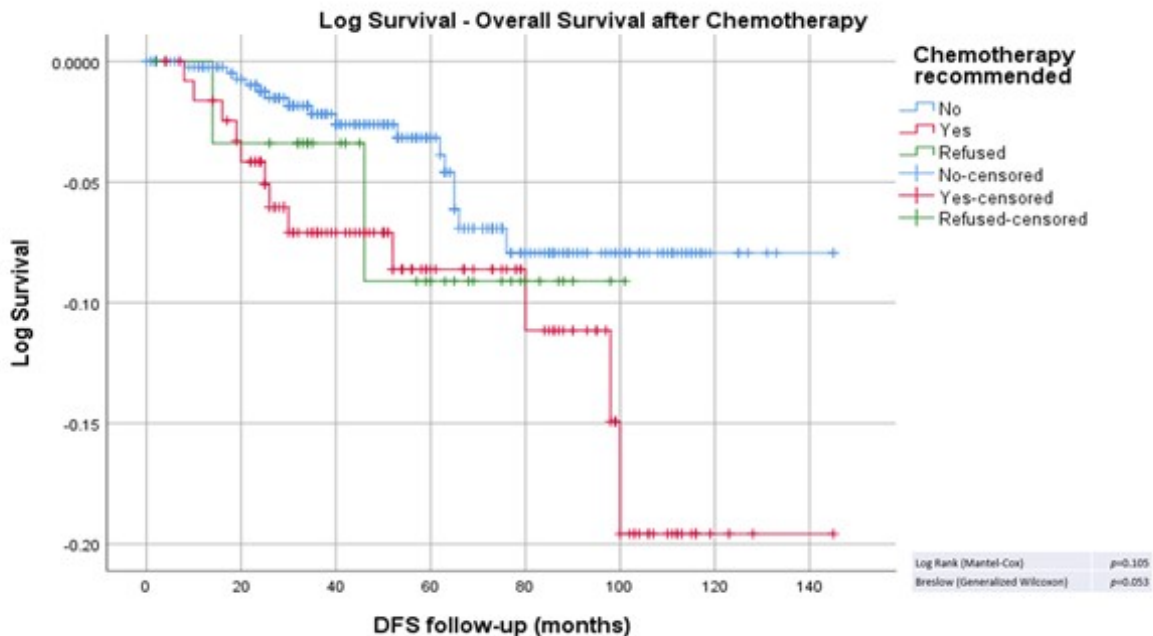
Design: All newly diagnosed ER/PR+, HER2 negative, lymph node negative breast cancer patients with available ODX-RS from 2008-2018 were included. The original pathology reports were reviewed and chart review was performed to obtain demographic data, document treatment plans and assess follow-up.

Results: There were 596 patients in our cohort. Median age was 61 years (range: 25-82). Median follow up was 49 months (mean: 59 months). There were 31 patients who were offered chemotherapy and refused (Table 1). Only 2 patients developed a locoregional and/or distant recurrences after a median follow up of 49 months, one of which also refused hormonal therapy. Most were older and approximately half were high risk by TAILORx cutoffs. A multinomial stepwise regression analysis demonstrated that statistically significant predictors associated with the

development of a locoregional recurrence were age ≤ 50 ($p=0.03$), not receiving hormonal therapy ($p=0.007$) and being offered chemotherapy and refusing ($p=0.013$). Significant predictors of the development of a distant recurrence were age ≤ 50 ($p=0.014$), associated DCIS with high nuclear grade ($p=0.008$) and grade 3 tumors ($p=0.032$). There was no significant difference in disease-free survival between patients who were offered chemotherapy and those who were offered and refused (Figure 1).

Age	Locoregional recurrence	Chemotherapy	ODX-RS				Total	p-value
			<11	11-15	16-25	>25		
≤ 50	Yes	Yes	0	1	2	0	3	0.1
		No	0	2	1	0	3	
		Refused	0	0	0	1	1	
		Total	0	3	3	1	7	
	No	Yes	1	2	18	12	33	<0.001
		No	19	22	24	1	66	
		Refused	0	2	1	3	6	
		Total	20	26	43	16	105	
> 50	Yes	Yes	0	0	1	0	1	0.706
		No	4	2	3	2	11	
		Refused	0	0	1	0	1	
		Total	4	2	5	2	13	
	No	Yes	3	3	28	56	90	<0.001
		No	105	102	135	16	358	
		Refused	1	2	9	11	23	
		Total	109	107	172	83	471	
Age	Distant Recurrence	Chemotherapy	ODX-RS				Total	p-value
			<11	11-15	16-25	>25		
≤ 50	Yes	Yes	0	1	2	1	4	0.687
		No	0	1	1	0	2	
		Refused	0	0	0	0	0	
		Total	0	2	3	1	6	
	No	Yes	1	2	18	11	32	<0.001
		No	19	23	24	1	67	
		Refused	0	2	1	4	7	
		Total	20	27	43	16	106	
>50	Yes	Yes	0	0	1	3	4	0.415
		No	1	0	2	1	4	
		Refused	0	0	1	0	1	
		Total	1	0	4	4	9	
	No	Yes	3	3	28	53	87	<0.001
		No	108	104	136	17	365	
		Refused	1	2	9	11	23	
		Total	112	109	173	81	475	

Figure 1 - 92



Conclusions: There was no significant difference in survival between patients who received chemotherapy and those who refused in most risk categories. Younger patients were also more likely to get locoregional or distant recurrences after refusal of chemotherapy.

93 NTRK Rearrangements (NTRK-R) Are Identified in a Rare Subset of Clinically Advanced and Metastatic Breast Carcinomas (MBC) With Both Secretory and Non-Secretory Histology

Mariangela Gomez¹, Ethan Sokol², Alexa Schrock², Douglas Lin², Natalie Danziger², Russell Madison², Douglas Mata², Brennan Decker², Tyler Janovitz², Richard Huang³, J. Keith Killian², Julia Elvin², Shakti Ramkissoon⁴, Kimberly McGregor², Jeffery Venstrom⁵, Jeffrey Ross⁶

¹SUNY Upstate Medical University, ²Foundation Medicine, Inc., Cambridge, MA, ³Foundation Medicine, Inc., Cary, NC, ⁴Foundation Medicine, Inc., Morrisville, NC, ⁵Foundation Medicine, Inc., San Francisco, CA, ⁶Upstate Medical University, Syracuse, NY

Disclosures: Mariangela Gomez: None; Ethan Sokol: *Employee*, Foundation Medicine, Inc.; *Stock Ownership*, Roche; Alexa Schrock: *Employee*, Foundation Medicine; *Stock Ownership*, Roche; Douglas Lin: *Employee*, Foundation Medicine, Inc.; *Stock Ownership*, Roche; Natalie Danziger: *Employee*, Foundation Medicine Inc.; Russell Madison: *Employee*, Foundation Medicine Inc.; *Stock Ownership*, Roche; Douglas Mata: *Employee*, Foundation Medicine, Inc.; Brennan Decker: *Employee*, Foundation Medicine; Tyler Janovitz: *Employee*, Foundation Medicine; Richard Huang: *Employee*, Foundation medicine; J. Keith Killian: *Employee*, Foundation Medicine; Julia Elvin: *Employee*, Foundation Medicine; *Stock Ownership*, Hoffmann-La Roche; Shakti Ramkissoon: *Employee*, Foundation Medicine; Kimberly McGregor: *Employee*, Foundation Medicine; *Stock Ownership*, ROCHE; Jeffery Venstrom: *Employee*, Foundation Medicine; Jeffrey Ross: *Employee*, Foundation Medicine

Background: The *NTRK* (Neurotrophic Tyrosine Receptor Kinase) gene family encodes three tropomyosin-related kinase (TRK) receptors (*NTRK1*, *NTRK2*, or *NTRK3*). *NTRK-R* have been associated with secretory MBC, but have not been studied in non-secretory MBC.

Design: Using an FDA-approved hybrid capture-based comprehensive genomic profiling (CGP) assay (FoundationOneCDx), a series of 14,481 MBC were sequenced to evaluate all classes of genomic alterations (GA).

Tumor mutational burden (TMB) was determined on 0.8 Mbp of sequenced DNA and microsatellite instability (MSI) was determined on 95 loci. PD-L1 expression was determined by IHC (Ventana Sp142) using inflammatory cell staining.

Results: 22 (0.2%) MBC featured *NTRK*-R involving 10 *NTRK1*, 0 *NTRK2* and 12 *NTRK3*. None of the *NTRK1*-R were canonical activating fusions. 4 (33%) of the 12 *NTRK3*-R cases featured known *NTRK* activating fusions with the transcription factor ETV6. These occurred in 2 metastatic secretory carcinomas, 1 metaplastic carcinoma and 1 pure high grade ductal carcinoma. The non-canonical *NTRK*-R rearrangements observed in our study include reciprocal fusions, events where the frame cannot be determined, or a fusion partner with an oligomerization domain was not found; these events may be indicative of an activating rearrangement event, such as a fusion; however, there is uncertainty whether these may be activating in all cases. 6/8 (75%) *NTRK1*-R and 5/7 (71%) *NTRK3*-R cases were ER+. 4 (18%) of 22 *NTRK*-R cases featured co-occurring *ERBB2* amplification, predominantly associated with *NTRK3*-R (27% of *NTRK3*-R, 17% of *NTRK1*-R). Among *NTRK3:ETV6* cases 1 (25%) featured a co-occurring *ERBB2* amplification and 3 (75%) were ER+. *NTRK1*-R were found exclusively (100%) in non-secretory MB including 1 inflammatory and 1 metaplastic carcinoma. Clinically significant co-altered genes included *ESR1* and *PIK3CA* at 17%, *PTEN* at 13%, *BRAF*, *NF1*, *FGFR3* all at 8% and *BRCA2* at 4% (no *BRCA1* GA) in the *NTRK1*-R tumors and *PIK3CA* at 42%, *PTEN* and *ESR1* at 17%, *FGFR1* at 8% and *BRCA1/2* at 0% in the *NTRK3*-R tumors. The median TMB was 2.5 mut/Mb for *NTRK1*-R and 1.3 mut/Mb for *NTRK3*-R cases. All cases were MSI stable and had no positive PD-L1 expression.

Conclusions: *NTRK*-R can occur in secretory, metaplastic and typical ductal MBC. *NTRK1*-R cases seen in this cohort do not involve known transcription factors and thus their responsiveness to *NTRK* targeted therapy needs further clinical validation. One-third of *NTRK3*-R involve fusions with the ETV6 transcription factor and are predominantly, but not exclusively found in secretory carcinomas. The high co-occurrence rate of *ERBB2* amplification with *NTRK*-R in MBC reinforces the utility of comprehensive genomic profiling to ensure detection of all relevant therapeutic targets. Given the widely known responsiveness of *NTRK*-R to anti-*NTRK*-R TKI drugs, further study on *NTRK*-R in MBC appears warranted.

94 The 21-Gene Recurrence Score (RS) in Special Histologic Subtypes of Breast Cancer: A Population-Based Study

H. Evin Gulbahce, The University of Utah, Salt Lake City, UT

Disclosures: H. Evin Gulbahce: None

Background: Although the US Federal Drug Administration (FDA) approved the use of RS testing in special types of breast cancer (BC) the data for the RS were derived from invasive ductal carcinoma- no special type and a small proportion of lobular cancers. The purpose of this study is to determine association of histologic types (HT) and RS, specifically high-risk RS, the group that needs systemic therapy, and HT as predictor of BC specific death.

Design: We used RS from Genomic Health linked to Surveillance Epidemiology End Result (SEER) registry of BC cases diagnosed 2004-2015. Demographic and clinicopathological information, and survival info were obtained. Women with ER+, HER2-, T1-T3 tumors were included. Multivariable logistic regression was used to evaluate association between HT and high-risk RS. Relationship between HT and low-, intermediate-, and high-risk RS were compared with chi-squared probability test. Kaplan-Meier curves were plotted and compared using log-rank test.

Results: 110,318 patients had RS testing. 23,220(21%) had low; 70,822(62.2%) intermediate; 16,276(14.6%) high RS. 80,476(73%) was ductal, 12,713(11.5%) lobular, 12,449(11.3%) mixed, 2,151(2%) mucinous, 610(0.6%) tubular 382(0.4%) micropapillary, 365(0.3%) salivary type, 208(0.2%) papillary, 49(0.04%) medullary, 26(0.02%) metaplastic, 26(0.02%) neuroendocrine, 863(0.8%) unknown type BC. The distribution of low-, intermediate-, high-risk RS was significantly different between HT. Significantly higher percentages of high-risk RS were identified in patients with ductal, medullary, and metaplastic types ($p < 0.001$). Lobular, tubular, mucinous, papillary types were significantly less likely to have high-risk RS. The odds of having high-risk was lower for lobular, mixed, mucinous, tubular and micropapillary types after multivariable adjustment for age, grade, PR status ($p < 0.05$). Low number of medullary and metaplastic carcinomas that were ER+ had higher odds of having high-risk RS. In patients with ≤ 2 cm

(T1) and >2cm (T2) tumors when ductal, lobular, mixed and other types combined together were compared, the survival was significantly different.

Table 1 Odds ratios for high-risk recurrence score (RS) among all women and women ≥50 years of age diagnosed with breast cancer in 2004 -2015 and had RS testing by histologic types, SEER registries.

	ALL AGES						50 YEARS AND OLDER						
	N	%	OR	CI		P*	N	%	OR	CI	P*		
Ductal	78,936	73.44	Reference					60,333	72.57	Reference			
Lobular	12,528	11.66	0.49	0.46	0.53	<0.01	10,358	12.46	0.52	0.48	0.56	<0.01	
Mixed	12,255	11.4	0.65	0.61	0.70	<0.01	9,611	11.56	0.65	0.60	0.70	<0.01	
Mucinous	2,117	1.97	0.82	0.69	0.98	0.03	1,605	1.93	0.78	0.63	0.96	0.02	
Tubular	607	0.56	0.59	0.37	0.93	0.03	424	0.51	0.63	0.37	1.05	0.08	
Micropapillary	378	0.35	0.71	0.52	0.96	0.03	312	0.38	0.60	0.42	0.85	<0.01	
Salivary Gland & Rare Types	356	0.33	0.76	0.51	1.11	0.15	244	0.29	0.77	0.49	1.21	0.26	
Papillary	204	0.19	0.67	0.39	1.17	0.16	174	0.21	0.51	0.26	0.99	0.05	
Medullary	48	0.04	9.65	3.77	24.73	<0.01	34	0.04	7.44	2.65	20.90	<0.01	
Metaplastic	26	0.02	7.34	2.55	21.15	<0.01	20	0.02	5.07	1.71	15.07	<0.01	
Neuroendocrine	25	0.02	0.70	0.23	2.17	0.54	21	0.03	0.32	0.07	1.57	0.16	
TOTAL	107,480	100					83,136	100					

OR: odds ratio; CI: confidence interval.

bold text designates statistical significance.

* p from a multivariate logistic regression, adjusted for grade, progesterone receptor status, and age

Conclusions: The studies on RS of special types of breast cancer has been limited and was addressed only in small studies until now. This is the largest, population based study of RS in HT that showed high-risk RS are identified in traditionally good prognostic subtypes. Some special subtypes, including micropapillary carcinoma, have lower odds of high-risk RS even after adjusting for grade, PR status and age

95 Evaluating the Significance of Atypical and Malignant Breast Lesions Arising in Fibroadenoma of the Breast

Kayla Hackman¹, Iskender Genco¹, Sabina Hajjiyeva¹
¹Northwell Health Lenox Hill Hospital, New York, NY

Disclosures: Kayla Hackman: None; Iskender Genco: None; Sabina Hajjiyeva: None

Background: While fibroadenomas (FAs) are the most common benign neoplasm of the breast, little data exists about clinical characteristics and prognostic value of FAs found to be directly associated with atypical and malignant lesions. Cases of FA diagnosed within our health system were reviewed to establish the exact clinical significance of these unique lesions.

Design: All FA cases diagnosed on core needle biopsy (CNB) between 2013 and 2020 within our department were screened to identify those with atypical and malignant lesions {(atypical lobular hyperplasia (ALH), lobular carcinoma in situ (LCIS), atypical ductal hyperplasia (ADH), flat epithelial atypia (FEA), ductal carcinoma in situ (DCIS), invasive ductal carcinoma (IDC), and invasive lobular carcinoma (ILC)} arising in FA. Cases with atypical or malignant lesions outside of FA on the same CNB were excluded. The relationship between CNB and excisional findings for each case were reviewed.

Results: A total of 1466 cases of FA diagnosed on CNB were identified. Among these, 17 cases showed atypical and/or malignant lesions arising in FA. The median age of patients at diagnosis was 53 years (range, 40-68 years). Of those 17 cases, nine were LCIS, two were LCIS+ILC, one was LCIS+DCIS, two were ADH, two were DCIS, and one case was DCIS+IDC. Each of these cases had a subsequent excisional specimen within our system. For LCIS, the excision showed LCIS in four cases, ADH in two cases, and LCIS+DCIS, LCIS+ILC, and only FA in one case each. For ADH, one showed DCIS and the other showed only FA. For DCIS, DCIS and DCIS+IDC were found on one case each upon excision. Lastly, for the LCIS+ILC, LCIS+DCIS and DCIS+IDC cases, both the biopsy and excision showed the same lesions.

Conclusions: There is a low percentage of FA harboring atypia or carcinoma; here we report the clinicopathologic features of 17 cases of atypia and carcinomas arising within FAs of the breast diagnosed on CNB and the findings on the subsequent excision. The presentation and gross characteristics of these tumors are indistinguishable from those of uncomplicated FAs. Lastly, 4 of 17 (24%) cases were upgraded upon excision, suggesting that complete excision of these lesions may be the recommended method of clinical management.

96 Expression of 'Tissue Specific' IHC Markers in Triple Negative Breast Cancer

Rachel Han¹, Sharon Nofech-Mozes², Fang-I Lu², Anna Plotkin¹, Wedad Hanna³, Elzbieta Slodkowska²
¹University of Toronto, Toronto, Canada, ²University of Toronto, Sunnybrook Health Sciences Centre, Toronto, Canada, ³Sunnybrook Health Sciences Centre, Toronto, Canada

Disclosures: Rachel Han: None; Sharon Nofech-Mozes: None; Fang-I Lu: None; Anna Plotkin: None; Wedad Hanna: None; Elzbieta Slodkowska: None

Background: Triple negative breast cancer (TNBC) represents a heterogenous group of breast carcinomas which lack expression of ER/PR and overexpression of HER2. ER/PR/HER2 negative metastases often present a diagnostic challenge as their distinction from TNBC has significant prognostic and therapeutic implications. The objective of this study was to evaluate the expression of 'tissue specific' IHC markers (Figure 1) on a large cohort of TNBC.

Design: Sections from tissue microarrays composed of 273 TNBC in triplicate 1mm cores were immunostained with a panel of 20 markers (2 different clones for 3 of them). Staining intensity was scored as 0, 1, 2, or 3 (0=no staining, 1=weak, 2=moderate, 3=strong). The percentage of positively stained tumour cells was assessed as a proportion of total tumour, and scored as 0, 1, 2, 3, or 4 (0=<1%, 1=1-10%, 2=10-24%, 3=25-49%, 4= \geq 50%). Percentage and intensity scores were added using a modified Allred method; combined scores \geq 2 were considered positive with the exception of mammaglobin, where any cytoplasmic staining was considered positive. BAP1 and SMAD4 were scored as retained vs. lost (no staining in tumor). Histologic tumour types were assigned according to WHO classification.

Results: Expression of all IHC markers is summarized in Table 1. Pankeratin was expressed in all TNBC but 4 metaplastic carcinomas (MC). CK7 was expressed in all but 11 cases, of which 7 were MC. GATA3 was expressed in 76% while mammaglobin was expressed in 43% of tumors (the latter often in single cells only). Among 198 TNBC-NOS, 5 (2%) lacked expression of SOX10, GATA3 and mammaglobin; of these, all were positive for CK7. Almost all TNBC showed no expression of Melan-A, Napsin A, PAX8 (SP348), SATB2 (EP281), TTF1, and had retained SMAD4.

Table 1. Expression of 20 ‘tissue-specific’ IHC markers in 273 cases of TNBC

IHC marker	Positive/retained expression	Diffuse positive expression (>50%)	Negative/loss of expression
AR	42% (115/273)	50% (57/115)	58% (158/273)
BAP1	96% (258/268)	n/a	4% (10/268)
CAIX	35% (95/272)	7% (18/272)	65% (177/272)
CDX2	12% (34/272)	4% (11/272)	88% (238/272)
CK5	82% (223/273)	57% (157/273)	18% (50/273)
CK7	96% (262/273)	91% (248/273)	4% (11/273)
GATA3	76% (207/271)	58% (156/271)	24% (64/271)
Mammaglobin	43% (114/267) ^a	6% (15/267)	57% (153/267)
Melan-A	<1% (1/270)	<1% (1/270) ^b	>99% (269/270)
Napsin A	0/269	0/269	100% (269/269)
NKX3.1	14% (37/273)	1% (3/273)	86% (236/273)
Pankeratin	99% (267/271)	96% (261/271)	1% (4/271)
PAX8 (clone SP348)	0/268	0/268	100% (268/268)
PAX8 (clone MPQ-50)	3% (9/269)	<1% (2/269)	97% (260/269)
p63	16% (43/269)	4% (10/269)	84% (226/269)
S100	44% (119/269)	13% (35/269)	56% (150/269)
SATB2 (clone EP281)	1% (3/267)	<1% (1/267)	99% (264/267)
SATB2 (clone SATBA4B10)	17% (47/268)	4% (10/268)	83% (221/268)
SMAD4	99% (266/268)	n/a	1% (2/268)
SOX10	64% (173/270)	60% (163/270)	36% (97/270)
TTF1 (clone SPT24)	1% (4/268)	<1% (2/268)	99% (264/268)
TTF1 (clone 8G7G3/1)	0/269	0/269	100% (269/269)
WT1	6% (16/269)	1% (4/269)	94% (253/269)

^aSingle cell staining in 25% (66/267); ^bweak intensity, negative for SOX10/S100, positive for CK7

Figure 1 - 96

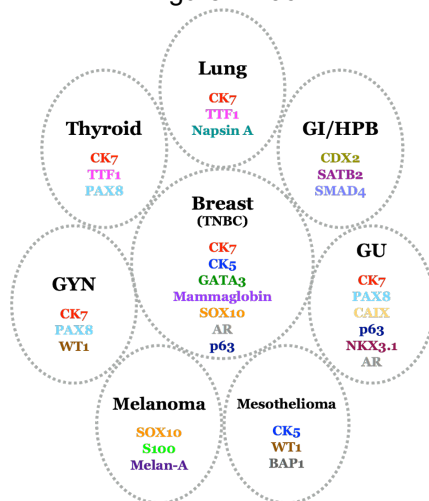


Figure 1. ‘Tissue specific’ IHC markers

Conclusions: Expression of SOX10, GATA3 and/or mammaglobin is present in 98% of TNBC-NOS. Expression of Melan-A, Napsin A, PAX8 (SP348), SATB2 (EP281), TTF1 (8G7G3/1), and/or loss of SMAD4 is highly specific for non-mammary origin. CDX2, NKX3.1 and WT1 can be variably expressed in TNBC and may lead to diagnostic challenges in the distinction of site of origin. The choice of PAX8, SATB2 and TTF1 clone can greatly help in delineating site of origin.

97 Morphological Breast Cancer Subtyping by Weakly Supervised Neural Networks

Matthew Hanna¹, Matthew Lee², Alican Bozkurt², Ran Godrich², Adam Casson², Patricia Raciti², Jillian Sue², Julian Viret², Donghun Lee², Leo Grady², Brandon Rothrock², Belma Dogdas², Thomas Fuchs², Jorge Reis-Filho¹, Christopher Kanan²

¹Memorial Sloan Kettering Cancer Center, New York, NY, ²Paige.AI, New York, NY

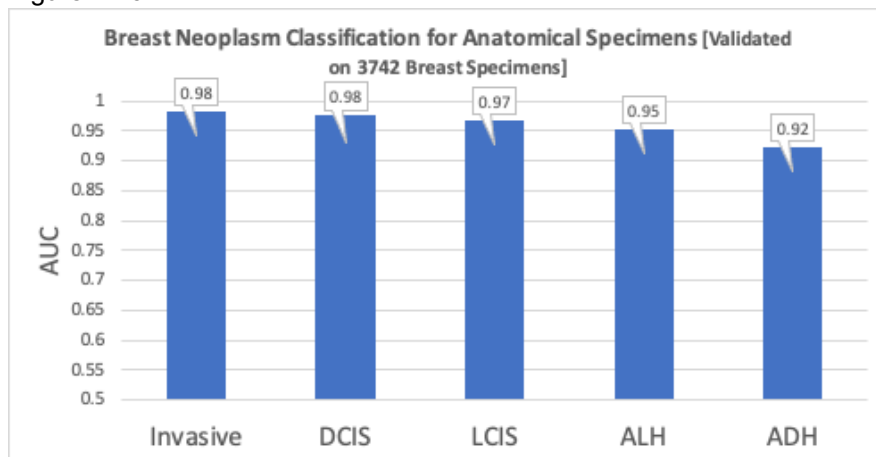
Disclosures: Matthew Hanna: *Consultant*, PaigeAI; Matthew Lee: *None*; Alican Bozkurt: *Employee*, Paige.AI; Ran Godrich: *Employee*, PaigeAI; Adam Casson: *Employee*, Paige.AI; *Employee*, Paige.AI; Jillian Sue: *Employee*, Paige.AI; Julian Viret: *None*; Donghun Lee: *None*; Brandon Rothrock: *None*; Belma Dogdas: *Employee*, Paige; *Stock Ownership*, Paige; Thomas Fuchs: *Employee*, Paige.AI Inc.; *Employee*, Paige.AI Inc.; Jorge Reis-Filho: *Consultant*, Paige; *Stock Ownership*, Paige; *Advisory Board Member*, Paige; Christopher Kanan: *Employee*, Paige.AI, Inc.

Background: Breast pathology includes a spectrum of benign, atypical/high risk, preinvasive, and invasive lesions. Diagnoses rendered on biopsies have a relative high discordance rate in interpretation, particularly without expert review. Detection and distinct classification of these lesions are required for appropriate patient management. Due to routine screening, breast specimens are common and high volume in pathology. Breast resection specimens may also be time consuming due to the number of glass slides and overall tissue area for histopathologic review. Machine learning has been shown to improve efficiency and accuracy of cancer detection in a variety of tissue types. Here, we hypothesized that such an algorithm can be trained to detect and subclassify clinically meaningful lesions in breast pathology with the potential to provide increased efficiency and accuracy to the histologic examination of slides of breast tissue.

Design: De-identified glass slides were scanned on Leica AT2 whole slide scanners (0.5 µm/pixel) from our institutional database were retrieved. Diagnoses were available from the pathology report. Using a machine learning architecture of multiple instance learning, an SE-ResNet50 Convolutional Neural Network (CNN) was trained using the same approach described in Campanella et al. (2019). Each input to the network consisted of whole slide images (WSIs). Classification performance for invasive carcinoma, ductal carcinoma in situ (DCIS), lobular carcinoma in situ (LCIS), atypical ductal hyperplasia (ADH), and atypical lobular hyperplasia (ALH) were determined. A split-sample testing and validation study design was employed for the development of the classifier.

Results: A dataset of 9,751 anatomical specimens (biopsy, 6,289; excision, 3,462) comprising 40,637 slides were used to train the CNN. The system was validated on WSI generated from 3,742 breast specimens (biopsy, 2,250; excision, 1,492) comprising 13,601 digital slides that were not included in the training of the CNN model. Results shows area under the receiver operating characteristic curve (AUC) classification of invasive carcinoma, DCIS, LCIS, ALH, and ADH as 0.98, 0.98, 0.97, 0.95, and 0.92, respectively. [Figure 1].

Figure 1 - 97



Conclusions: The trained CNN had high performance in classifying breast lesions including invasive carcinoma, DCIS, LCIS, ADH, and ALH. Future work includes histologic typing of invasive breast cancers and the detection

of microinvasion and calcifications, as well as assessing generalizability of the results utilizing independent real-world data.

98 Upstage Rates of Pleomorphic, Florid, and Classic Lobular Carcinoma In Situ Diagnosed on Core Needle Biopsies: A Seven Year Single Institution Retrospective Study

Lakshmi Harinath¹, Evgeny Ozhegov¹, Alexander Strait², Tatiana Villatoro³, Beth Clark¹, Jeffrey Fine⁴, Jing Yu⁴, Gloria Carter¹, Rohit Bhargava¹

¹UPMC Magee-Womens Hospital, Pittsburgh, PA, ²Magee Womens Hospital, Pittsburgh, PA, ³University of Pittsburgh Medical Center, Pittsburgh, PA, ⁴University of Pittsburgh, Pittsburgh, PA

Disclosures: Lakshmi Harinath: None; Evgeny Ozhegov: None; Alexander Strait: None; Tatiana Villatoro: None; Jeffrey Fine: *Stock Ownership*, Splntelx, Inc.; Jing Yu: None; Gloria Carter: None; Rohit Bhargava: *Advisory Board Member*, Eli Lilly & Company

Background: There is practice heterogeneity regarding optimal management of classical type lobular carcinoma in-situ (CLCIS) when diagnosed on core need biopsy (CNB). Now with recognition of LCIS variants, florid (FLCIS) and pleomorphic (PLCIS) types, the management has become even more complicated. The primary aim of this study was to determine the upstage rates of CLCIS, FLCIS and PLCIS when diagnosed on CNB. The secondary goal was to determine outcome of cases that are not upstaged.

Design: Our institutional pathology database was searched from Jan 1, 2013 to current time for patients with LCIS diagnosed on CNB and underwent subsequent excision. Radiologic findings were noted for asymmetry, mass, lesion, distortion, enhancement, calcifications. The upstage rate (defined as invasive carcinoma and ductal carcinoma in-situ [DCIS] on excision) was calculated for all cases and specifically for cases with calcifications only (true upstage rate). Follow up outcome data was obtained on patients who were not upstaged on excision.

Results: A total of 94 cases were identified (CLCIS= 75, FLCIS =15 and PLCIS=4). Most cases had multiple radiologic findings including calcifications (63%), mass (30%), non-mass enhancement (23%), asymmetry (15%), distortion (15%), and hypoechoic lesion (7%). Of the 94 cases, 18 cases were upstaged. The upstage rate for FLCIS/PLCIS (9/19: 47.3%) was significantly higher compared to CLCIS (9/75: 12%, p-value= 0.0015). Of the 76 patients that were not upstaged, none developed invasive carcinoma or DCIS during follow up (average 46 months). We then examined 39 cases with calcifications only as the radiologic finding (CLCIS=31, FLCIS=6, PLCIS=2). The upstage rate for FLCIS/PLCIS (2/8: 25%) was higher compared to CLCIS (1/31: 3.2%), but the difference was not statistically significant (p-value: 0.1011). Of the 36 patients that were not upstaged, none developed invasive carcinoma or DCIS during follow up (average 47 months).

Conclusions: All LCIS types that are associated with imaging findings other than calcifications should be excised. CLCIS associated with imaging findings of calcifications only, may be observed since the upstage rate is low. Additional studies are needed for LCIS variants diagnosed on core needle biopsy with imaging findings of calcification only, to determine appropriate management.

99 Breast Tumor Measurement After Neoadjuvant Chemotherapy Using the 8th Edition of the American Joint Committee on Cancer Staging System: Impact on Estimates of Tumor Size and Discrepancies with Residual Cancer Burden Class

Dawn Harter¹, Johann D. Hertel¹, Siobhan O'Connor², Benjamin Calhoun¹

¹The University of North Carolina at Chapel Hill, Chapel Hill, NC, ²University of North Carolina School of Medicine, Chapel Hill

Disclosures: Dawn Harter: None; Johann D. Hertel: None; Siobhan O'Connor: None; Benjamin Calhoun: *Consultant*, Luminex Corp

Background: In the 8th Edition of the American Joint Committee on Cancer Staging System (yAJCC) for breast cancer after neoadjuvant chemotherapy (NAC), tumor size is based on the largest focus of residual tumor, excluding treatment-related fibrosis. The goal of this study was to assess the impact of strict adherence to yAJCC

criteria on residual breast tumor size and discrepancies between yAJCC stage and Residual Cancer Burden (RCB) class.

Design: Breast cancer resections after NAC from 2016-2020 were identified in the Anatomic Pathology laboratory information system. Stage IV and neoadjuvant endocrine therapy alone were exclusion criteria. Tumor size, ypT category and focality were reassessed using current yAJCC criteria and compared to the original reports. A mean of 32 slides per case were reviewed (range, 11-92).

Results: A total of 260 cases met inclusion criteria, including 80 (31%) TNBCs, 74 (28%) HER2+, and 106 (41%) hormone receptor-positive/HER2-negative (HR+/HER2-). Slide review is complete for 84/260 (32%) randomly selected cases, including 24 (29%) TNBCs, 23 (27%) HER2+ and 37 (44%) HR+/HER2-. Of the 74 cases with residual tumor, the reassessed tumor size and ypT category differed from the original report in 37 (50%) and 34 (46%) cases, respectively. In all of these cases, the tumor size or ypT category was smaller/lower on review. The 34 cases with lower ypT categories included 27% of TNBCs, 69% of HER2+ and 47% of HR+/HER2- ($p=0.04$). Of the 239 cases with residual tumor in the original report, 12 (5%) were classified as multifocal versus 43/74 (58%) after review ($p<0.001$). The reassessed yAJCC stage group differed from the original report in 14 (19%) cases (all down-staged). There were 95/239 (40%) cases with yAJCC/RCB discrepancies in the original reports versus 38/74 (51%) after slide review ($p=0.08$). The yAJCC/RCB discrepant cases in the original reports included 43% of TNBCs, 34% of HER2+ and 34% of HR+/HER2- versus 38% of TNBCs, 35% of HER2+ and 57% of HR+/HER2- after review ($p=0.18$).

Conclusions: Strict adherence to yAJCC criteria for measurement of the residual breast tumor after NAC resulted in smaller tumor size, lower ypT category and lower yAJCC stage in a subset of cases. More tumors were classified as multifocal. There was no significant change in the frequency of yAJCC/RCB discrepancies.

100 Clinical and Pathologic Features Associated with Invasive Breast Carcinoma with 2018 ASCO/CAP Group ISH 2 Results (HER2/CEP17 ratio ≥ 2.0 and Average HER2 Copy Number of < 4.0)

Raza Hoda¹, Patrick McIntire¹, Miglena Komforti¹, Erinn Downs-Kelly¹

¹Cleveland Clinic, Cleveland, OH

Disclosures: Raza Hoda: None; Patrick McIntire: None; Miglena Komforti: None; Erinn Downs-Kelly: None

Background: HER2-targeted therapies have proved to improve clinical outcome in patients (pts) with HER2-amplified invasive breast carcinomas, compared to those with HER2-negative carcinomas. Accurate appraisal of HER2 status is integral in intendance of pts with breast carcinoma. In 2018, ASCO/CAP updated HER2 testing guideline to address uncommon results using dual-probe in-situ hybridization (ISH). Cases with *HER2*/CEP17 ratio ≥ 2.0 but average *HER2* copy number < 4.0 signals per cell (ISH Group 2) are no longer considered eligible for anti-HER2 therapy, when corresponding HER2 immunohistochemistry (IHC) is 0, 1+, or 2+. ISH Group 2 results are rare and represented 0.8% of cases in the seminal HERA trial; thus, prognostic and predictive data remain limited.

Design: The institutional database was interrogated. Pts diagnosed between 01/01/12-12/31/14 with invasive, recurrent, or metastatic breast carcinoma with HER2 FISH testing performed at our center were identified. All cases with *HER2*/CEP17 ratio ≥ 2.0 and average *HER2* copy number < 4.0 were selected. When available, pt age, tumor size, lymph node status, histologic subtype, tumor grade, hormone receptor status, HER2 IHC results, treatment regimen (targeted HER2, cytotoxic, hormone, and radiation therapies), and follow-up were recorded. Differences in categorical variables were assessed with χ^2 and Fisher exact tests, where applicable, and in noncategorical variables with Student *t* test. Statistical significance was established at $P<.05$.

Results: During the study period, 40 pts had breast carcinoma reclassified as ISH Group 2 (Table 1). Median age was 62 years (mean, 61 y; range, 27-93 y). Median tumor size was 20 mm (mean, 23 mm; range, 5-109 mm); 52% were pT1 tumors. The most common histologic type was invasive carcinoma of no special type (30/40; 75%). Twelve (36%) of 33 pts who had lymph node assessment showed nodal involvement. Twenty-one (53%) of 40 pts received anti-HER2 therapy, 8 of whom were treated in the neoadjuvant setting. Three (40%) of these 8 pts achieved pathologic complete response (pCR). Pts treated with HER2-targeted therapy were younger and had tumors of higher histologic grade, compared to pts without anti-HER2 therapy; however, these differences were not

statistically significant ($P=.29$ and 1.0 , respectively). The only significant difference between pts treated with and without anti-HER2 therapy was administration of cytotoxic chemotherapy ($P<.001$). Overall, clinical outcome was similar between the two groups.

Table 1. Clinical and pathologic features of 40 patients with breast carcinoma with 2018 American Society of Clinical Oncology/College of American Pathologists ISH Group 2 results ($HER2/CEP17$ ratio ≥ 2.0 and average $HER2$ copy number <4.0 signals/cell), treated with and without targeted HER2 therapy.

Feature	Group 2 Patients treated with anti-HER2 therapy (n = 21)	Group 2 Patients treated without anti-HER2 therapy (n = 19)	P
Age, median, (mean), [range], y	57 (59) [27-87]	65 (64) [37-93]	.29
$HER2/CEP17$ ratio, median, (mean), [range]	2.3 (2.3) [2.0-3.1]	2.1 (2.2) [2.0-3.3]	.17
$HER2$ copy number, median, (mean), [range]	3.6 (3.5) [2.5-3.9]	3.6 (3.4) [2.2-3.8]	.33
Pathologic tumor stage, No. (%)			.17
T1	11 (52)	12 (63)	
T2	8 (38)	4 (21)	
T3	1 (5)	1 (5)	
T4	1 (5)	1 (5)	
Data not available	0	1 (5)	
Lymph node involvement, No. (%)			.69
Yes	6 (29)	6 (32)	
No	12 (57)	9 (47)	
Data not available	3 (14)	4 (21)	
Histologic grade, No. (%)			1.0
1	1 (5)	1 (5)	
2	6 (28)	11 (58)	
3	14 (67)	7 (37)	
Hormone receptor status, No. (%)			.19
Hormone receptor +	12 (57)	15 (79)	
Hormone receptor -	9 (43)	4 (21)	
$HER2$ Immunohistochemistry result, No. (%)			1.0
Negative (0 or 1+)	4 (19)	9 (48)	
Equivocal (2+)	2 (9)	5 (26)	
Positive (3+)	1 (5)	0	
Not performed	14 (67)	5 (26)	
Tumor histology, No. (%)			1.0
Invasive carcinoma of no special type	15 (71)	15 (79)	
Invasive lobular carcinoma, classic or pleomorphic types	4 (19)	0	
Invasive ductal carcinoma with mixed features ^a	1 (5)	4 (21)	
Metaplastic carcinoma	1 (5)	0	
Radiation therapy, No. (%)			.58
Received	10 (48)	7 (37)	
Did not receive	11 (52)	11 (58)	
Data not available	0	1 (5)	
Cytotoxic chemotherapy, No. (%)			<.001 ^b
Received	20 (95)	6 (32)	
Did not receive	1 (5)	12 (63)	
Data not available	0	1 (5)	

Endocrine therapy, No. (%)			.33
Received	10 (48)	12 (63)	
Did not receive	11 (52)	6 (32)	
Data not available	0	1 (5)	
Clinical status, No. (%)			1.0
No evidence of disease	13 (62)	13 (68)	
Alive with recurrent and/or metastatic disease	3 (14)	1 (5)	
Died of disease	5 (24)	3 (16)	
Died of other causes	0	2 (11)	
Clinical follow-up, median (mean), [range], m	76 (66) [2-101]	79 (72) [3-101]	.55

Abbreviations: HER2, human epidermal growth factor receptor 2; ISH, in-situ hybridization; m, months; y, years.

^a Invasive ductal carcinoma with mixed features encompasses cases of invasive ductal carcinoma with special histological features, including mucinous and micropapillary features.

^b Statistically significant *P* value < .05 by Student's *t* test, Fisher's exact test, or χ^2 , where applicable.

Conclusions: Scarcity of ISH Group 2 tumors shrouds our understanding of anti-HER2 therapy in such pts. This retrospective study with median follow-up of 6 years shows that pts with ISH Group 2 tumors had similar clinical outcomes, irrespective of treatment with HER2-targeted therapy. Further analysis of our cohort and evaluation of patient outcomes in the prospective setting would provide valuable data.

101 Dual Detection of Extracellular and Intracellular Domains of HER2/ERBB2 Reveals Distinct Patterns of Isoform Expression with Mechanistic and Therapeutic Implications
 Michael Hsieh¹, Hidetoshi Mori¹, Jasmine Rosa², Hyeongsun Moon³, Louis Schuetter², Qian Chen², Joshua Snyder⁴, Alexander Borowsky⁵
¹University of California, Davis, Davis, CA, ²UC Davis Medical Center, Sacramento, CA, ³School of Veterinary Medicine, UC Davis, Davis, CA, ⁴Duke University Medical Center, Durham, NC, ⁵UC Davis Health System, Sacramento, CA

Disclosures: Michael Hsieh: None; Hidetoshi Mori: None; Jasmine Rosa: None; Hyeongsun Moon: None; Louis Schuetter: None; Qian Chen: None; Joshua Snyder: None; Alexander Borowsky: None

Background: A HER2 isoform called p95HER2 is generated from alternative splicing or a post-translational modification by protease. p95HER2 can induce constitutive activation of downstream signaling pathways via an intracellular tyrosine kinase domain. Moreover, the consequence of truncated extracellular domain (ECD) is the lack of a Trastuzumab binding domain, leading to drug resistance. Detection of p95HER2 is limited in current recommendations for HER2 testing, which include detection of the intracellular domain (ICD) of HER2 by immunohistochemistry (IHC) and HER2 DNA amplification by Fluorescent In-Situ Hybridization. p95HER2 is known to be observed frequently in HER2+ tumors, but the proportion of p95HER2 produced by either alternative splicing or protease activity and its resulting clonal distribution in tumors is unknown. Hence, we sought to assess the patterns of ECD loss in HER2+ breast cancers.

Design: 39 HER2+ cases, which were pre-tested with both Herceptest IHC and Pathvysion two color FISH, were collected from the diagnostic biopsy service at UC Davis. ECD and ICD of HER2 were visualized using fluorescence based IHC, and imaging analysis was performed with a multi-spectral imaging microscope. Full-length versus p95HER2 was judged by cell positivity for both ECD and ICD versus only ICD.

Results: Our multiplex-IHC revealed four distinct patterns: 'Pattern 1' is full length HER2 (FL-HER2) possessing both ECD and ICD; 'Pattern 2' is fully p95HER2 which only stained positively for ICD; 'Pattern 3' is a mixture of subclonal p95HER2 and FL-HER2 tumors; and 'Pattern 4' is a mixture of various levels of ECD within the lesion

expressing both p95HER2 and FL-HER2. The analysis showed the following rates: 28.2% (Pattern 1), 12.8% (Pattern 2), 28.2% (Pattern 3) and 30.7% (Pattern 4).

Figure 1 - 101

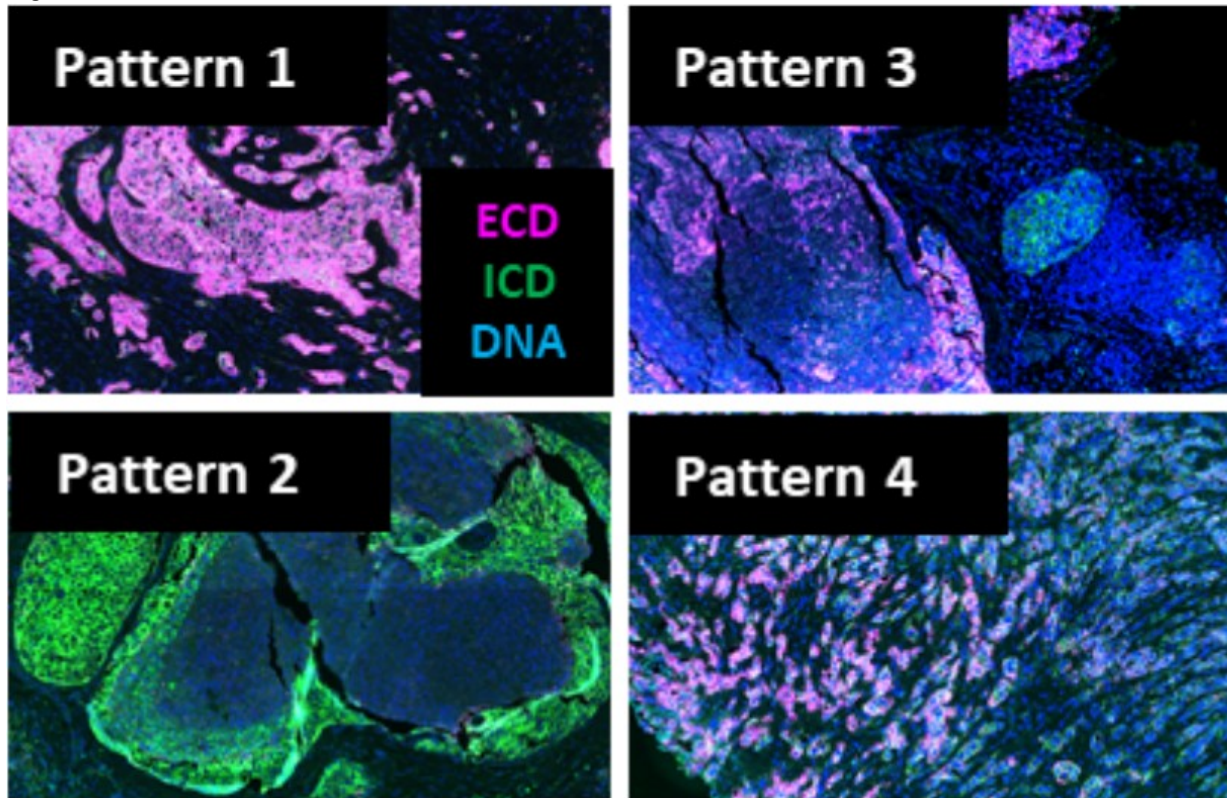


Figure. Multiplex IHC analysis for identifying p95HER2. Breast cancer tissues were stained for detecting ECD (magenta) and ICD (green) of HER2 and DNA (blue). There are 4 patterns identified: (Pattern 1) full length HER2 (FL-HER2), (Pattern 2) p95HER2, (Pattern 3) subclonal p95HER2 and FL-HER2 and (Pattern 4) mixture of p95HER2 and FL-HER2.

Conclusions: Here we effectively show ECD domain loss in Herceptest-positive samples in patterns 2, 3 and 4. Because p95HER2 has implications with respect to Trastuzumab resistance, it is important to add efficient p95HER2 detection to our current clinical workflow. This should help determine better therapeutic options for targeting p95HER2, such as a strategy to inhibit specifically the HER2 tyrosine kinase domain or novel targeting neopeptides and/or N-terminus of p95HER2.

102 Clinicopathologic and Molecular Characterization of Low-Grade Early-Stage Breast Carcinoma with Unusual HER2 Overexpression

Natasha Hunter¹, Lisa Han², Eric Konnick¹, Thing Rinda Soong³

¹University of Washington, Seattle, WA, ²University of Chicago, Chicago, IL, ³University of Pittsburgh, Pittsburgh, PA

Disclosures: Natasha Hunter: None; Lisa Han: None; Eric Konnick: None; Thing Rinda Soong: None

Background: Breast tumors that overexpress human epidermal growth factor receptor 2 (HER2) generally display a high-grade histology and a more aggressive clinical phenotype than HER2-negative tumors, requiring chemotherapy and HER2-directed therapies at lower pT and pN stages to achieve comparable outcomes to patients with luminal A and B phenotypes. Identifying carcinomas that are HER2-driven is therefore critical. HER2-positivity is very rare in low-grade tumors, and its biologic implication remains unclear in that setting. We aimed to characterize the clinicopathologic and molecular profiles of these tumors with unusual HER2 expression.

Design: We identified 22 Nottingham grade 1 invasive carcinomas that were confirmed HER2-positive by standard guidelines via immunohistochemistry and/or fluorescence in-situ hybridization studies on core biopsies. Hormone receptor profiles were assessed using immunohistochemistry. Histology was reviewed by two independent pathologists. Fourteen cases had sufficient tissue for genomic evaluation, and were examined by a clinically validated next generation sequencing (NGS) assay that interrogates the full coding sequences of 340 genes for mutations and copy number variations (CNVs). Frequencies of molecular alterations and clinicopathologic features in subgroups were compared by Fisher's exact test.

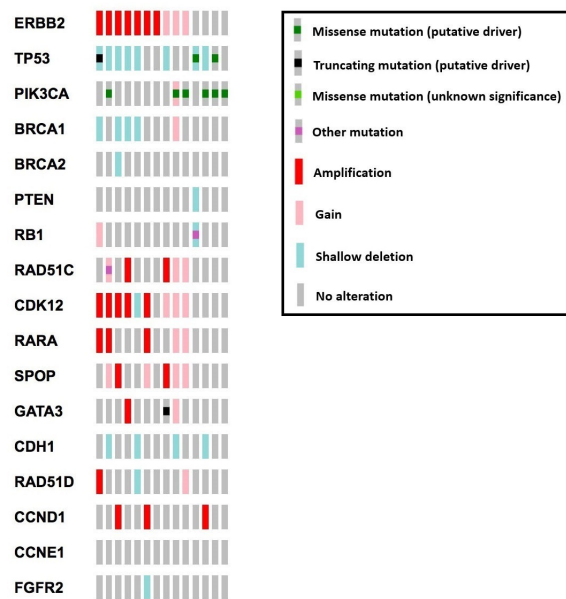
Results: Median age was 57 years (range: 36-72). The majority (81%) of tumors were invasive ductal carcinoma, and most (86%) were <2 cm in size (Table in Figure 1). Eight (36%) cases had positive lymph nodes at the time of resection (macrometastases: 4 ; micrometastases: 4). Five tumors were upgraded to Nottingham grade 2 upon excision. No change in HER2 status in resection samples was detected in re-tested specimens (8/22). All except one sample were ER positive. More than half (54%) received HER2-directed therapy, and none experienced a recurrence or disease-related death with a median follow-up of 351 days (range: 21-4732). Ten of 14 sequenced samples exhibited gain (n=3) or amplification (n=7) of *ERBB2*. No point mutation in *ERBB2* was identified. *PIK3CA* (43%) and *TP53* (21%) comprised the most common genetic alterations predicted to be pathogenic in this cohort (Figure 2). No significant association of genetic alteration with clinical or pathologic features was noted. BluePrint molecular subtyping analysis is in process.

Figure 1 - 102

Patient and tumor features of low-grade HER2-positive invasive carcinoma in breast (N=22)	
Characteristics	N (%)
Demographics	
Median age at diagnosis (years)	57 (range: 35-72)
Caucasian	20 (90)
African American	1 (5)
Unknown race	1 (5)
Pathology	
<u>Tumor subtype</u>	
Ductal	18 (82)
Mucinous	2 (9)
Others	2 (9)
<u>Tumor upgrade in resection</u>	
	5 (23)
<u>Tumor stage</u>	
pT1	21 (95)
pT2	1 (5)
<u>Nodal stage</u>	
pN0	14 (64)
pN0(mi)	4 (18)
pN1	3 (13)
pN2	1 (5)
<u>Hormone receptor status</u>	
ER-positive	21 (95)
PR-positive	21 (95)
Therapy	
Adjuvant chemotherapy	12 (55)
Neoadjuvant chemotherapy	2 (9)
HER2-directed therapy	11 (59)
Unknown	4 (18)

Figure 2 - 102

Select recurrent genetic alterations detected in low-grade HER2-positive invasive carcinoma in breast



Conclusions: To our knowledge, this is the first and largest series evaluating HER2-positive low-grade breast carcinoma using a comprehensive NGS panel. Results confirm presence of *ERBB2* CNVs underlying HER2 positivity in most of the tumors. A minority of these cases lack apparent *ERBB2* genetic alterations, suggesting possible tumor heterogeneity, or alternative pathway(s) contributing to HER2 protein overexpression. The findings warrant further studies to define which patients may be spared HER2-directed therapy and related toxicity.

103 Accuracy and Comparison of Core Needle Biopsy Diagnoses with Excision Specimen Diagnoses in Fibroepithelial Lesions of Breast

Romana Idrees¹, Alka Rani¹, Muhammad Usman Tariq¹
¹Aga Khan University Hospital, Karachi, Pakistan

Disclosures: Romana Idrees: None; Alka Rani: None; Muhammad Usman Tariq: None

Background: Breast lump is the commonest symptom with which patients present in breast clinic. Histological tissue diagnosis is a universally accepted means of definitive diagnosis of a breast lump. Fibroepithelial lesions (FEL) of the breast are biphasic neoplasms composed of a proliferation of both epithelial and stromal components and include fibroadenoma (FA) and phyllodes tumor (PT). PT are related with recurrence and warrants an excision with safe margins. Therefore, PT needs to be differentiated from FA which isn't straightforward on core needle biopsy (CNB). Our aim was to assess the accuracy of CNB diagnosis of FA and PT by comparing it with diagnosis on subsequent excision specimen

Design: At total of 166 cases of FEL of breast who underwent CNB and subsequent complete excision between January 2001 and December 2019 were included in our study. Microscopy glass slides of these cases were blindly and independently reviewed for diagnoses by two pathologists.

Results: Out of 166 cases, 125 (75%) were reported as a definite diagnosis on CNB and 41(25%) cases were reported as FEL with differential diagnosis of FA & PT. On CNB, 76 cases were diagnosed as FA and 49 cases as PT while 110 cases were diagnosed as FA and 56 cases as PT on excision. (Table 1). Among 125 cases, CNB diagnosis and excision biopsy diagnosis were concordant in 113 (90.4%) cases. Among 12 cases with discordant diagnoses, 3 (25%) cases diagnosed as FA on CNB were diagnosed as PT on excision. Tumor size in these cases

was 6 cm, 12.5 cm and 17.5 cm. Nine (75%) cases diagnosed as PT on CNB were diagnosed as FA on excision. These tumors ranged in size from 1.8 to 6.5 cm and median was 4.5 cm.

In 23 cases, PT were further categorized into benign, borderline and malignant categories on CNB. One out of 8 benign PT on CNB was upgraded to borderline PT on excision specimen. One out of 14 borderline PT on CNB was upgraded to malignant PT and another case was downgrade to benign PT on excision specimen. One case diagnosed as malignant PT on excision remained malignant on excision specimen. Two cases diagnosed as conventional FA on CNB turned out to be complex FA on excision specimen. One case each of juvenile FA and complex FA diagnosed on CNB was also diagnosed as same on excision specimen.

Overall diagnostic accuracy of fibroepithelial lesions on CNB is 90.4% with sensitivity 89% and specificity 93%. Positive predictive value was 96% and negative predictive value was 81.6%.

Table 1. Correlation between the diagnoses rendered on CNB and excision specimen. (n=166)

CNB diagnosis	Excisional biopsy diagnosis	
	Fibroadenoma	Phyllodes Tumor
Fibroadenoma (n=76)	73 (96%)	3 (4%)
Phyllodes Tumor (n=49)	9 (18.4%)	40 (81.6%)
Fibroepithelial lesion with differential diagnosis of fibroadenoma and phyllodes tumor (n=41)	28 (61%)	13 (39%)

- CNB shows good accuracy and overall good concordance with diagnoses made on excision specimen.
- All cases which were underreported as FA on CNB were more than 5 cm in size. Therefore, one should always think about the possibility of PT in tumor measuring >5cm in size.
- Juvenile fibroadenoma and complex adenoma can impose diagnostic challenge for pathologist on CNB and can be misdiagnosed as PT, causing unnecessary surgical intervention.
- Diagnostic accuracy can be improved by correlating with radiological findings.

104 Interobserver Variability in the Measurement of the Metastatic Tumor Size on Sentinel Lymph Nodes of Breast Carcinoma

Zena Jameel¹, Carlos Aneses-Gonzalez, Jose De Jesus¹, Marilyn Rosa¹
¹H. Lee Moffitt Cancer Center & Research Institute, Tampa, FL

Disclosures: Zena Jameel: None; Carlos Aneses-Gonzalez: None; Jose De Jesus: None; Marilyn Rosa: None

Background: Pathological evaluation of lymph nodes in breast cancer comprises the assessment of excised nodes from sentinel lymph nodes and /or lymph node dissection. The distinction among isolated tumor cells (ITCs), micrometastases and macrometastases is important for patient management and prognosis. Based on the most recent 8th edition of the AJCC staging manual, the size of a tumor deposit should be determined by measuring the largest dimension of any group of cells that are confluent or contiguous. Yet, we have encountered difficulties and subjectivity regarding how this concept is applied in practice.

Design: A survey of 10 microscopic images of lymph nodes involved by metastatic carcinoma was shared with a large group of practicing pathologists to determine the variability in measuring the extent of metastatic foci. Images were all taken at 1x magnification from AE1/3 stained slides and included 3 options to measure metastatic foci (A, B, C) without providing the foci size, and one option categorized as uncertain (not sure/other, D). For analysis, responses were aggregated as ITCs, micrometastases and macrometastases. Demographic information was also collected.

Results: A total of 88 pathologists completed the survey, the majority of which practice general pathology (75%). 69% would seek consultation to reach consensus in difficult cases. 49% have been in practice for over 10 years. We observed significant variability regarding how metastatic deposits are measured, with responses ranging from ITCs, micrometastases and macrometastases, sometimes in the same case (Table 1). Cases with extranodal extension (ENE) were prompt to more subjectivity (Cases 5, 9 and 10). In case 5, responses ranged from ITCs up

to macrometastases with 25% of responders unsure of how to measure it (Figure 1). In case 9, all options constituted macrometastases but 64% of participants opted to exclude the size of the ENE from the measurement. For case #10, the majority of participants (81%, Figure 2) classified the lymph node as negative in an image showing a focus of ENE/soft tissue tumor deposit. In cases with higher degree of concordance in metastases classification (6, 8), all given options constitute micrometastases.

Table 1. Tumor deposit classification based on responses (89%)

Case	Responses (%)				
	ITC	Micromet	Macromet	Negative	Not Sure/Other
1	50	43	0	0	7
2	0	59	35	0	6
3	0	7	79	0	14
4	0	13	81	0	6
5	6	20	49	0	25
6	0	99	0	0	1
7	0	50	43	0	7
8	0	96	0	0	4
9	0	0	95	0	5
10	n/a	n/a	11	81	8

Legends: ITC: isolated tumor cells; Micromet: micrometastasis; Macromet: macrometastasis

Figure 1 - 104

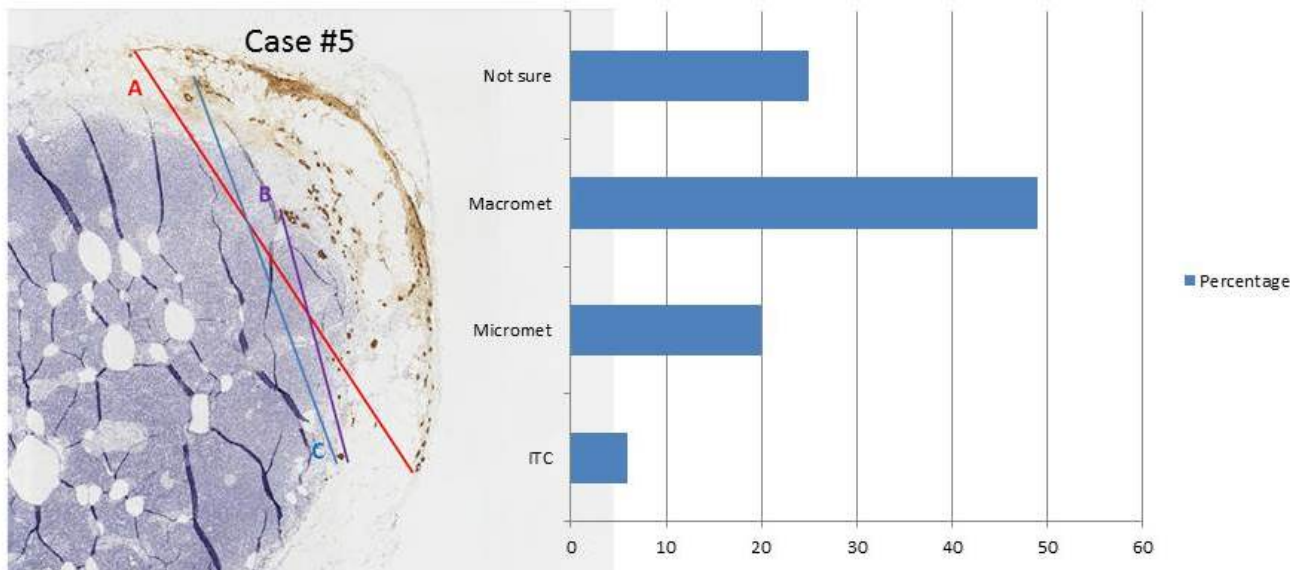
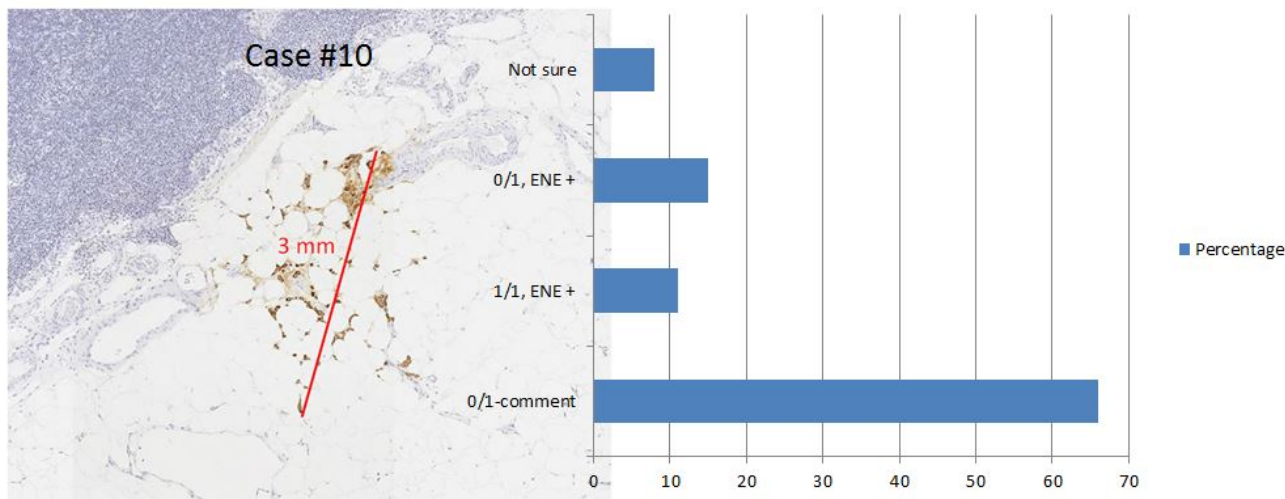


Figure 2 - 104



Conclusions: Our results underscore the inherent difficulty and thus variability that exist when measuring and classifying small metastatic tumor deposits in breast sentinel lymph nodes, even when guidelines have been already established.

105 Risk Stratification for Management of Breast Cancer Patients Using Genomic Testing in Needle Core Biopsies: Lessons Learned During the COVID-19 Pandemic and Future Implications

Hani Katerji¹, David Hicks¹, Bradley Turner¹, Ioana Moisini¹, Huina Zhang¹, Xi Wang², Linda Schiffhauer², Ajay Dhakal³, Alissa Huston², Carla Falkson²

¹University of Rochester Medical Center, Rochester, NY, ²University of Rochester, Rochester, NY, ³Wilmot Cancer Institute, University of Rochester Medical Center, Rochester

Disclosures: Hani Katerji: None; David Hicks: None; Bradley Turner: None; Ioana Moisini: None; Huina Zhang: None; Xi Wang: None; Linda Schiffhauer: None; Ajay Dhakal: None; Alissa Huston: None; Carla Falkson: None

Background: The COVID-19 pandemic has affected just about every aspect of life, including screening, diagnosis, treatment, and follow-up care for breast cancer patients. In March 2020, state governments and federal agencies recommended that healthcare systems delay elective care. In response, the COVID-19 Pandemic Breast Cancer Consortium Expert Opinion suggested the use of core biopsies for genomic testing to help triage patients for decisions about surgical vs. systemic treatment during the pandemic. This provided a unique opportunity to assess the feasibility and clinical utility of obtaining prognostic genomic information prior to making surgical or neoadjuvant treatment decisions in a real-world practice. Our clinic participated in a pre-operative quality project using Mammaprint (MP), a 70 gene prognostic assay, and Blueprint (BP), an 80-gene molecular subtyping assay, in order to assess their efficacy and effectiveness in treatment planning for newly diagnosed breast cancer patients. Here we report our initial findings.

Design: From April to September 2020, our multidisciplinary breast cancer clinic sent all breast core biopsies with a diagnosis of breast cancer for MP and BP testing as part of the routine workflow. Typically, genomic testing is performed on the surgical excision specimen (Standard workflow, Figure 1). In our study, turnaround time (TAT) was evaluated using the Rapid Results workflow (Figure 1). When genomic results differed from IHC/FISH results, or suggested a different treatment plan than did clinical factors alone, we referred to this as “reclassification”.

Results: MP and BP results were available for 95.3% of patients (n=201/211). The average TAT from biopsy to test results was 10.02 days, with an average lab TAT of 5.04 days. Results were available for tumor conference discussions 100% of the time. MP and BP resulted in reclassification 32% of the time (Table 1). Of the 65 patients where MP/BP re-classified results, treatment plans aligned with genomic results in 97% of cases.

Reclassification Rate vs. pathology IHC/FISH or Clinical Factors	# Patients	% Patients
ER+ (path IHC)--> Basal:	1/150	0.67%
Triple Negative (path IHC/FISH)--> Luminal A (BP)	2/26	7.69%
Triple Negative (path IHC/FISH)--> Luminal B (BP)	2/26	7.69%
HR-/HER2+ (path IHC/FISH)--> Basal (BP)	1/6	16.7%
Triple Positive (path IHC/FISH)--> Luminal B (BP)	7/19	36.8%
Triple Positive (path IHC/FISH)--> Luminal A (BP)	1/19	5.26%
Clinically High Risk (T2+ or LN+ and ER+)--> Luminal A (BP)	26/67	38.8%
Clinically Low Risk (<t2, In=""> MP Ultra-Low </t2,>	16/26	61.5%
Total Re-Classification Rate	65/201	32.3%

Figure 1 - 105

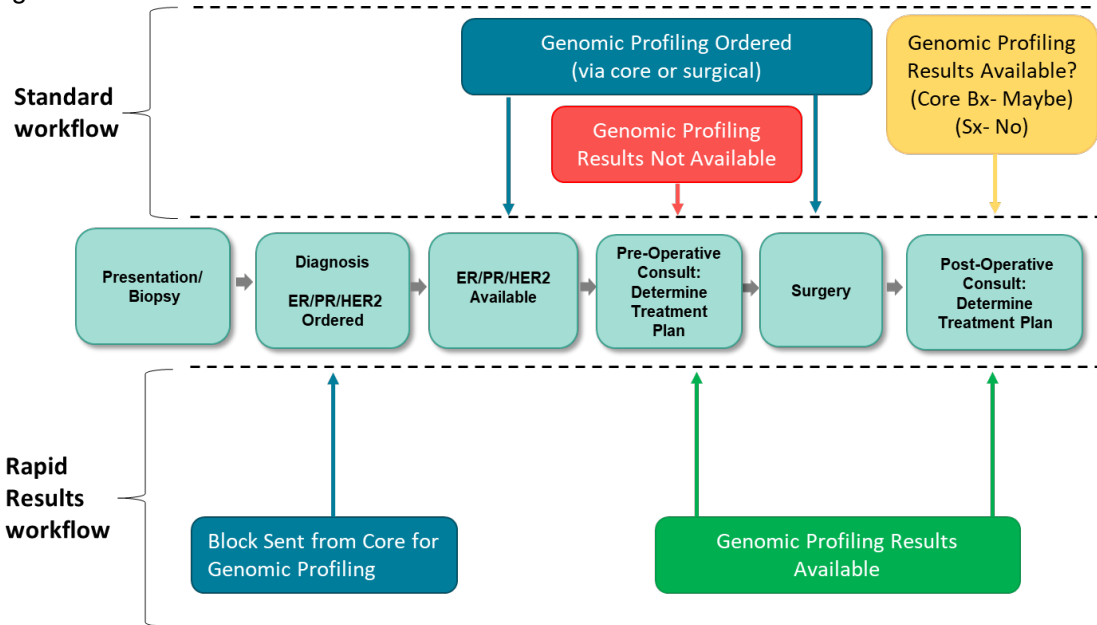
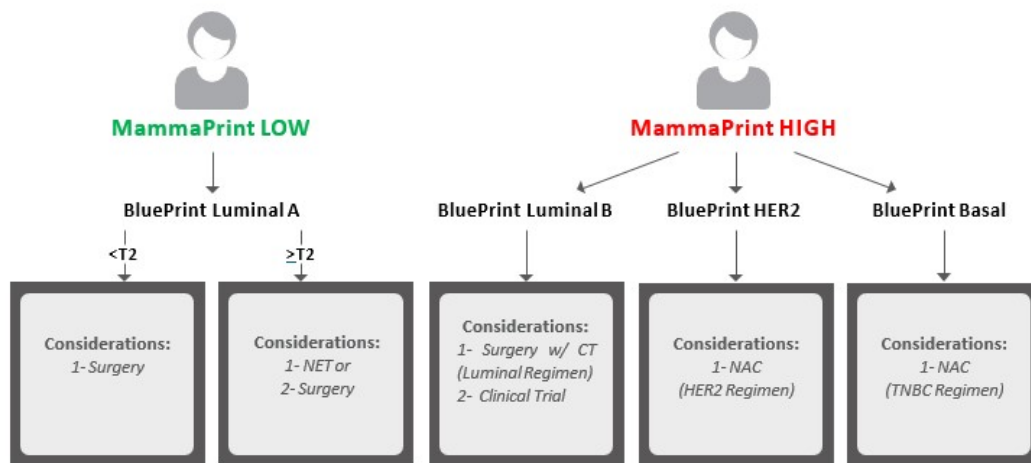


Figure 2 - 105

Pre-operative Treatment Algorithm Utilizing MP/BP Results

For Early Stage Breast Cancer Patients



Abbreviations: NET- Neoadjuvant Endocrine Therapy; NAC= Neoadjuvant Chemotherapy; CT= Chemotherapy; TNBC= Triple Negative Breast Cancer

Conclusions: Utilization of the Rapid Results workflow enabled genomic results to be incorporated into tumor conference peri-operative discussions in 100% of cases, resulting in better informed decisions about peri-operative

treatment planning. Although the Rapid Results workflow was designed for triage of patients during the COVID-19 pandemic, this approach has great potential for clinical utility beyond the pandemic (Figure 2).

106 Computerized Quantification of Tumor Infiltrating Lymphocyte (TIL) Density on H&E Images is Associated with Recurrence Risk in Ductal Carcinoma in Situ (DCIS)

Haojia Li¹, Pingfu Fu², Paula Toro², Anant Madabhushi², Mangesh Thorat³

¹CCIPD, Case Western Reserve University, Cleveland, OH, ²Case Western Reserve University, Cleveland, OH, ³Wolfson Institute of Preventive Medicine, Barts CRUK Cancer Centre, London, United Kingdom

Disclosures: Haojia Li: None; Pingfu Fu: None; Paula Toro: None; Anant Madabhushi: *Advisory Board Member, Aiforia Inc; Primary Investigator, Bristol Myers-Squibb; Grant or Research Support, AstraZeneca; Grant or Research Support, Boehringer-Ingelheim;* Mangesh Thorat: None

Background: Ductal Carcinoma in Situ (DCIS) is a pre-invasive form of breast cancer. The annual rate of progression to invasive disease is approximately 1% in DCIS treated by surgery alone. Therefore, it's critical to identify high risk DCIS, which would benefit from adjuvant treatment. Recent evidence suggests that the tumor immune microenvironment, especially, density of Tumor Infiltrating Lymphocytes (TILs) in DCIS is associated with the risk of recurrence and progression to micro and Invasive Breast Carcinoma. TIL quantification by pathologists is time-consuming and suffers from substantial inter-observer variability. In this study, we used computerized image analysis and machine learning approaches to quantitatively determine the density of TILs in DCIS and evaluate its association with probability of recurrence.

Design: Representative H&E Whole Slide Images (WSIs) and corresponding outcome information (recurrence events) from 119 DCIS patients (61 patients with a recurrence event either invasive progression or local recurrence and 59 patients censored) belonging to the no adjuvant treatment arm of the UK/ANZ DCIS trial were retrieved and collected from Queen Mary university of London. WSIs were scanned using 3DHistech scanners at 43x magnification. A Convolutional Neural Network (CNN) model described by Saltz *et.al* in 2018 for lymphocyte infiltration classification was applied on the DCIS slide images. TIL density was predicted by the CNN model inside each individual DCIS and the associated micro-environment (up to 250 um from DCIS boundary) as illustrated in Figure 1. The patients were classified as corresponding to high vs. low TIL density by applying the median TIL density value across all the patients as the threshold.

Results: A threshold of 24% of TIL density was applied to distribute the patients into high vs. low TIL density group. The patients in high TIL density group had a significantly worse Disease Free Survival (DFS) compared to those in low TIL density group, with Hazard Ratio (HR)=1.88 (95% Confidential Interval=1.14~3.11, p=0.014) from log-rank test in Kaplan–Meier (KM) survival analysis as shown in Figure 2.

Figure 1 - 106

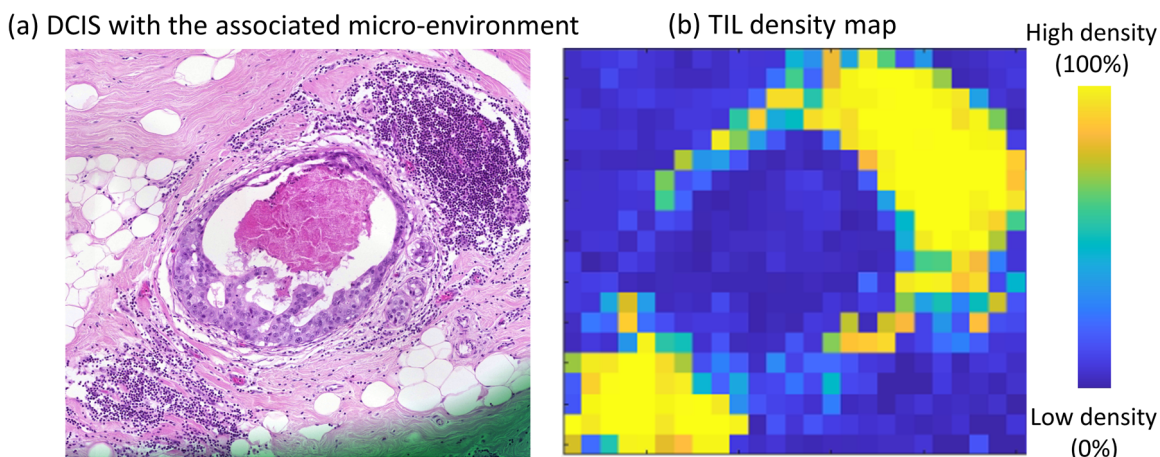


Figure 1: CNN model predicted TIL density map (b) on the H&E slide image of DCIS and the associated micro-environment

Figure 2 - 106

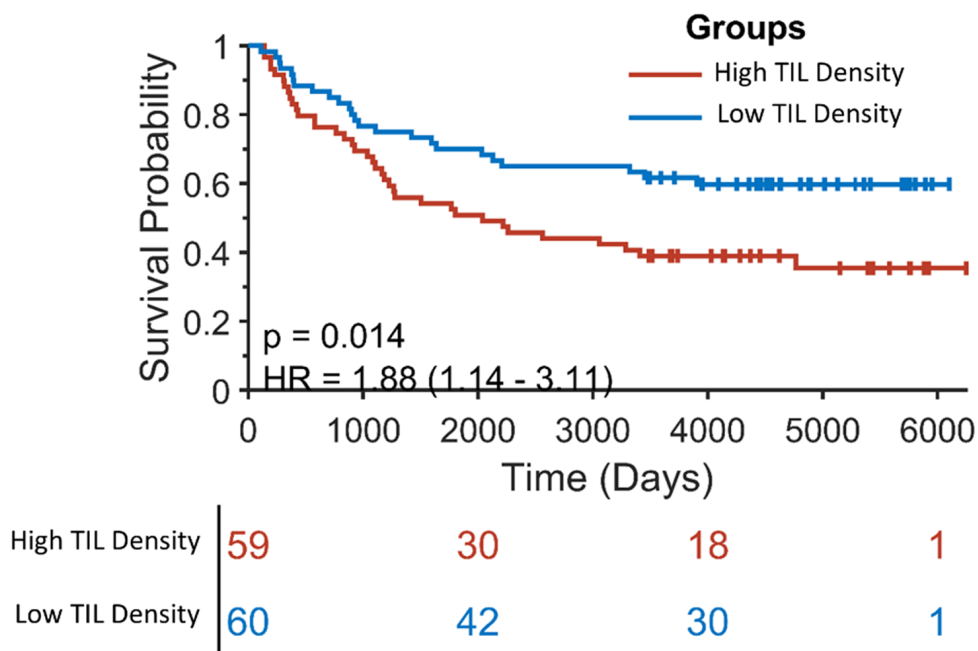


Figure 2: KM curve estimates of DCISs in high TIL density group vs. low TIL density group with DFS as the end point.

Conclusions: A stronger lymphocytic response, represented by high density of infiltrated lymphocytes, is associated with worse prognosis in terms of DFS in patients suffering from DCIS.

107 FOXC1: A Specific Biomarker for Triple Negative Breast Cancer Diagnosis and Classification

Ming Li¹, Hong Lv¹, Siyuan Zhong¹, Shuling Zhou¹, Anqi Li¹, Hongfen Lu, Wentao Yang¹
¹Fudan University Shanghai Cancer Center, Shanghai, China

Disclosures: Ming Li: None; Hong Lv: None; Siyuan Zhong: None; Shuling Zhou: None; Anqi Li: None; Hongfen Lu: None; Wentao Yang: None

Background: Forkhead box transcription factor C1 (FOXC1) expression has been identified as a specific biomarker for basal-like breast cancer (BLBC) in previous studies. However, few studies have investigated FOXC1 protein expression in surrogate molecular breast carcinoma subtypes defined by immunohistochemistry (IHC). This study aimed to investigate the diagnostic utility of the IHC-based FOXC1 expression in breast cancer subtyping and evaluate its correlation with histology subtypes, other biomarkers and clinicopathologic parameters in triple-negative breast cancer (TNBC).

Design: FOXC1 expression was evaluated using IHC in a large cohort of 2443 invasive breast cancer patients. Receiver operating characteristic (ROC) curves were used to assess the diagnostic ability of FOXC1 expression in predicting TNBC and identify the best cutoff value of FOXC1 staining. FOXC1 expression was correlated with clinicopathological parameters and other molecular markers in TNBC.

Results: The expression rate of FOXC1 in TNBC (77.84%) was significantly higher than in luminal A (5.3%), luminal B (8.2%) and human epidermal growth factor receptor 2 (HER2) positive (26.0%) subtypes. The area under the ROC curve (AUC) values confirmed the high diagnostic value of FOXC1 for TNBC prediction (AUC=0.861, p<0.001). The cutoff value of 1% showed a maximized sum of sensitivity (77.27%) and specificity (90.54%), while the 10% cutoff showed a higher specificity value (94.43%). In TNBC, FOXC1 expression was

significantly associated with younger age and aggressive tumor phenotypes (higher histology grade and higher Ki-67 expression). Furthermore, FOXC1 positive expression was mainly observed in invasive breast carcinoma (IBC) of no special type (NST, 94.21%), metaplastic carcinoma (83.33%) and adenoid cystic carcinoma (AdCC, 100%), while rarely observed in carcinoma with apocrine differentiation (1.69%). Correspondingly, FOXC1 expression was significantly associated with the expression of basal markers (CK14 and CK5/6) but negatively correlated with apocrine related markers (AR and GCDFP15) in TNBC.

Table 1 Correlation between FOXC1 expression with molecular markers in TNBC

Immunohistochemical markers	Overall	FOXC1 Positive(n=288)		FOXC1 negative (n=82)		p
AR						<0.001
negative	197	194	98.48	3	1.52	
positive	173	94	54.34	79	45.66	
GCDFP15						<0.001
negative	237	229	96.62	8	3.38	
positive	133	59	44.36	74	55.64	
GATA3						0.001
negative	65	62	95.38	3	4.62	
positive	305	226	74.10	79	25.90	
CK5/6						<0.001
negative	119	72	60.50	47	39.50	
positive	251	216	86.06	35	13.94	
CK14						<0.001
negative	183	108	59.02	75	40.98	
positive	187	180	96.26	7	3.74	
Ki-67						<0.001
<20%	64	16	25.00	48	75.00	
≥20%	306	273	89.22	34	11.11	

Conclusions: In conclusion, FOXC1 was a highly specific marker for TNBC. In TNBC, FOXC1 expression was positively correlated with basal markers, and negatively correlated with apocrine-related markers, which suggested that immunohistochemical detection of FOXC1 expression can be used as an additional diagnostic tool for prediction of triple-negative phenotype and further classification in TNBC.

108 RUNX3/SOX9 Expression in Relapsed ER+ Breast Cancer

Hui Liu¹, Hui Liu¹

¹The Affiliated Hospital of Xuzhou Medical University, Xuzhou, China

Disclosures: Hui Liu: None

Background: About 70% of breast cancer express estrogen receptor α (ERα). Tamoxifen is an agent used to treat patients with ER+ breast cancer. Despite the initial response of most patients with ER+ breast cancer to the treatment of tamoxifen, 30% - 40% of patients are subjected to drug resistance, tumor relapse and metastasis within 15 years. Therefore, it is important to further probe into the mechanism of breast cancer undergoing tamoxifen resistance. Overactivation of the Wnt signaling pathway is confirmed to contribute to tamoxifen resistance. RUNX3 is a tumor-suppressor gene that could inhibit the Wnt signaling pathway by regulating SOX9 expression. SOX9 (Sex-determining region Y-box 9) is a well-documented gene that could activate Wnt signaling pathway and has been confirmed to be related to tumor recurrence, metastasis and drug resistance. The purpose of this study is to study the expression of RUNX3 and SOX9 in primary and corresponding

relapsed breast cancer tissues to clarify the relationship between RUNX3 and SOX9 and whether RUNX3 or SOX9 was related to breast cancer tamoxifen resistance.

Design: 20 pairs of primary/relapsed formalin fixed paraffin embedded (FFPE) tissues of hormone receptor-positive breast cancer patients treated with tamoxifen from 2008. Tissue microarray (TMA) consisting of 200 breast cancer patients was prepared. The expression of RUNX3 and SOX9 was detected using immunohistochemistry staining and interpreted by experienced pathologists in the form of H-Score. The results were displayed as a heat map. Furthermore, RUNX3, SOX9 expression was detected in TMA of 200 ER+ breast cancer patients in the form of H-Score. Pearson correlation analysis was performed based on the scoring results.

Results: An analysis of the staining results of 20 primary/relapsed pairing samples showed that the positive staining patterns of both RUNX3 and SOX9 were clear nuclear staining. The expression of RUNX3 in relapsed specimen was significantly lower than that of the paired primary specimen ($P = 0.0410$), and the expression of SOX9 in the relapsed specimen was significantly higher than that of the corresponding primary specimen ($P = 0.0496$) (Figure 1). Analysis of TMA staining results involving 200 cases of ER+ breast cancer showed that the RUNX3 expression was significantly negatively related to the SOX9 expression ($R = -0.209$, $P = 0.008$) (Figure 2).

Figure 1 - 108

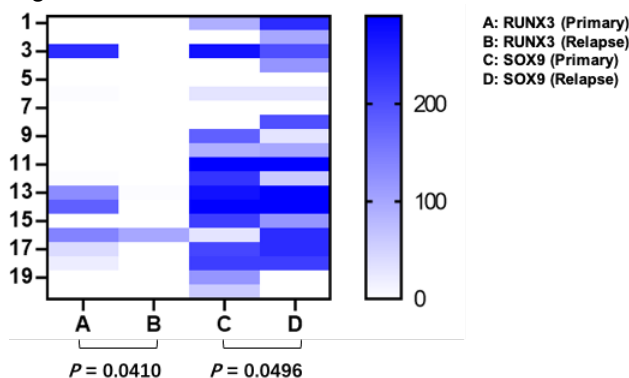
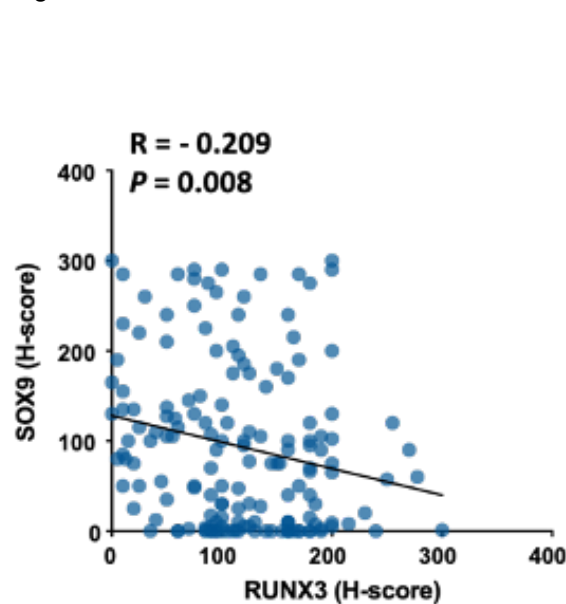


Figure 2 - 108



Conclusions: The study confirmed that RUNX3 decreased significantly in ER+ breast cancer relapsed specimens and SOX9 increased significantly on the contrary after tumor relapse. RUNX3 expression showed a significantly negative correlation with SOX9 expression. SOX9 might mediate tamoxifen resistance and breast cancer recurrence in ER+ breast cancer and could be negatively regulated by RUNX3.

109 Response to Neoadjuvant Therapy with Trastuzumab in Invasive Breast Cancers with Different HER2 FISH-Positive Pattern

Hong Lv¹, Qianming Bai¹, Hongfen Lu¹, Xiaoyan Zhou², Wentao Yang¹

¹Fudan University Shanghai Cancer Center, Shanghai, China, ²Fudan University Shanghai Cancer Center, Shanghai Medical College, Fudan University, Shanghai, China

Disclosures: Hong Lv: None; Qianming Bai: None; Hongfen Lu: None; Xiaoyan Zhou: None; Wentao Yang: None

Background: HER2-positive breast cancer patients may have different HER2/CEP17 ratios and HER2 copy numbers. Outcomes of HER2-positive breast cancer patients treated with neoadjuvant therapy combined with trastuzumab are also different. We aim to identify the relationship between different groups of HER2-FISH-positive results and pathologic complete response (pCR) of patients treated with neoadjuvant therapy combined with trastuzumab.

Design: 114 HER2-positive invasive breast cancer patients who received neoadjuvant therapy with trastuzumab and chemotherapy were collected. According to FISH results, 114 patients were divided into three groups. Group 1: HER2/CEP17 < 2.0 and HER2 copy number ≥6.0; Group 2: HER2/CEP17 ≥2.0 and HER2 copy number ≥4.0 and < 6.0; Group 3: HER2/CEP17 ≥2.0 and HER2 copy number ≥6.0. The efficacy of neoadjuvant therapy in three groups was analyzed.

Results: Among 114 patients, 113 were invasive ductal carcinomas and 1 case was invasive micropapillary carcinoma. 58 cases (58/114,50.9%) were luminal B type, and 56 cases (56/114,49.1%) were HER2 overexpression. 9 patients were included in FISH group 1, of which 3 (3/9,33.3%) were luminal B type and 6 (6/9,66.7%) were HER2 overexpression type. 21 patients were in FISH group 2, included 13 patients (14/21,66.7%) with luminal B type and 7 (7/21,33.3%) with HER2 overexpression type. There were 84 patients in FISH group 3, 41 (41/84,48.8%) with luminal B type and 43 (43/84,51.2%) with HER2 overexpression. There was no significant difference in molecular subtype among three groups ($\chi^2=3.269$, $P=0.195$). Totally, 33 patients (33/114,28.9%) achieved pathological complete response (pCR), and 81 cases (81/114,71.1%) were non-pCR. According to Miller-Payne grading system, 39 cases (39/114,34.2%) were grade 5, among which 6 patients still had residual cancer cells in axillary lymph nodes. 75 patients (75/114,65.8%) were grade 1-4. In FISH group 1, 4 cases (4/9,44.4%) achieved pCR and 5 (5/9,55.6%) were non-pCR. In FISH group 2, only 1 case (1/21, 4.8%) achieved pCR and 20 (18/21, 95.2%) were non-PCR. In FISH group 3, the number of pCR cases was 28 (28/84,33.3%) and non-pCR was 56 (56/84,66.7%). The pCR rate of neoadjuvant therapy in the second group was significantly lower than that in the other two groups, and there was significant difference in pCR rate among the three groups ($\chi^2=8.811$, $P=0.009$).

Table1:Molecular subtype and PCR status of different groups

	Group1	Group2	Group3	χ^2	p
molecular subtype				3.269	0.195
luminalB	3(33.3%)	14(66.7%)	41(48.8%)		
HER2 overexpression	6(66.7%)	7(33.3%)	43(51.2%)		
PCR status				8.811	0.009
PCR	4(44.4%)	1(4.8%)	28(33.3%)		
non-PCR	5(55.6%)	20(95.2%)	56(66.7%)		

Conclusions: Although all were invasive breast cancers with positive HER2-FISH results, patients with HER2/CEP17 ≥2.0 and HER2 copy number ≥4.0 and <6.0 seem to respond less favorably to trastuzumab-containing neoadjuvant treatment compared with other groups. The biological characteristics of this group of patients were worthy of further study.

110 Breast MRI-Detected Pseudoangiomatous Stromal Hyperplasia: Microvessel Analysis and Radiologic Features

Sundis Mahmood¹, Roberta diFlorio-Alexander², Todd Miller³, Jonathan Marotti²

¹Dartmouth-Hitchcock Medical Center, Lebanon, NH, ²Dartmouth-Hitchcock Medical Center, Geisel School of Medicine at Dartmouth, Lebanon, NH, ³Dartmouth Geisel School of Medicine, Lebanon, NH

Disclosures: Sundis Mahmood: None; Roberta diFlorio-Alexander: None; Jonathan Marotti: None

Background: The term "pseudoangiomatous" was given to the benign entity pseudoangiomatous stromal hyperplasia (PASH) because of the slit-like interanastomosing spaces lined by myofibroblasts that mimic blood vessels. However, PASH can be found in MRI biopsies of enhancing lesions, suggesting a significant vascular component might be present. The aims of this study were to evaluate the microvasculature of PASH using digital image analysis and to correlate findings with MRI features.

Design: PASH detected and biopsied by breast MRI was identified from a retrospective review of all MRI-guided breast biopsies performed at our institution from 2004-2019. One section from each case was immunostained with CD31 (Dako, 1:50) and scanned (Aperio AT2, Leica Biosystems) at 40x resolution. A representative field of PASH away from terminal duct lobular units (TDLUs), PASH immediately adjacent to TDLUs, non-PASH stroma adjacent to TDLUs, non-PASH fibrous stroma, and adipose tissue was selected for each case (Aperio ImageScope, Leica Biosystems). Microvessel density was determined for the selected fields using the Aperio Microvessel Analysis Algorithm (Leica Biosystems). Paired t-test and ANOVA with Tukey's multiple comparisons test were used to identify differences in mean microvessel density between the histologic areas. MRI features were reviewed by a breast radiologist.

Results: 10 cases of PASH detected and biopsied by MRI were identified (2% of all MRI breast biopsies). There was no difference in the mean microvessel density between PASH and non-PASH stroma ($p=0.7411$). PASH adjacent to TDLUs (Figure 1A-B) contained increased microvessel density compared to PASH away from TDLUs ($p=0.0008$) (Figure 1C-D), non-PASH fibrous stroma ($p=0.0003$), and adipose tissue ($p<0.0001$). Similarly, non-PASH stroma adjacent to TDLUs contained increased microvessel density compared to non-PASH fibrous stroma ($p=0.0056$) and adipose tissue ($p=0.0092$). There was no difference in the mean microvessel density between PASH adjacent to TDLUs and non-PASH stroma adjacent to TDLUs ($p=0.9965$). The mean size of PASH on MRI was 2.4 cm (range 0.7-5.0 cm). MRI review showed 8/10 cases were non-mass enhancement (Figure 2), 10/10 had increased background parenchymal enhancement, and 7/10 progressive or plateau kinetics.

Figure 1 - 110

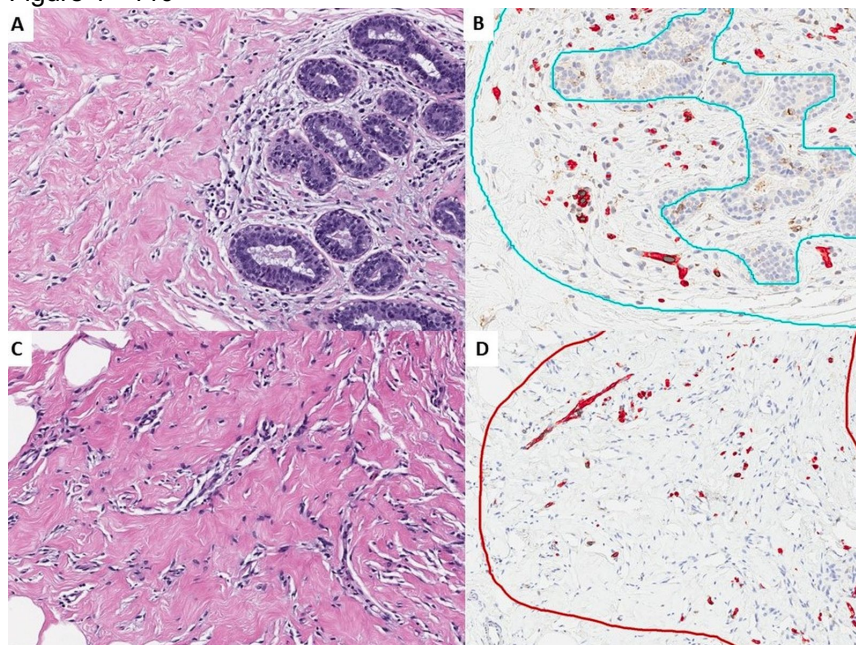
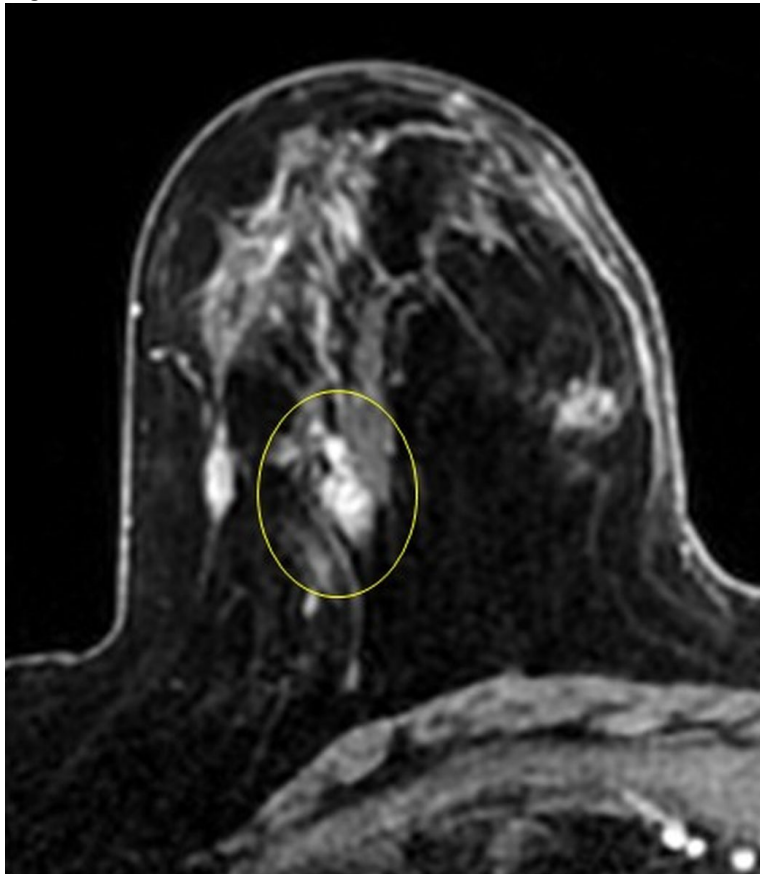


Figure 2 - 110



Conclusions: In this preliminary study evaluating MRI-detected PASH, digital image analysis showed a similar microvessel density between PASH and non-PASH stroma. Microvessel density was highest immediately adjacent to TDLUs; since the majority of cases displayed non-mass enhancement, further investigation of the epithelial-stromal interface as a possible contributing factor to the MRI findings of PASH is warranted.

111 Low ER Positive Breast Cancers are Characterized by Aggressive Histologic Features

Sundis Mahmood¹, Kristen Muller¹

¹Dartmouth-Hitchcock Medical Center, Lebanon, NH

Disclosures: Sundis Mahmood: None; Kristen Muller: None

Background: Breast cancers with low estrogen receptor (ER) expression, defined by 1-10% ER positivity, are infrequent, and their clinicopathological features are not well characterized. There are data that suggest low ER+ tumors are heterogeneous in both behavior and biology and often have gene expression profiles more similar to ER-negative cancers. We sought to characterize the clinical and pathological features of low ER+ breast cancers at our institution.

Design: Our pathology database was searched for all invasive breast cancers from 2012 to 2020. Invasive tumors with low ER expression (1-10%) were included. ER, progesterone receptor (PR) and HER2 (by dual-probe FISH) were performed on the core needle biopsies. Immunohistochemical assays were performed on paraffin-embedded tissue sections fixed in 10% neutral buffered formalin for 6-72 hours using the polymer system technique with appropriate controls. The assays were performed according to the manufacturer's instructions using Anti-ER (SP1) and Anti-PR (16) antibodies. ER was repeated on the surgical specimen in a minority of cases.

Results: Twenty-four cases were identified. All patients were female (mean age 60 ± 12.5 years). Histologic type was predominantly invasive ductal carcinoma (22/24, 92%), and tumor size ranged from 0.3 cm to 10.0 cm (mean = $3.1 \text{ cm} \pm 2.4 \text{ cm}$). Twenty-three cases were high-grade (96%), and one was intermediate-grade (4%). Ductal carcinoma in-situ and lymphovascular invasion were present in 43% of cases. Interestingly, ten (42%) tumors showed solid, sheet-like growth with associated necrosis, and among these, eight had pushing borders with prominent stromal lymphoplasmacytic inflammation, resembling the morphology described in basal-like or medullary-like breast cancers. Fourteen patients underwent axillary staging; metastases were present in five patients (N0 = 9, ITC = 1, N1 = 1, N2 = 0, N3 = 3). ER staining ranged from 1% to 10% with the majority showing weak expression. PR was negative in 75% of cases. HER2 was positive in a single (4%) case. One patient received neoadjuvant chemotherapy and showed a pathologic complete response in the surgical specimen. ER was repeated on four surgical specimens per oncologist request, which all again revealed low ER expression. The average Oncotype DX recurrence score was 44 (n=6). 52% of patients received hormone therapy, 74% received radiation therapy, and 86% received chemotherapy. Follow-up was available for 22 patients (mean 31.7 mos.); three patients developed recurrences, two of whom died of disease, while 19 patients currently have no evidence of disease.

Conclusions: The findings from our study support the notion that invasive breast cancers with low levels of ER expression often show aggressive histologic features.

112 Malignant Phyllodes Tumors: Re-classification with Consensus Guidelines and Subsequent Patient Outcomes

Patrick McIntire¹, Raza Hoda¹, Miglena Komforti¹, Erinn Downs-Kelly¹
¹Cleveland Clinic, Cleveland, OH

Disclosures: Patrick McIntire: None; Raza Hoda: None; Miglena Komforti: None; Erinn Downs-Kelly: None

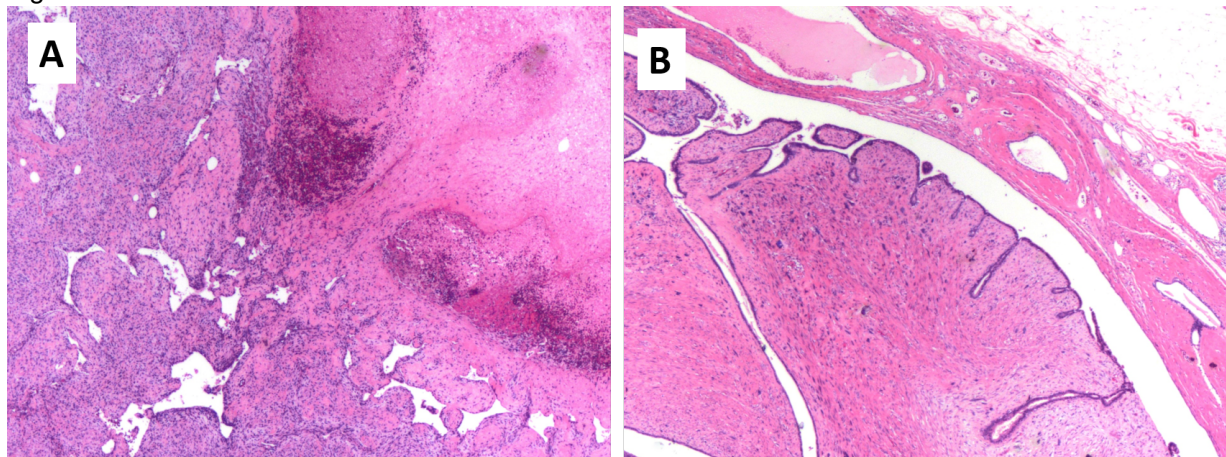
Background: Histologic classification of Phyllodes tumors (PT) is challenging due to the complex morphologic features and historically ambiguous diagnostic criteria. Criteria have been addressed by Tan et al. in 2016¹. Herein, we re-review all malignant PT (Figure 1A) diagnosed at our institution and re-classified them based Tan et al. consensus guidelines, correlating with outcome.

Design: All primary resection specimens of malignant PT were identified in the pathology files at our institution. H&E stained sections were reviewed by four AP board-certified, breast fellowship-trained pathologists. For each case, morphologic variables delineated in *Tan et al.* (i.e. stromal overgrowth, atypia, tumor border, presence of heterologous elements, presence of stromal overgrowth, necrosis) were scored, according to their guidelines. Following review, cases were reclassified as benign, borderline (low-grade malignant) or malignant. All discrepancies were discussed until there was a group consensus. The reviewing pathologists were blinded to patient outcomes.

Results: The final cohort consisted of 20 cases of malignant PT from 20 patients diagnosed between 1994 and 2019. The patients were all female with an average age of 57.5 years (range: 36-88 years). Upon reclassification, 5/20 were 'down-graded' to borderline PT (Figure 1B). All borderline PT demonstrated a nodular growth pattern (100%) and one had a definitively infiltrative stromal interface (20.0%). Stromal cell atypia was moderate in three (60.0%, 3/5) and marked in two (40.0%, 2/5). Stromal cellularity was mild in one (20.0%, 1/5), moderate in two (33.3%, 2/6) and marked in three (60.0%, 3/5). All five borderline tumors had pleomorphic tumoral giant cells and 'leaf-like' growth (100%, 5/5). No stromal overgrowth, necrosis or heterologous elements were present in the borderline tumors (0/5). All tumors were excised to negative margins. Of the borderline tumors, there was neither recurrence nor metastases recorded. Follow-up data for borderline PT ranged from 1.5-180 months.

In contrast, malignant PT resulted in 4/15 locoregional recurrences (26.6%) and 3/15 metastases (20.0%), overall 46.7%. No tumors were re-classified as benign.

Figure 1 - 112



Conclusions: The recent PT consensus guidelines are useful in the distinction between borderline and malignant PT¹. Application of these guidelines allowed for re-classification into biologically relevant disease categories. None of the re-classified borderline PT resulted in locoregional recurrence or metastatic disease.

1. Tan BY et al. 2016. Phyllodes tumours of the breast: a consensus review. *Histopathology*, 68(1), pp.5-21.

113 Clinicopathologic Findings in Breast Patients Status Post-Neoadjuvant Hormonal Therapy with Deferred Surgery Due to the SARS-CoV-2 (COVID-19) Pandemic

Harshita Mehrotra¹, Swetha Gaddam², Dhananjay Chitale²

¹Henry Ford Health System, Detroit, MI, ²Henry Ford Hospital, Detroit, MI

Disclosures: Harshita Mehrotra: None; Swetha Gaddam: None; Dhananjay Chitale: None

Background: The COVID-19 pandemic has presented oncologists with considerable challenges in providing effective care to patients with invasive breast cancer (IBC), while minimizing risk of exposure to this vulnerable high-risk population and assuring efficient utilization of resources. Per COVID 19 Pandemic Breast Cancer Consortium guidelines, patients with estrogen receptor positive (ER+) and HER2 negative early IBC (T1N0, T2 or N1 disease) could be safely placed on neoadjuvant endocrine therapy (NET) and surgery delayed for 6 to 12 months. Traditionally, these patients have been treated with upfront surgery and the current literature on the effect of delaying surgery in this cohort is limited. We aim to evaluate whether NET can be offered as a viable therapeutic alternative in this population.

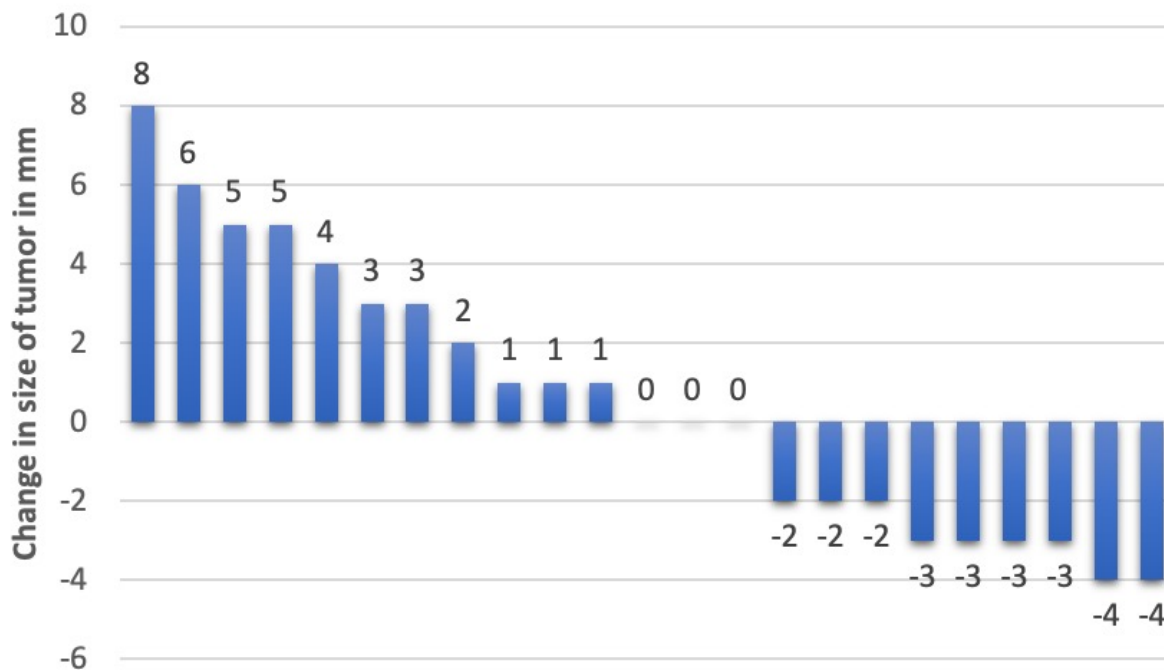
Design: Retrospective chart and pathology slides review was done for patients with ER+ IBC treated with NET followed by definitive surgery between 04/01/2020 and 09/30/2020. Tumor dimensions by ultrasonography (USG) at the time of biopsy were taken as pretreatment size and dimensions on pathological analysis of definitive surgical specimen were taken as posttreatment size. Statistical analysis was done using paired t-test and Pearson correlation in Microsoft excel version 16.42.

Results: Thirty-three patients fulfilled the inclusion criteria. Patient characteristics and treatment details are given in attached table 1 and waterfall plot for change in the tumor size for invasive ductal carcinoma (IDC) in figure 1. Given the significant known and observed discordance in radiological and pathological size in invasive lobular carcinoma (ILC), we excluded these patients from our analysis and got no statistically significant change in tumor size ($p = 0.44$). There was no correlation of treatment response with age, ethnicity, pretreatment size of tumor, histologic grade, ER status or duration of treatment. Comparing morphology of biopsy vs surgical resection, there were minimal histological changes of NET such as reduced cellularity, foamy histiocytes, necrosis, and fibrosis.

Patient Characteristics			
Age (years)	41 – 87 (mean 65)		
Ethnicity (no. of patients)	Caucasians 24	African Americans 6	Others 3
Reproductive status (no. of patients)	Postmenopausal 31	Premenopausal 2	
Histological type (no. of patients)	Invasive Ductal (IDC) 23	Invasive Lobular (ILC) 7	Mixed (IDC+ ILC) 3
Radiological (USG) size of tumor at biopsy (mm)	IDC 5 – 28 (mean 12.9)	ILC 6-30 (mean 13)	Mixed 8 – 64 (mean 28.3)
Nottingham grade (of 3)	One 14	Two 17	Three 18
ER status (%)	30 – 100 (median 100)		
PR status (%)	0 – 100 (median 85)		
Type of Hormonal therapy (no. of patients)	Anastrozole 16	Letrozole 13	Tamoxifen 4
Duration of treatment (months)	2.9 – 27.6 (median 5.6)		
Adverse Effects (no. of patients)	Hot flashes 1	Mood Changes 1	Myalgia 1
Pathological Size of tumor on definitive surgery (mm)	IDC 6 – 24 (mean 13.5)	ILC 1.5 – 65 (mean 27.9)	Mixed 10 – 69 (mean 32.5)
change in size of tumor (mm)	IDC -4 to 8	ILC -9.5 to 35	Mixed -3 to 9
P(T<=t) one-tail	IDC 0.44	ILC 0.05	Mixed 0.40

Figure 1 - 113

CHANGE IN SIZE OF TUMOR POST NEO-ADJUVANT ENDOCRINE THERAPY



Conclusions: NET can be safely offered to patients with ER+ early breast carcinoma for 6 to 9 months to defer surgery in this small cohort. However, this needs to be confirmed by larger prospective studies. No significant post-NET morphologic changes were noted in the tumor. ILC infiltrates as single cords with less conspicuous mass lesion, underestimating the tumor size on USG as highlighted by a significant discordance between USG and pathological size in our data set.

114 Pathobiologic Stratification of Oncotype DX Recurrence Scores and Comparative Validation of Three Surrogate Models

Anas Mohamed¹, Aisha Kousar², Takeda Kotaro², Joseph Geradts¹

¹Vidant Medical Center/East Carolina University, Greenville, NC, ²East Carolina University, Greenville, NC

Disclosures: Anas Mohamed: None; Aisha Kousar: None; Takeda Kotaro: None

Background: The Oncotype DX Recurrence Score (RS) is widely used by clinicians to predict recurrence and benefit from chemotherapy in ER-positive, N0 and N1 breast cancer patients. Cost and unavailability are two major disadvantages of the test. Multiple surrogate models have been developed to predict RS at no extra cost using different histologic and immunohistochemical parameters. This study aims to estimate the correlation of three surrogate models with the Oncotype DX RS, and to predict Oncotype DX risk category based on histologic type, tumor grade, and biomarker profile.

Design: A retrospective study of four hundred breast cancer cases received between 2005 and 2020 with available Oncotype DX RS was performed at our institution. Tumor size, histologic type, combined tumor grade, tubular grade, nuclear grade, mitotic grade, and biomarker profile were reviewed. RS was calculated by three surrogate models that do not include Ki67: Breast Cancer Prognostic Score (BCPS) (Geradts et al 2010), Magee 0 (Flanagan et al 2008), and Magee 2 (Klein et al 2013). The categorical concordance (Fig.1) and correlation (Fig.2) of each surrogate model with the Oncotype DX RS were calculated.

Results: Out of 400 cases, 322 cases (81%) were invasive ductal carcinoma, and 32 cases (8%) were invasive lobular carcinoma. 133 cases (33%) were low grade, 213 cases (53%) were intermediate grade, and 54 cases (14%) were high grade. All cases were ER-positive, 91% were PR-positive, and 97% were Her2-negative. BCPS showed the best categorical concordance (73%) with conventional cutoffs, and 54% concordance with TAILORx cutoffs. Both Magee models yielded similar and a slightly better categorical concordance (58%) than BCPS with TAILORx cutoffs. Only 4% of low grade tumors had a RS>25, compared to 12% of intermediate grade, and 35% of high grade tumors. About 14% of invasive ductal carcinomas had a RS>25, compared to only 1 of 32 cases of invasive lobular carcinoma (Table1). Among tumors with high PR expression, only 6% had a RS>25.

Pathologic Parameters	Conventional. Low Risk		Conventional. Intermediate Risk		Conventional. High Risk
	TAILORx. Low Risk	TAILORx. Intermediate Risk		TAILORx. High Risk	
	<11	11-17	18-25	26-30	>30
Histologic Type					
Invasive Ductal Carcinoma (n=322)	88 (27%)	113 (35%)	75 (23%)	19 (6%)	27 (8%)
Invasive Lobular Carcinoma (n=32)	7 (22%)	18 (56%)	6 (19%)	1 (3%)	0
Tumor Grade					
Low Grade (n=133)	42 (32%)	56 (42%)	29 (22%)	3 (2%)	3 (2%)
Intermediate Grade (n=213)	63 (30%)	83 (39%)	41 (19%)	13 (6%)	13 (6%)
High Grade (n=54)	5 (9%)	17 (31%)	13 (24%)	5 (9%)	14 (26%)
ER					
High (Allred Score 7-8) (n=366)	111 (30%)	142 (39%)	69 (19%)	17 (5%)	27 (7%)
Low (Allred Score 3-6) (n=34)	1 (3%)	12 (35%)	14 (41%)	0	7 (21%)
PR					
High (Allred Score 7-8) (n=282)	96 (34%)	133 (47%)	38 (13%)	10 (4%)	5 (2%)
Low (Allred Score 3-6) (n=83)	10 (12%)	21 (25%)	32 (39%)	6 (7%)	14 (17%)
Negative (Allred Score 0-2) (n=35)	1 (3%)	4 (11%)	13 (37%)	4 (11%)	13 (37%)
Her2					
Negative (n=389)	109 (28%)	153 (39%)	80 (21%)	19 (5%)	28 (7%)
Positive/Equivocal (n=11)	0	3 (27%)	3 (27%)	2 (18%)	3 (27%)

Figure 1 - 114

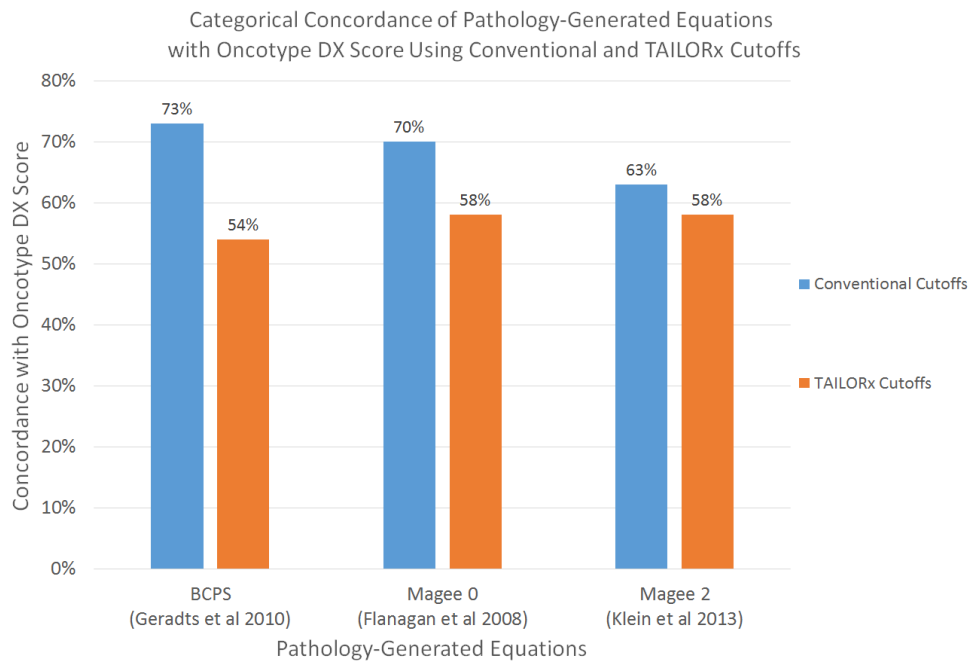
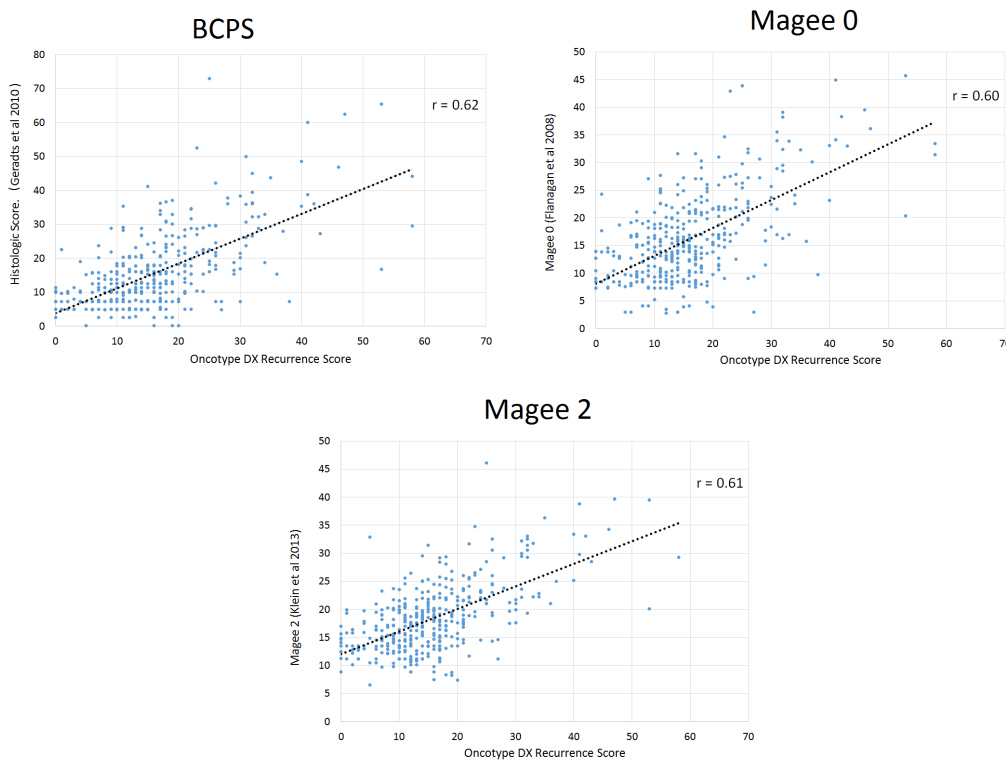


Figure 2 - 114



Conclusions: The three surrogate models demonstrated comparable correlation with the Oncotype DX RS. Categorical concordance of the three models was better when conventional cutoffs were used. A high Oncotype DX RS was observed only in a small percentage of invasive lobular carcinomas, low grade carcinomas, and tumors with high PR, suggesting that these types of tumors may not require Oncotype testing.

115 Can Automated Histomorphometric Analysis Accurately Classify Intraductal Proliferative Lesions of the Breast?

Amir Momeni Boroujeni¹, Ellen Alexander², Emily Bachert¹, Faisal Mahmood¹, Stuart Schnitt²
¹Brigham and Women's Hospital, Harvard Medical School, Boston, MA, ²Brigham and Women's Hospital, Boston, MA

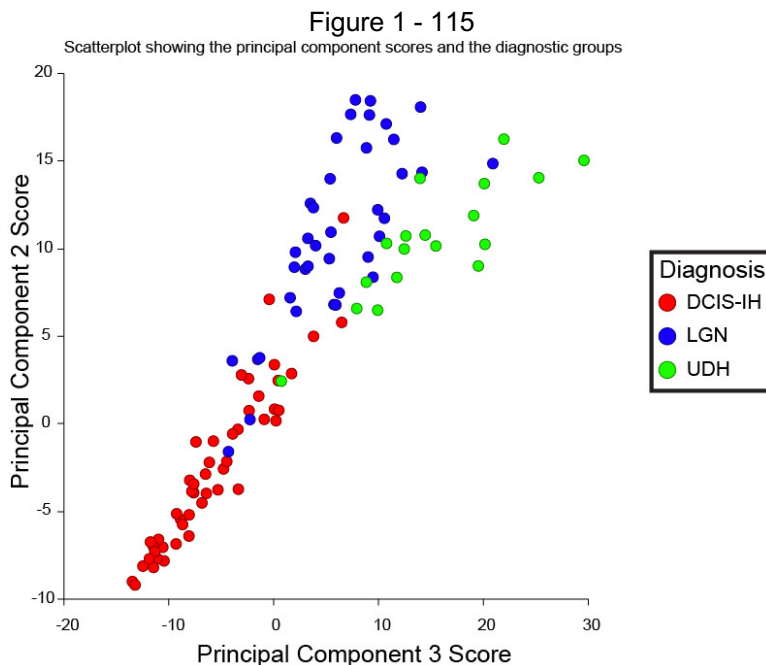
Disclosures: Amir Momeni Boroujeni: None; Ellen Alexander: None; Emily Bachert: None; Faisal Mahmood: None; Stuart Schnitt: None

Background: Diagnosis of breast intraductal proliferations is based primarily on qualitative assessment of cytological and architectural features. However, interobserver variability in classification as usual ductal hyperplasia (UDH), atypical ductal hyperplasia (ADH), and ductal carcinoma in situ (DCIS) has been repeatedly documented. In this study, we assessed the accuracy of automated histomorphometric evaluation of H&E sections using computational approaches for classifying these lesions.

Design: Representative foci of UDH, ADH, low grade ductal carcinoma in situ (DCIS-L), and intermediate or high grade DCIS (DCIS-I/H) from 150 consecutive breast core needle biopsies were photographed at 400x (total: 250 images). After annotation of the images, the STARDIST algorithm was used to segment the nuclei and extract histomorphometric features. Descriptive analysis followed by training of a random forest classifier was performed. For this initial analysis, ADH and DCIS-L were analyzed as a single low-grade neoplasia (LGN) group.

Results: DCIS-I/H had the largest nuclear area size (median: 36.1 μm^2) with high variability in size (interquartile range (IQR): 20.0 μm^2). LGN and UDH had similar median nuclear areas (26.6 μm^2 vs 28.4 μm^2). However, LGN had less nuclear size variation than UDH (IQR: 7.3 μm^2 vs 8.9 μm^2). UDH nuclei showed higher variability in hematoxylin staining intensity than LGN and DCIS-I/H (median hematoxylin SD: 0.06 vs 0.05 and 0.04 respectively). Conversely, LGN nuclei were darker than nuclei in DCIS-I/H and UDH (median hematoxylin intensity: 0.35 vs 0.34 and 0.32 respectively). These differences were all statistically significant (ANOVA $P < 0.001$ for all). Principal component analysis followed by K-means clustering with silhouette analysis showed that the nuclei are best clustered into 3 groups.

The 250 images were split into test and training groups using stratified randomization with 100 images assigned to the test group. A random forest classifier was trained to distinguish between UDH, LGN, and DCIS-I/H. At the image-level, the model was 91% accurate; 4/9 discrepancies involved misclassification of UDH as LGN or DCIS-I/H. The remainder were misclassifications between LGN and DCIS-I/H (Figure).



Conclusions: Objective, automated histomorphometric measures show significant differences among intraductal proliferations of the breast. These measures can be used to train probabilistic models to potentially serve as diagnostic support tools for pathologists. Our model, solely based on nuclear features, achieved an accuracy of 91% which may potentially be improved by quantifying and incorporating architectural features.

116 INSM1 Expression in Invasive Breast Carcinomas with a Focus on Neuroendocrine Neoplasms

Saleh Najjar¹, Gregor Krings², Yunn-Yi Chen², Sandra Shin³, Kimberly Allison¹, Gregory Bean¹

¹Stanford Medicine/Stanford University, Stanford, CA, ²University of California, San Francisco, San Francisco, CA, ³Albany Medical College, Albany, NY

Disclosures: Saleh Najjar: None; Gregor Krings: None; Yunn-Yi Chen: None; Sandra Shin: None; Kimberly Allison: None; Gregory Bean: None

Background: The current WHO classification of breast tumors defines breast neuroendocrine (NE) neoplasms as invasive carcinomas characterized by a combination of NE morphology and extensive immunoreactivity to NE markers. Insulinoma-associated protein 1 (INSM1) is an emerging nuclear marker of NE differentiation. Studies on INSM1 expression in the breast are very limited. Here, we characterize immunohistochemical expression of INSM1 in breast carcinomas (BCs) enriched for NE neoplasia, with comparisons to synaptophysin (SYN) and chromogranin (CHR).

Design: A cohort of 115 primary BC (73 whole sections, 42 tissue microarray cores) were evaluated for INSM1, SYN and CHR by immunohistochemistry. The series was enriched with cases demonstrating cytologic and architectural NE features (n=75), including solid papillary carcinoma (SPC), NE tumor, small cell NE carcinoma and large cell NE carcinoma, as well as other BCs (invasive ductal NST, lobular, metaplastic, etc). Cases ranged from Nottingham grade 1-3. Expression was assessed by the percentage of cells expressing the marker at any intensity. Bivariate correlations and comparison of means were conducted using Spearman's correlation and paired t-test, respectively.

Results: Overall, 48%, 41% or 25% of the cases was positive for INSM1, SYN and CHR, respectively. INSM1 expression correlated with SYN and CHR expression (0.53, $p < 0.01$ and 0.39, $p < 0.01$); INSM1 was positive in 31/42 (73%) SYN-positive cases and in 18/26 (69%) CHR-positive cases. Expression of all three markers was seen in 18 cases. SYN was the only positive marker in 4 cases; 1 case was only positive for CHR. INSM1 was the only positive marker in 19 cases; this included 13 carcinomas without overt NE morphology (n=36), compared to 0 or 1 case for SYN and CHR, respectively. Expression was most often focal in this setting. INSM1 also showed focal staining in normal epithelium. Among SPCs (n=15), INSM1, SYN or CHR was positive in 66%, 80% and 53% of cases, respectively. INSM1 expression correlated with ER and PR expression (0.22, $p = 0.039$ and 0.44, $p < 0.01$), similar to SYN and CHR. Among grade 3 BCs with NE morphology (n=31), INSM1, SYN or CHR was positive in 53%, 60% and 36% of cases, respectively. There was no statistically significant difference in INSM1 expression between invasive and in situ carcinoma.

Conclusions: INSM1 is an additional marker in the arsenal to assess NE differentiation. Among BCs, the sensitivity of INSM1 appears intermediate between SYN and CHR, but may be less specific.

117 Are Metaplastic Carcinomas with Osseous Differentiation and Primary Osteosarcomas of the Breast One and the Same?

Grace Neville¹, Christopher Fletcher², Deborah Dillon³, Stuart Schnitt²

¹Brigham and Women's Hospital, Harvard Medical School, Boston, MA, ²Brigham and Women's Hospital, Boston, MA, ³Harvard Medical School, Boston, MA

Disclosures: Grace Neville: None; Christopher Fletcher: None; Deborah Dillon: None; Stuart Schnitt: None

Background: The distinction between metaplastic breast carcinomas with heterologous osseous differentiation (MBC) and primary breast osteosarcomas (OS) may be difficult. Histologic evidence of epithelial differentiation, co-

existent ductal carcinoma in situ, and/or immunohistochemical (IHC) evidence of epithelial differentiation support a diagnosis of MBC. However, some have suggested that virtually all breast lesions with osseous differentiation are MBC, even if no histologic or IHC evidence of epithelial differentiation is demonstrable (presuming malignant phyllodes tumor is excluded). In this study, we profiled malignant tumors of the breast with osseous differentiation to determine if MBC and OS are genomically distinct entities.

Design: Ten MBC with osseous differentiation and 5 osseous breast tumors without histologic or immunophenotypic evidence of epithelial differentiation or features of phyllodes tumor were identified from our institutional and consult files (2013-2020). All patients were female with a median age of 59 years (range 31-82 years). Median tumor size was 2.9 cm (range 2-14 cm). Malignant osseous foci were macrodissected and analyzed by hybrid-capture next generation sequencing (Oncopanel), interrogating the full coding regions of 447 genes for mutations and copy number variations (CNVs). In four cases, separate areas showing epithelial differentiation were also sequenced.

Results: Overall, the most commonly altered genes were TP53 (n= 9), PIK3CA (n= 8), CDKN2A (n=6), CDKN2B (n= 6), MTAP (n= 6), TERT (n= 6) and PTEN (n= 4). Thirteen cases showed one of two mutational patterns: TP53 mutation +/- PTEN inactivation (n=7) or PIK3CA mutation +/- TERT +/- CNKN2A inactivation (n=6). Two cases showed both patterns. Cases classified as MBC or OS according to traditional histopathologic and IHC criteria were represented equally by both genomic patterns (Table 1). Four cases with separate analysis of osseous and epithelial areas showed similar genomic profiles in both areas of the same tumor.

Pathogenic Mutations	MBC with Osseous differentiation										Pure Osseous Tumors					
P53	■	■	■	■	■	■	■	■	■	■	■	■	■	■	■	■
PIK3CA	■	■	■	■	■	■	■	■	■	■	■	■	■	■	■	■
TERT	■	■	■	■	■	■	■	■	■	■	■	■	■	■	■	■
PTEN	■	■	■	■	■	■	■	■	■	■	■	■	■	■	■	■
Deep Deletions (2 Copy)																
CDKN2A	■	■	■	■	■	■	■	■	■	■	■	■	■	■	■	■
CDKN2B	■	■	■	■	■	■	■	■	■	■	■	■	■	■	■	■
MTAP	■	■	■	■	■	■	■	■	■	■	■	■	■	■	■	■

Conclusions: Malignant breast tumors classified as MBC with osseous differentiation and as OS are not distinct at the genomic level, suggesting that there is no role for genomic profiling in this differential diagnosis. Since patients with MBC and OS may be treated with different chemotherapeutic regimens, this remains an important differential diagnosis that should continue to be made according to traditional histopathologic and IHC criteria.

118 Biomarkers Expression in Triple Negative Breast Cancer (TNBC)

Sharon Nofech-Mozes¹, Rachel Han², Ekaterina Olkhov-Mitsel³, Fang-I Lu¹, Anna Plotkin², Wedad Hanna³, Elzbieta Slodkowska¹

¹University of Toronto, Sunnybrook Health Sciences Centre, Toronto, Canada, ²University of Toronto, Toronto, Canada, ³Sunnybrook Health Sciences Centre, Toronto, Canada,

Disclosures: Sharon Nofech-Mozes: None; Rachel Han: None; Ekaterina Olkhov-Mitsel: None; Fang-I Lu: None; Anna Plotkin: None; Wedad Hanna: None; Elzbieta Slodkowska: None

Background: TNBC is biologically diverse with limited therapeutic options and poor prognosis. Molecular profiling studies identified 4 major subtypes (Basal-like 1 and 2, mesenchymal and luminal-androgen-receptor); however, in most settings these are not clinically available. We studied the expression of biomarkers by immunohistochemistry to enhance our understanding of its heterogeneity possibly guiding targeted therapies in TNBC.

Design: TMAs from 273 TNBCs were stained with p53, p16, RB1, BRCA1 associated protein-1 (BAP1), PD-L1 (SP142), androgen receptor (AR) and MMRs (MLH1, PMS2, MSH2, MSH6). P53 was scored as abnormal (A)

based on diffuse nuclear, complete absence or diffuse cytoplasmic staining. P16 was considered overexpressed (OE) based on block type strong nuclear/cytoplasmic staining. RB1, BAP1 and MMR were scored as lost (L) or retained (R). PD-L1 staining $\geq 1\%$ in inflammatory cells/ tumor area was considered positive. AR was assessed in semi quantitative manner (<1 , 1-10, 11-25, $>25\%$) and was considered positive when expressed in $>10\%$. Fisher exact test was performed to assess the significance of biomarker expression proportions in different histologic subtypes. Unsupervised cluster analysis was performed using the 'pheat map' () function in R package version 1.0.12.

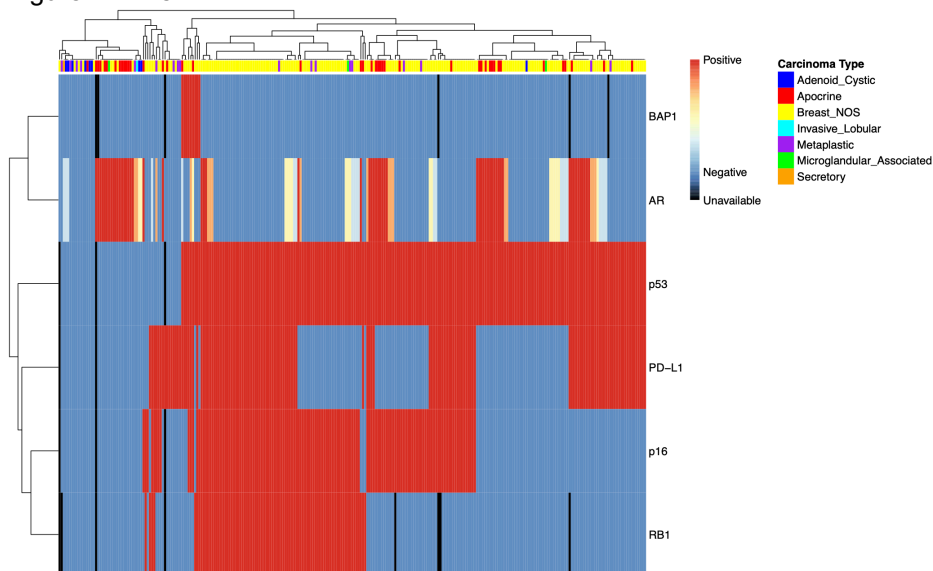
Results: The results are summarized in Table 1. AR was positive in 33.4% of TNBC, (25.5, 74.4, 22% in NOS, apocrine (AC) and metaplastic carcinomas (MC; $P < 0.001$). PD-L1 was positive in 48% of all cases (57.4, 23.8, 38.9% in NOS, AC and MC types $p = 0.0002$). Among NOS, AC and MC P53 was A in 90.3, 64.3 and 50% ($p < 0.001$); P16 was OE in 60.2, 26.2 and 44.4% ($p < 0.001$); RB1 was L in 38.7, 7.1 and 22.2% ($p = 0.00025$); and BAP1 was L in 3.6%, 4.9% and 0% ($p = 0.646$). All the tumors except one NOS case with PMS2-L had intact MMR stains. Unsupervised cluster analysis (Figure 1) identified three major molecular clusters (C1-3; described left to right). C1: RB-R, p53-normal, p16- usually normal; these can be further clustered into AR+/PD-L1- and AR-/PD-L1+/- subclasses; most of the cases were of special type. C2: RB-L, p53-A and almost always p16-OE; the majority were NOS, AR negative and PD-L1 $> 50\%$. C3: RB-R, p53-A, +/-p16OE, PD-L1 $> 50\%$ and AR+ between C1 and C2. BAP1-L cases were p53-A and PD-L1+.

Table 1: Biomarkers expression by histologic type:

Histologic Classification	Number of cases	Androgen Receptor				PD-L1+ /available cores	P53-A	P16-OE	RB1-L	BAP1-L
		$<1\%$	1-10%	11-25%	$>25\%$					
All cases	273	160	21	18	74	130/271	216/270	138/270	84/265	9/268
NOS	198	134	13	13	38	113/197	177/196	118/196	75/194	7/194
Apocrine	43	7	4	1	31	10/42	27/42	11/42	3/42	2/41
Metaplastic	18	13	1	1	3	7/18	9/18	8/18	4/18	0/18
AdCC	9	5	2	2	0	0/9	2/9	0/9	0/9	0/9
MGA associated	3	1	0	1	1	0/3	2/3	1/3	2/3	0/3
Secretory	1	0	1	0	0	0/1	0/1	0/1	1/1	0/1
ILC	1	0	0	0	1	0/1	0/1	0/1	1/1	0/1

AdCC= adenoid cystic carcinoma, MGA= microglandular adenosis, NA= not available, A=abnormal, OE=overexpressed, L=loss

Figure 1 - 118



Conclusions: By IHC three major clusters of TNBC based on p53, p16 and RB can be identified. AR is expressed across the major TNBC subtypes. PDL-1 is positive in significantly higher proportion of TNBC-NOS. BAP1 loss is rare and MMR abnormalities are exceedingly rare in TNBC. These findings highlight potential predictive markers for targeted therapies that could be further tested in clinical trials.

119 Metastatic Breast Carcinoma to Mucosal Sites: A Clinical/Pathologic Review

Fernando Alekos Ocampo Gonzalez¹, Paolo Gattuso¹, Vijaya Reddy¹, Indu Agarwal¹

¹Rush University Medical Center, Chicago, IL

Disclosures: Fernando Alekos Ocampo Gonzalez: None; Paolo Gattuso: None; Vijaya Reddy: None; Indu Agarwal: None

Background: Metastatic breast carcinoma to mucosal sites is not a common clinical manifestation, but it can be confused clinically, radiographically and pathologically with a primary neoplasm. We undertook a retrospective study to assess mucosal site metastasis and evaluated these according to age, histopathologic subtypes, prognostic markers, time to metastasis and survival

Design: We performed a retrospective search of our pathology records from 1993-2020 looking for any metastatic breast carcinoma to mucosal sites. With these cases identified, we then performed a search of medical records for data on age, subtype, prognostic markers, time from primary diagnosis to mucosal metastases, survival and presence of other metastases.

Results: 56 total cases were identified, all female. The mean age at metastatic diagnosis was 57.2 years, (31 to 93 years). The distribution by histologic subtype showed 28 (50%) cases of ductal carcinoma, 26 (46%) of lobular carcinoma and 2 mixed (4%). The most common location for metastasis was gastrointestinal (GI) tract with 19 cases, followed by respiratory with 15, gynecologic with 14, genitourinary with 5 and eye with 3. Lobular carcinoma was more common in gastrointestinal (72%) and gynecological (85%), while ductal carcinoma was more common in respiratory (100%), eye (100%) and genitourinary (60%) sites. Regarding prognostic markers, 64% of cases were ER positive, 37.5% were PR positive and 12.5% were HER2 positive by immunohistochemistry. The average time to mucosal metastasis was 5.6 years (1-35 years). Five patients had mucosal metastases diagnosed concurrently with breast primary, and two cases were diagnosed before a primary breast carcinoma was identified. Survival data was available for 28 patients, with an average survival after diagnosis of 1.9 years (6 months-7 years). Data on other metastases was available for 23 patients, with 15 presenting with previous metastases to other sites, most commonly body fluids (8 cases), bone (7 cases), other mucosal sites (4 cases) and central nervous system and liver (3 cases each).

Conclusions: Metastatic breast carcinoma can uncommonly metastasize to most mucosal sites, and should be considered for any patient who presents with carcinoma of these sites. On our study, lobular carcinoma showed a predilection for the GI and gynecological tracts, while ductal carcinoma exhibited preference for respiratory and genitourinary sites, as well as the eye. Attention must be brought to any history of breast malignancy even if remote, since several cases can be diagnosed even 30 years after the original diagnosis. Metastatic breast carcinoma should also be considered in cases where no breast primary has been diagnosed, as it can be a rare first manifestation of already metastatic disease. Metastasis to mucosal sites tends to portend a bad prognosis, owing to co-existence with more widespread metastatic disease and short survival.

120 Histologic Features of the Tumor Bed Following Neoadjuvant Chemotherapy for Breast Cancer: Relationship to Presence of Residual Disease and Tumor Subtype

Ricardo Pastorello¹, Alison Laws², Samantha Grossmith³, Claire King⁴, Monica McGrath², Elizabeth Mittendorf², Tari King⁵, Stuart Schnitt⁵

¹Hospital Sírio Libanês, São Paulo, Brazil, ²Dana-Farber Cancer Institute, Brigham and Women's Cancer Center, Boston, MA, ³Dana-Farber Cancer Institute, Boston, MA, ⁴DFCI, Boxford, MA, ⁵Brigham and Women's Hospital, Boston, MA

Disclosures: Ricardo Pastorello: None; Samantha Grossmith: None; Claire King: None; Monica McGrath: None; Tari King: None; Stuart Schnitt: None

Background: Evaluation of the tumor bed after neoadjuvant chemotherapy (NAC) for breast cancer is imperative to accurately determine response to treatment, guide further therapy, and assess prognosis. Whether tumor bed features differ based on the presence or absence of residual carcinoma or by tumor subtype has not been previously studied in detail.

Design: We reviewed H&E-stained sections of the post-treatment surgical specimens for 665 patients with stage I-III breast cancer treated with NAC followed by surgery from 2004-2014 blinded to pre-treatment characteristics. The tumor bed in each case was evaluated for minimal changes, mild edema, fibrosis/scarring, elastosis, mucin, myxoid change, hemosiderin deposition, hemosiderin-laden macrophages, and foamy macrophages. The frequency of each feature was compared for cases with and without a pathologic complete response (pCR; ypT0/is ypN0) and between tumor subtypes.

Results: Among the 665 cases, there were 278 lumpectomy and 387 mastectomy specimens. Breast cancer subtypes included 242 hormone receptor-positive/HER2-negative (HR+/HER2-) tumors (36.4%), 216 (32.5%) HER2+ cancers, and 207 (31.1%) HR-HER2- tumors (TNBC). pCR was seen in 7.9%, 37.0%, and 37.7%, of HR+/HER2-, HER2+ cancers, and TNBC respectively (p<0.001). As shown in the Table, for all tumor subtypes, elastosis, mucin, and myxoid change were all significantly more frequent in the tumor bed of cases without a pCR (all p<0.02). Conversely, foamy and hemosiderin-laden macrophages were significantly more common in those with a pCR (both p≤0.001). Most of these differences were also seen for each tumor subtype; however, among HER2+ tumors, there were no significant differences in tumor bed macrophages in cases with and without a pCR.

Table. Distribution of tumor bed changes in patients with (n=177) and without pCR (n=488) by tumor subtype

<u>Tumor subtype</u>	<u>Tumor bed changes</u>	<u>Type of response</u>		<u>p value</u>
		pCR	Not pCR	
All subtypes (n=665)	Minimal changes (n=20)	14 (7.9%)	6 (1.2%)	<0.001
	Mild edema (n=461)	121 (68.4%)	340 (69.7%)	0.746
	Fibrosis/scarring (n=656)	172 (97.2%)	484 (99.2%)	0.061
	Stromal elastosis (n=212)	30 (16.9%)	182 (37.3%)	<0.001
	Stromal mucin (n=32)	3 (1.7%)	29 (5.9%)	0.024
	Myxoid change (n=92)	3 (1.7%)	89 (18.2%)	<0.001
	Hemosiderin deposition (n=384)	104 (58.8%)	280 (57.4%)	0.750
	Foamy macrophages (n=166)	70 (39.5%)	96 (19.7%)	<0.001
	Hemosiderin-laden macrophages (n=356)	113 (63.8%)	243 (49.8%)	0.001
HR+/HER2- (n=242)	Minimal changes (n=3)	1 (5.3%)	2 (0.9%)	0.218
	Mild edema (n=164)	11 (57.9%)	153 (68.6%)	0.337
	Fibrosis/scarring (n=241)	18 (94.7%)	223 (100.0%)	0.079
	Stromal elastosis (n=94)	2 (10.5%)	92 (41.3%)	0.008
	Stromal mucin (n=20)	0 (0.0%)	20 (9.0%)	0.380
	Myxoid change (n=46)	0 (0.0%)	46 (20.6%)	0.029
	Hemosiderin deposition (n=132)	10 (52.6%)	122 (54.7%)	0.861
	Foamy macrophages (n=39)	12 (63.2%)	27 (12.1%)	<0.001
	Hemosiderin-laden macrophages (n=110)	12 (63.2%)	98 (43.9%)	0.106
HER2+ (n=216)	Minimal changes (n=9)	6 (7.5%)	3 (2.2%)	0.080
	Mild edema (n=160)	59 (73.8%)	101 (74.3%)	0.934
	Fibrosis/scarring (n=209)	76 (95.0%)	133 (97.8%)	0.428
	Stromal elastosis (n=67)	18 (22.5%)	49 (36.0%)	0.038
	Stromal mucin (n=11)	2 (2.5%)	9 (6.6%)	0.219
	Myxoid change (n=29)	3 (3.8%)	26 (19.1%)	0.001
	Hemosiderin deposition (n=106)	38 (47.5%)	68 (50.0%)	0.723
	Foamy macrophages (n=60)	26 (32.5%)	34 (25.0%)	0.235
	Hemosiderin-laden macrophages (n=110)	44 (55.0%)	66 (48.5%)	0.358

TNBC (n=207)	Minimal changes (n=8)	7 (9.0%)	1 (0.8%)	0.005
	Mild edema (n=137)	51 (65.4%)	86 (66.7%)	0.850
	Fibrosis/scarring (n=206)	78 (100.0%)	128 (99.2%)	1.000
	Stromal elastosis (n=51)	10 (12.8%)	41 (31.8%)	0.002
	Stromal mucin (n=1)	1 (1.3%)	0 (0.0%)	0.377
	Myxoid change (n=17)	0 (0.0%)	17 (13.2%)	0.001
	Hemosiderin deposition (n=146)	56 (71.8%)	90 (69.8%)	0.757
	Foamy macrophages (n=67)	32 (41.0%)	35 (27.1%)	0.038
	Hemosiderin-laden macrophages (n=136)	57 (73.1%)	79 (61.2%)	0.082

Conclusions: Among breast cancer patients treated with NAC, the frequency of several tumor bed changes differed significantly according to presence of residual disease. In particular, stromal alterations were significantly more common in the tumor bed of patients with residual carcinoma, while macrophage infiltration was more frequent in those with a pCR. Whether or not histologic features of the tumor bed are associated with outcome following NAC requires further study.

121 Conventional and Digital Ki67 Quantification in Luminal, HER2-Negative Breast Cancer: Which One Correlates Better with Oncotype DX?

Laura Pons¹, Ahmad Altaieb, Esperanca Ussene², Anna Martinez-Cardus³, Paula Rodríguez-Martínez⁴, Pedro Fernandez⁵

¹Hospital Germans Trias i Pujol, Fundació IGTiP, ²Vila Franca de Xira Hospital, Pathology Department, ³Department of Medical Oncology-ICO, Spain, ⁴Hospital Germans Trias i Pujol, Badalona, Spain, ⁵Hospital Germans Trias i Pujol, Universidad Autónoma de Barcelona, Barcelona, Spain

Disclosures: Laura Pons: None; Ahmad Altaieb: None; Esperanca Ussene: None; Anna Martinez-Cardus: None; Paula Rodríguez-Martínez: None; Pedro Fernandez: None

Background: Ki67 immunohistochemical evaluation is subject to high intra- and inter-observer variability. Therefore, digital counting (DC) methods have been designed and compared to conventional counting (CC) in attempt to homogenize and improve its usefulness.

It is conceivable that Ki67 expression and Oncotype DX recurrence score (ORS) should be positively correlated, given that Ki67 is one of the major contributors to the multigene panel. In a time in which digital pathology is gaining adepts, conventional and digital Ki67 quantification methods seem to correlate well with each other. The aim of this study is to confirm this high correlation in our daily practice, and also determine which of these methods correlates better with the prognostic capacity of Oncotype DX.

Design: A total of 89 cases of luminal Her-2 negative breast cancers were analyzed. At least three randomly selected high-power fields were evaluated with a Ki67 digital algorithm (Ventana). A minimum of 100 cells/field for CC and 500 cells for DC were counted in each field in all cases. A Ki67 cutoff of 25% positive cells (institutional mean) was used for surrogate molecular subtype classification (luminal A-like vs luminal B-like).

The ORS was obtained in 55 cases that were subsequently correlated with CC and DC methods using the Pearson correlation coefficient (r).

Results: Ki67 quantification by CC and DC methods showed an excellent intraclass coefficient correlation of 0.81 (95%CI: 0.73-0.89). We found a higher correlation of conventional Ki67 quantification with ORS (r=0.45, p<0.001), than with digital method (r=0.39, p=0.003), even then both were significantly correlated.

Conclusions: In conclusion, we have shown that CC and DC methods correlate well enough to consider stopping manual counting. We have also shown that both methods correlate positively with Oncotype DX recurrence score, and this correlation is higher with the conventional method.

122 Outcome of B3 Breast Biopsies at the Largest London-Based Screening Centre, 2019

Michael Rathbone¹, Soha El Sheikh¹

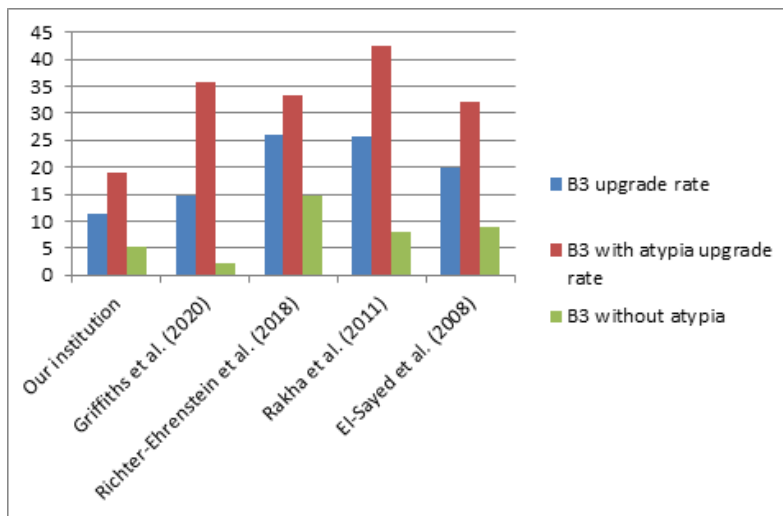
¹Royal Free London NHS Foundation Trust, London, United Kingdom

Disclosures: Michael Rathbone: None; Soha El Sheikh: None

Background: Diagnostic breast biopsies in the UK are assigned a B code to guide further treatment. The most complex and heterogeneous group of abnormalities, with the most interobserver variability is the B3 “lesion of uncertain malignant potential” category. The proportion of B3 lesions varies across institutions nationally and internationally with a 5% rate in the UK (1999-2006), 4.5% in Germany, 11.9% in Italy, 17% in Switzerland, and 8% in the US (Shaaban *et al*). Our aim is to assess the outcome of B3 lesions at our centre, in comparison with national and international data.

Design: We identified all breast biopsies received in 2019 and divided the cases using B category. We then further subclassified the B3 lesions into: lesions with ductal atypia (atypical intraductal epithelial proliferation AIDEP/ADH/FEA, atypia in papillary lesion or radial scar), in situ lobular neoplasia, papillary lesion without atypia, radial scar, fibroepithelial lesion and other. Using our records and the NHS Breast Screening Programme (NHSBSP), we obtained the final excision histology, and calculated the malignant upgrade rate or positive predictive value (PPV) to comply with the NHSBSP H5 classification: invasive carcinoma, DCIS and confirmed LCIS.

Results: Of a total the 4168 B coded breast biopsies received in 2019, 375 were B3 (9.0%) and 296 (79%) had available outcome data. There were 84 cases of AIDEP with a PPV of 14%; 77 papillary lesions without atypia with a PPV of 1.3%; 57 cases of in situ lobular neoplasia with a PPV of 22.8% and radial scars without atypia with a 9.8% PPV. Figure 1 compares the PPV of total B3 cases, B3 with atypia and B3 without atypia, with the results from large recent studies.



Conclusions: The data show that our institution has a high rate of classifying biopsies as B3 (9%) compared with large studies (range 4.5 to 6.7%). Whereas our PPV rate for B3 lesions without atypia was within expected limits, the PPV for B3 lesions with atypia was significantly lower at 19.1%. The increased B3 rate combined with the lower PPV suggests overuse of the B3 category in diagnostic biopsies, which has management implications.

Our possible overuse of B3 is under investigation through a blinded, multi-consultant review of the B3 cases with atypia, to measure the degree of interobserver variability, and explore whether changes to our routine practice need to be considered.

123 Comprehensive Analysis of Immunohistochemical Estrogen Receptor Expression in Mammary Normal Epithelial Elements: Generating Contemporary Data on “Internal Positive Control”

Renan Ribeiro e Ribeiro¹, C. James Sung², M. Ruhul Quddus², Katrine Hansen¹, Kamaljeet Singh¹
¹Women and Infants Hospital, Providence, RI, ²Women & Infants Hospital/Alpert Medical School of Brown University, Providence, RI

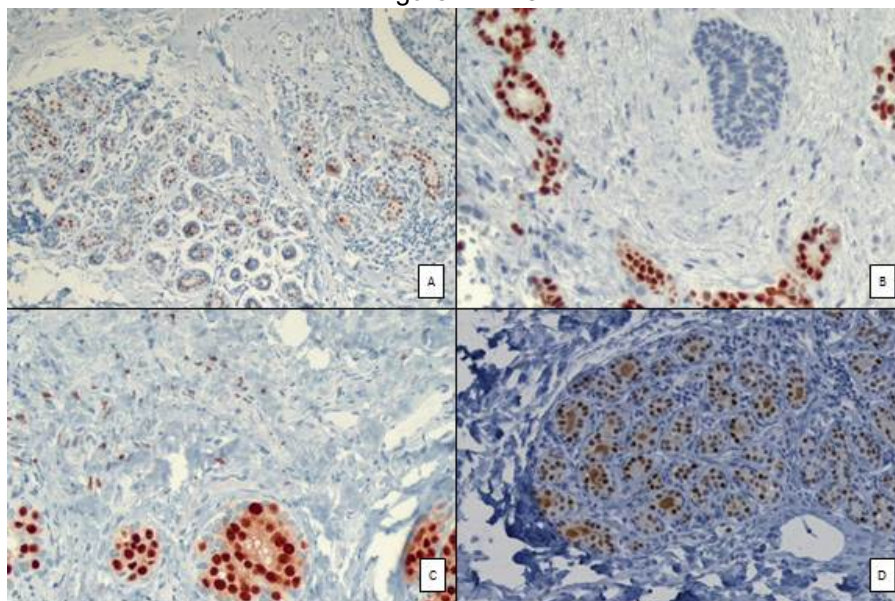
Disclosures: Renan Ribeiro e Ribeiro: None; C. James Sung: None; M. Ruhul Quddus: None; Katrine Hansen: None; Kamaljeet Singh: None

Background: The 2020 CAP/ASCO guidelines on Estrogen receptor (ER) immunohistochemistry (IHC) testing of breast cancer recommend routine evaluation of "internal normal epithelial elements (INEE)" on each tested slide. The expert panel recommends reporting internal control status with 0% to 10% ER (low ER +) staining in carcinoma. Contemporary data on ER IHC in mammary INEE is lacking, as most studies investigating this are from the last century. Our aim was to investigate the distribution and intensity of ER IHC expression in breast INEE.

Design: The ER IHC slides on consecutive breast carcinomas during 2011 from a single institution were reviewed. Dako's ER PharmDx™ Kit (Cat # SK310) was used on Dako Autostainer Link 48 instrument. Dewaxing (60°C in oven x 1 hour), rehydration, antigen retrieval (pH=6.1) & peroxidase blocking (x5 minutes) was followed by incubation with primary antibody (Dako, clone ER-2-123+1D5), secondary antibody, and DAB chromogen-substrate system. The ER extent (0-100%) and intensity (score of 0, 1+ to 3+) was recorded in carcinoma, and INEE and an Allred score was computed.

Results: Total 283 ER slides comprising of 250(88%) needle biopsies, 25(9%) excisions, and 8(3%) skin biopsies with 60(21%) DCIS, 135(48%) invasive, and 87(31%) invasive and in-situ carcinomas and 1 benign biopsy were reviewed. Figure 1A shows the typical ER staining pattern of INEE. The INEE were absent in 48(17%) cases. Completely ER- lobules and ducts were identified in 1(0.6%) and 9(4.2%) samples, respectively. Focal ER- INEE (Figure 1B) were present in 74/235(31%) samples, most of which were ER- ducts (71/74). The mean Allred score for ducts was significantly lower than lobules (5.73 versus 5.33; p=0.023). The INEE were either absent or ER- in 9 of 45 (20%) ER-/ER low+ carcinomas. The ER- INEE did not correlate with age or ER- status of carcinoma. Stromal cell ER nuclear staining (Figure 1C) was present in 104(37%) cases and dermal fibroblasts nuclei were ER+ in 4(50%) skin biopsies. Aberrant cytoplasmic ER staining (Figure 1C) was noted in carcinomas, INEE and histiocytes in 19(6.7%), 29(10.2%) and 5(1.8%) cases, respectively. ER positive secretions (Figure 1D) were found in 31(11%) cases.

Figure 1 - 123



Conclusions: We report absent INEE and ER- INEE in 17% and 4.8% breast samples, respectively. Benign breast lobules show most consistent ER staining when compared to ducts, and should therefore be treated as the most reliable INEE while evaluating ER IHC.

124 Heterogeneity of Immunohistochemical Estrogen Receptor Expression in Breast Carcinoma: Hitherto Unexplored Phenomenon

Renan Ribeiro e Ribeiro¹, Katrine Hansen¹, M. Ruhul Quddus², C. James Sung², Kamaljeet Singh¹
¹Women and Infants Hospital, Providence, RI, ²Women & Infants Hospital/Alpert Medical School of Brown University, Providence, RI

Disclosures: Renan Ribeiro e Ribeiro: None; Katrine Hansen: None; M. Ruhul Quddus: None; C. James Sung: None; Kamaljeet Singh: None

Background: Estrogen receptor (ER) immunohistochemistry (IHC) expression is an important biomarker in breast carcinoma (BC). A BC (in-situ and invasive) with >1% ER staining in the tumor cell nuclei is classified as ER positive (ER+). The visual guides (in 10% increments) published with the College of American Pathologists ER guidelines show intermix of ER+ and ER- nuclei (Fig1A, 20% nuclei staining). There is no data on heterogeneity in ER expression in breast cancer. Our aim was to investigate the prevalence and describe patterns of ER heterogeneity in BC.

Design: The ER IHC slides on consecutive BC during 2011 from a single institution were reviewed. Dako’s ER PharmDx™ Kit (Cat # SK310) was used on Dako Autostainer Link 48 instrument. Dewaxing (60°C in oven x 1 hour), rehydration, antigen retrieval (pH=6.1) & peroxidase blocking (x5 minutes) was followed by incubation with primary antibody (Dako, clone ER-2-123+1D5), secondary antibody, and DAB chromogen-substrate system. The extent (0-100%) and intensity (score of 0, 1 to 3+) of ER staining was recorded in BC (invasive and in-situ), lobules, and ducts. Allred scores for each epithelial element was computed. A BC with 0-10% staining was classified as low ER+. The ER heterogeneity was defined as differentially ER staining tumor cell sub-populations that displayed abrupt change in ER staining intensity (eg. Fig1B, ER- & ER+ DCIS, 20% nuclei staining).

Results: Total 282 ER IHC slides from 262 patients comprising of 249 (88%) needle biopsies, 25(9) excisions and 8(3%) skin biopsies with 60(21%) DCIS, 135(48%) invasive, and 87(31%) invasive and in-situ BCs were reviewed. Heterogeneity of ER IHC expression was found in 11(3.9%) BCs (Table 1). All 11 cases were grade 2 or 3 and contained ER- or low ER+ carcinoma components. Ten of 11 BC (except 1 LCIS) were originally classified as ER+. Three patterns of heterogeneity were identified in in-situ BC (8 DCIS, 1 LCIS): type I (n=4) with low ER+ and ER+ DCIS (Fig 2A), type II (2 DCIS, 1 LCIS) with ER- and ER+ in-situ BC populations (Fig 2B), and type III (n=2) with ER- and ER low+ staining (Fig 2C). One case of invasive ductal carcinoma showed distinct ER- and ER+ components and 1 case showed discordant ER staining in in-situ (ER- DCIS) and invasive (ER+) components (Fig 2D). Aberrant cytoplasmic ER staining was noted in 19 carcinomas (6.7%), 29 internal normal epithelial elements (10.2%), and histiocytes 5(1.8%). Aberrant ER staining in luminal secretions was identified in 31 slides (11%).

Case	Sample type	Age (years)	Diagnosis	Overall ER extent (%)	Overall ER intensity	Heterogeneity type
Case 1	Biopsy	53	DCIS G3	40	Strong	Type I Low+ and Pos
Case 2	Biopsy	38	DCIS G2-3	40	Moderate	Type I Low+ and Pos
Case 3	Biopsy	71	Pleomorphic LCIS	5	Moderate	Type I Low+ and Pos
Case 4	Excision	57	IDC G2 DCIS G2-3	90 60	Moderate Moderate	Type II Neg and Pos
Case 5	Excision	64	DCIS G3	70	Strong	Type II Neg and Pos
Case 6	Biopsy	50	IDC G2 DCIS G2-3	80	Strong	DCIS (neg) IDC (pos)
Case 7	Biopsy	59	DCIS G3	40	Weak	Type III Neg and Low
Case 8	Biopsy	59	DCIS G3	40	Weak	Type III Neg and Low
Case 9	Biopsy	67	DCIS G3	60	Moderate	Type I Low+ and Pos
Case 10	Biopsy	58	IDC G2	60	Weak	Type II Neg and Pos
Case 11	Biopsy	59	DCIS G3	30	Strong	Type II Neg and Pos

Figure 1 - 124

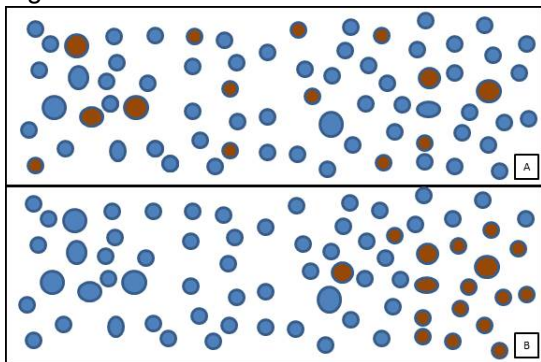
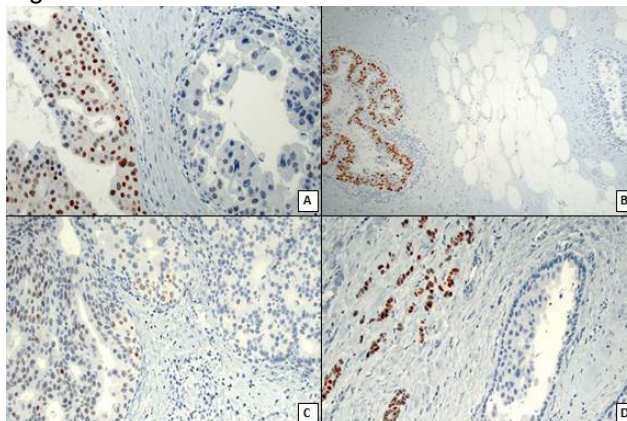


Figure 2 - 124



Conclusions: We report ER heterogeneity in 6% DCIS and ER discordance between in-situ and invasive carcinoma in 1.1% BC. All ER heterogeneous BC contain ER- or low ER+ component, but in routine practice they are classified as ER positive. Further studies are needed to refine the BC ER heterogeneity criteria and investigate its clinical relevance. Retesting of ER on excisional specimens may be considered for DCIS that are ER negative on core biopsy.

125 Interobserver Agreement of Programmed Death-Ligand 1 (PD-L1) Scoring in Triple Negative Breast Cancers

Stephanie Richards¹, Shabnam Samankan², Rochelle Freire³, Isildinha Reis³, Anthony De La Cruz³, Merce Jorda³, Carmen Gomez-Fernandez³

¹Jackson Memorial Hospital/University of Miami Hospital, Miami, FL, ²Mount Sinai Hospital Icahn School of Medicine, New York, VA, ³University of Miami Miller School of Medicine, Miami, F

Disclosures: Stephanie Richards: None; Shabnam Samankan: None; Rochelle Freire: None; Isildinha Reis: None; Anthony De La Cruz: None; Merce Jorda: None; Carmen Gomez-Fernandez: None

Background: Multiple studies have shown increased PD-L1 expression by immunohistochemistry (IHC) in triple negative breast cancers (TNBC). Atezolizumab is currently the only FDA-approved checkpoint inhibitor being used to treat TNBC, and treatment requires PD-L1 (Ventana sp142) immune cell (IC) staining $\geq 1\%$. However, Pembrolizumab has also shown promising results in clinical trials. Qualification for Pembrolizumab therapy requires PD-L1 (Dako 22c3) Combined Positive Score (CPS), currently being investigated at cutoff values of ≥ 1 and ≥ 10 . Breast pathologists must be familiar with these cutoffs and be able to accurately assess tumor PD-L1 positivity with these different antibodies. This goal of this study was to assess the interobserver agreement in calculating PD-L1 (Dako 22c3) CPS amongst breast pathologists at our institution in preparation for clinical use.

Design: 45 cases of TNBC from a three year period (2017-2019) were reviewed. Each case was stained for PD-L1 (Dako 22c3). The cases were independently evaluated by four breast pathologists (two senior pathologists and two junior pathologists), and the CPS were recorded.

The data were analyzed in terms of percent concordance between pathologists at CPS ≥ 1 and ≥ 10 as well as actual numerical values. Interrater agreement between pathologists was assessed for every pathologist duo and for the agreement of all pathologists. For each outcome, the observed percentage agreement/concordance and the Cohen's kappa statistic (κ) were reported. In addition, the Shrout-Fleiss intraclass correlation coefficient (ICC) was reported as a measure of the interrater reliability. Statistical analysis was performed in SAS 9.4.

Results: At CPS ≥ 1 , there was fair agreement amongst all four pathologists (48.9%, $\kappa = 0.328$), moderate agreement between the two junior pathologists (86.7%, $\kappa = 0.444$), and moderate agreement between the two senior pathologists (80%, $\kappa = 0.601$). Similar results were noted at CPS ≥ 10 , with fair concordance amongst all four raters

(44.4%, $\kappa=0.321$), moderate agreement between the two junior pathologists (73.3%, $\kappa=0.481$), and moderate agreement between the two senior pathologists (82.2%, $\kappa=0.530$).

When the data were analyzed for interrater reliability at actual CPS value, there was moderate correlation between all four pathologists (ICC=0.534), moderate-to-good correlation between the two junior pathologists (ICC=0.738), and moderate correlation between the two senior pathologists (ICC=0.666).

Conclusions: There was overall fair-to-moderate agreement between breast pathologists in calculating PD-L1 CPS. As the PD-L1 CPS will be used to define the population of breast cancer patients which will receive treatment with Pembrolizumab, agreement amongst breast pathologists is critical. The data suggest that group training, consensus scoring, or digital image analysis for PD-L1 IHC could be helpful at our institution.

126 Comparison Study of a 2nd Generation HER2 Gene Protein Assay with Individual HER2 IHC and ISH Assays and Its Implications for Intratumoral Heterogeneity

Mark Robida¹, Hiro Nitta¹, Shrividhya Srinivasan², Bingbing Song³, Joseph Castillo², Jessica Baumann¹, Timothy Wilson², Richard Huang⁴, Sanne de Haas⁵, Charmi Patel⁶, Luciana Molinero², Yijin Li², David Chen², Jennifer Giltnane²

¹Roche Tissue Diagnostics, Tucson, AZ, ²Genentech, Inc., South San Francisco, CA, ³Ventana Medical Systems, Inc., Tucson, AZ, ⁴Foundation Medicine, Inc., Cary, NC, ⁵F. Hoffmann-La Roche Ltd, Basel, Switzerland, ⁶University of California, San Diego, San Diego, CA

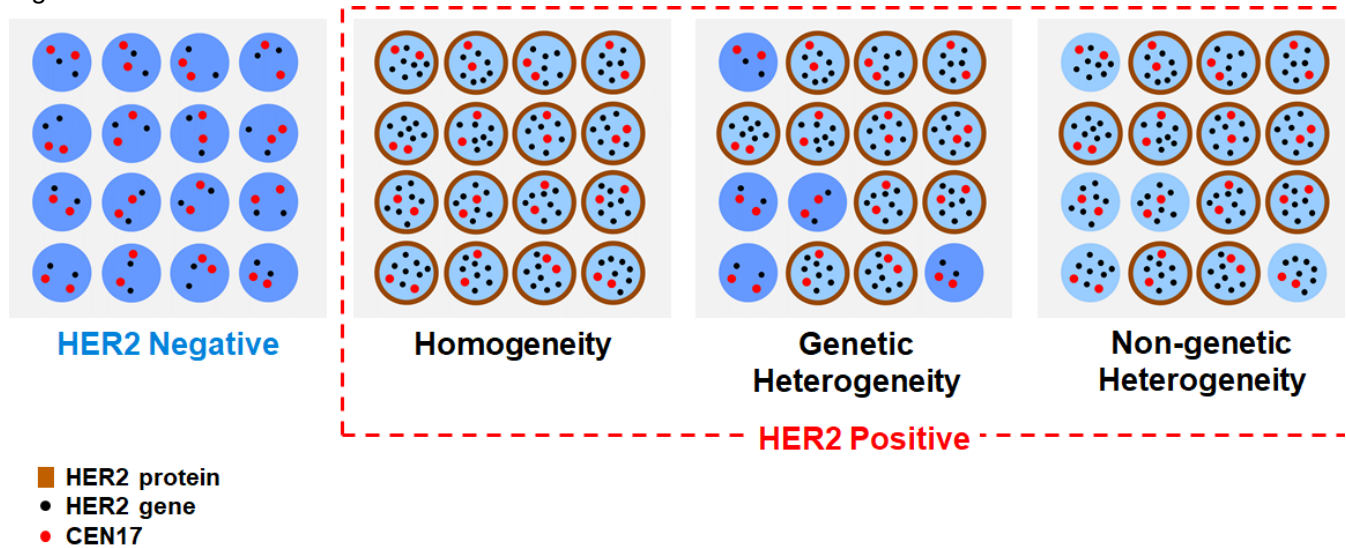
Disclosures: Mark Robida: *Employee*, F. Hoffmann LaRoche; *Employee*, F. Hoffmann LaRoche; Hiro Nitta: *Employee*, Roche Tissue Diagnostics; Shrividhya Srinivasan: *None*; Jessica Baumann: *None*; Richard Huang: *Employee*, Roche; Sanne de Haas: *Employee*, F. Hoffmann - La Roche Ltd.; *Stock Ownership*, F. Hoffmann - La Roche Ltd; Charmi Patel: *Employee*, Roche tissue Diagnostic (was working with the company last year); David Chen: *Employee*, Genentech

Background: The 2018 ASCO/CAP Guidelines for HER2 Testing in Breast Cancer emphasizes concurrent IHC and ISH evaluation to determine HER2 status in cases classified as equivocal with intratumoral heterogeneity. Furthermore, recent studies show that HER2 genetic and non-genetic heterogeneity may predict resistance to neoadjuvant HER2-targeted therapy, showing the importance of HER2 heterogeneity analysis for patient treatment planning. Our objective was to develop a 2nd generation HER2 gene protein assay (GPA) to simultaneously assess both HER2 protein expression and HER2 gene status on a single slide, and then to compare the performance of our HER2 GPA with individual immunohistochemistry (IHC) and *in situ* hybridization (ISH) assays.

Design: We designed a fully-automated HER2 GPA that combined IHC using the 4B5 rabbit monoclonal antibody with an oligo-based ISH assay for use on an automated staining system. To assess performance of the GPA, we compared the staining of the HER2 GPA to that of the individual 4B5 IHC assay and to two CE IVD approved on-market bright-field ISH assays across 101 clinically HER2-positive, procured breast cancer samples.

Results: The technical performance of the GPA was equivalent to that of the individual IHC and superior to that of the individual ISH assays. Overall pass rates were higher for the HER2 ISH component of the GPA (100%) compared to the two CE IVD approved ISH assays (88.1% and 93.1%, respectively). When scored according to the 2018 ASCO/CAP Guidelines, the IHC portion of the GPA and individual 4B5 IHC had a 95.1% concordance rate when binned into the three categories of negative, equivocal, and positive. In cases with an IHC vs. ISH scoring discrepancy, ISH results were concordant with the GPA IHC score over the standard IHC score 60% of the time. The ISH portion of the GPA and an on-market ISH assay had a 98.9% concordance rate, with the 4B5 IHC alone agreeing with the GPA ISH score in the lone discrepant case. Analysis of the GPA results found heterogeneity in 26.7% of cases, with non-genetic heterogeneity found in 19.8% of cases and genetic heterogeneity in 6.9% of cases.

Figure 1 - 126



Conclusions: We have demonstrated that the GPA is technically robust and has high concordance to individual HER2 IHC and ISH assays. Because it allows for simultaneous evaluation of HER2 protein expression and gene amplification at the cellular level, the GPA is a powerful tool for identifying patients with HER2 intratumoral heterogeneity and HER2 protein and gene dissociation.

127 Digital Validation of Breast Biomarkers (ER, PR, AR and HER2) in Cytology Specimens Using Three Different Scanners

Abeer Salama¹, Matthew Hanna¹, Brie Kezlarian¹, Marc-Henri Jean¹, Oscar Lin¹, Christina Vallejo¹, Dilip Giri, Edi Brogi¹, Marcia Edelweiss¹

¹Memorial Sloan Kettering Cancer Center, New York, NY

Disclosures: Abeer Salama: None; Matthew Hanna: *Consultant*, PaigeAI; Brie Kezlarian: None; Marc-Henri Jean: None; Oscar Lin: *Consultant*, Hologic; *Consultant*, Janssen; Christina Vallejo: None; Dilip Giri: None; Edi Brogi: None; Marcia Edelweiss: None

Background: Technical advancements in the field of digital pathology has yielded new opportunities for a digital and remote work environment. We sought to evaluate the utility of the digital review of breast cancer markers using whole slide images (WSI) from formalin fixed paraffin embedded (FFPE) cytology cell blocks (CBs) using 3 different scanners.

Design: Breast cancer CBs sampled from 20 patients (1 breast, 8 lymph nodes, 9 pleural fluid, 2 chest wall) with available immunohistochemical prognostic markers (IHC) and reported using conventional microscopy were included. All glass slides were scanned (20 H&E, 20 ER, 20 PR, 16 AR and 20 HER2) on 3 different scanners (Leica GT450, Phillips Ultrafast Scanner, and 3DHistech P1000) at 40x equivalent resolution (0.25 um/pixel). Four breast pathologists with cytology experience reviewed the IHC digital images and recorded the semi-quantitative scoring for each marker blinded for the reported results. Discrepancies between reads were adjudicated and determined to be clinically relevant if a change in reporting was identified (i.e. positive vs negative) between paired microscopic/digital interpretations.

Results: The overall concordance between microscopic/digital pairs was 99.6% with excellent agreement between Leica vs 3DHistech, moderate agreement between Leica vs Philips and good agreement between Philips vs 3DHistech scores, all significant (P <0.001), see Figure 1.

In total we had 228 IHC reads (60 each for ER, PR, HER2 and 48 for AR) with 3 discrepancies seen in the same case using the 3 different scanners and corresponding to 1.3% of paired reads. Clinical significance of these discrepancies is questionable as the difference was from 1% to 0% nuclear staining for PR.

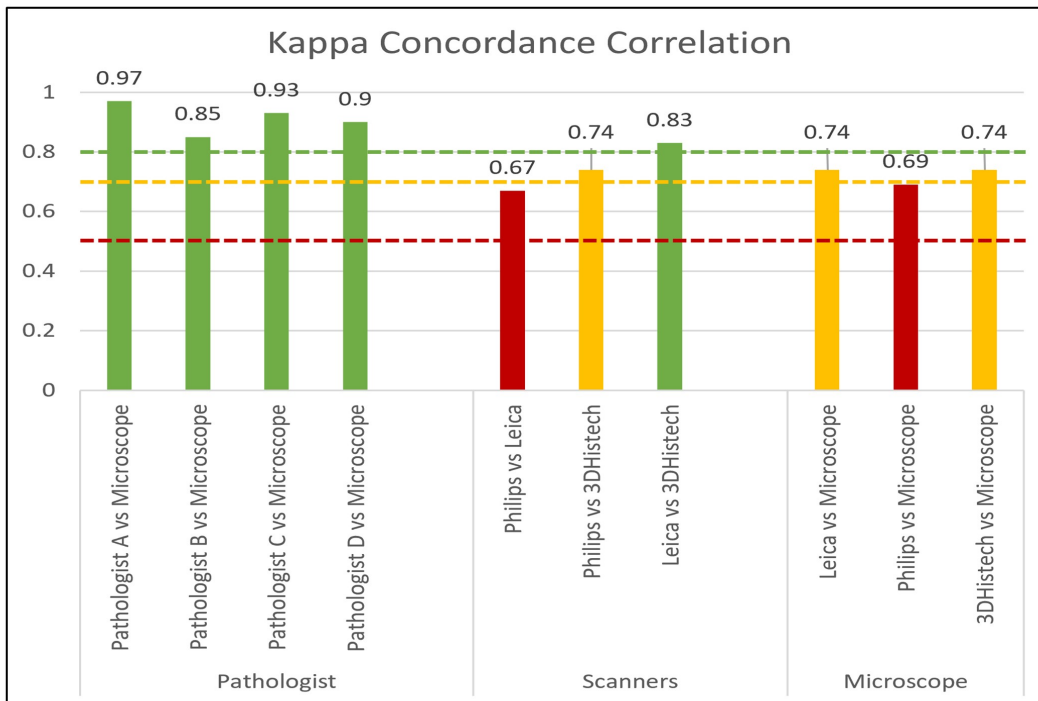
Quality assurance review of WSI prior to digital readings showed that, of the 96 glass slides scanned on the 3 scanners (total=288 scanned images), 23%(n=65) required rescanning due to label barcode detection failures, 14%(n=39) due tissue detection failures, and 2%(n=5) due to out of focus scans. The first-time successful scan rate and average number of rescans to successfully scan each slide are shown in Table 1. After remediation of the slide labels and manual software scanner adjustments, failures decreased to total of 3 images (1%).

Table1: First-time successful scan rate and average number of rescans to successfully scan for each slide

1st time successful scan	CB	ER	PR	AR	HER2
	H&E				
Positive Negative	NA	14 6	7 13	12 4	2 18
Leica	85%	80%	80%	81%	80%
Philips	75%	35%	35%	38%	20%
3DHistech	85%	80%	80%	75%	15%
Average # rescans	CB	ER	PR	AR	HER2
Leica	1.3	1.5	1.5	1.5	1.3
Philips	2.6	1.3	1.7	1.7	2.1
3DHistech	1	2	1	1	1.5

Figure 1 - 127

Figure1:



The p-value corresponds to a two-sided hypothesis test comparing reader-averaged accuracy with each scanner to the microscope (>0.5 moderate agreement, >0.7 good agreement, >0.8 strong agreement).

Conclusions: To our knowledge, this study is the first to address the accuracy of WSI of breast IHC in CBs to validate primary reporting using 3 different scanners. Digital scanning is a reliable method for ER, PR, AR and HER2 score assessment in CBs.

128 Multiple Instance Learning Predicts Recurrence from the Nuclear Morphology in Both Lymph Node Positive and Negative ER+ Breast Cancer H&E Slides

Daniel Shao¹, Cheng Lu¹, Haojia Li², Pingfu Fu¹, Anant Madabhushi¹

¹Case Western Reserve University, Cleveland, OH, ²CCIPD, Case Western Reserve University, Cleveland, OH

Disclosures: Daniel Shao: None; Cheng Lu: None; Haojia Li: None; Pingfu Fu: None; Anant Madabhushi: *Advisory Board Member, Aiforia Inc; Primary Investigator, Bristol Myers-Squibb; Primary Investigator, Astrazeneca; Primary Investigator, Boehringer-Ingelheim*

Background: Background: Estrogen Receptor Positive (ER+) breast cancer (BCa) makes up nearly two-thirds of all BCa diagnoses in the United States. Nearly all ER+ Lymph Node (LN) positive BCa patients will receive chemotherapy, but not all patients will benefit from it. For LN- patients, the criteria for chemotherapy varies widely between different clinics. The ability to prognosticate risk of recurrence and mortality with respect to LN status would enable physicians to develop more appropriate treatment plans for their patients. This study involves the use of machine learning approach called Multiple Instance Learning (MIL) to identify the prognostic ability of computer extracted feature of cancer nuclei on H&E images for predicting short-term (<10 years) recurrence-free survival (RFS) in LN- and LN+ breast cancer patients. Unlike traditional machine learning approaches which examine the tumor appearance on average, the MIL approach aims to identify the specific regions on whole slide images most reflective of cancer prognosis.

Design: Digitized H&E slides of ER+ BCa tissue from the Cancer Genome Atlas were divided into an LN+ group (n=315) and an LN- group (n=344). The LN+ and LN- groups were further separated into training sets (LN+ = 252, LN- =275) and testing sets (LN+=63, LN- =69). Ten 2000 X 2000 pixel patches were randomly selected from the tumor region of each slide, and 4663 features relating to nuclear morphology were extracted from each patch. For each training set, first the feature list was narrowed down to the 12 most informative features according to Relief-MI feature ranking. The top identified features were used to train the MIL classifier in conjunction with the Earth Mover's Distance Kernel (EMD-Kernel) to predict short-term recurrence and mortality. Classifiers specific to LN+ (+), and LN- (-) patients were constructed. Performance of M+ and M- were respectively evaluated on the LN+ and LN- test sets by Kaplan-Meier Survival analysis and Cox Proportional Hazards (CPH) analysis controlling for age, progesterone receptor status, HER2 status, and TNM-stage.

Results: The 12 top features measured various aspects of nuclear shape, haralick nuclear texture, cell cluster graphs, cell run length, and delaunay triangulation.

LN+ patients identified as high-risk by M+ had significantly worse outcomes compared to those with predicted RFS (Hazard Ratio (HR)=3.85, 95% Confidence Interval (CI)=1.61 - 9.2, p=0.002). M- demonstrated significant risk stratification of LN- patients (HR=5.10, CI=1.93 - 13.5, p=0.001). CPH showed both S- (HR=4.6, CI=1.3-16.3, p=0.017) and S+ (HR=3.24, CI=1.0-10.4, p=0.048) are prognostic of RFS, independent of leading clinical variables (age, progesterone receptor status, HER2 status, TNM-stage).

Table 1: Patient table indicating distribution of clinical variables and patient outcome for LN- and LN+ groups.

Table 1: Patient table indicating distribution of clinical variables and patient outcome for LN- and LN+ groups.

Clinical Variables	Count (Percentage)	
	TCGA LN-	TCGA LN+
Age		
<50 years	110 (35%)	72 (21%)
>=50 years	205 (65%)	278 (79%)
PR Status		
pr+	47 (15%)	52 (15%)
pr-	268 (84%)	297 (85%)
HER2		
her2+	17 (15%)	36 (22%)
her2-	97 (85%)	127 (78%)
T-stage (diam)		
t1 (<=20mm)	59 (19%)	118 (34%)
t2 (<50mm)	187 (59%)	181 (52%)
t3 (>=50mm)	69 (22%)	51 (14%)
Outcome		
Non-RFS	31 (10%)	37 (11%)
RFS	284 (90%)	323 (89%)

Figure 1 - 128

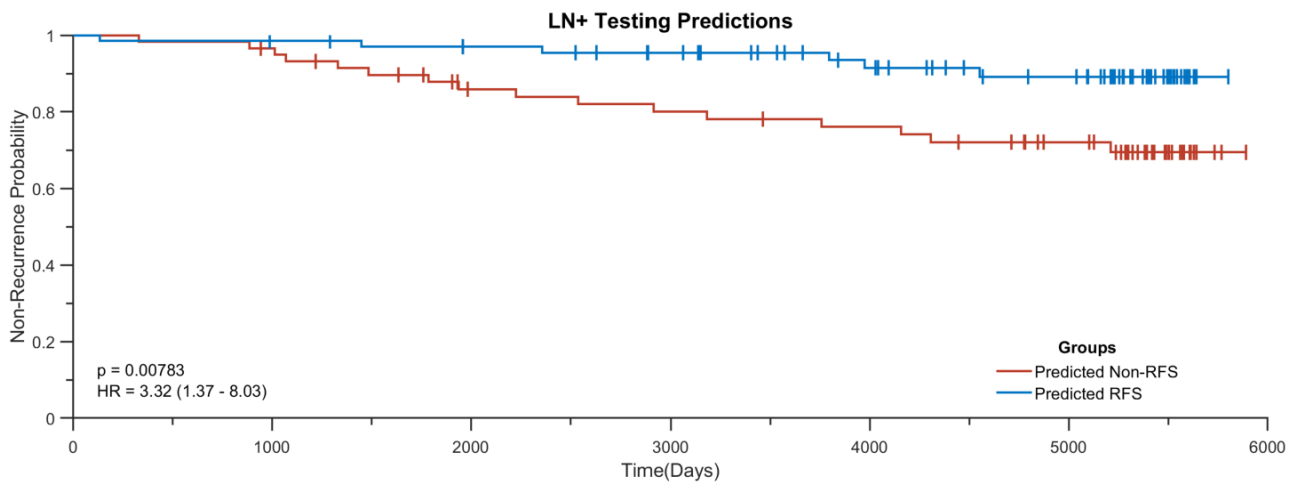
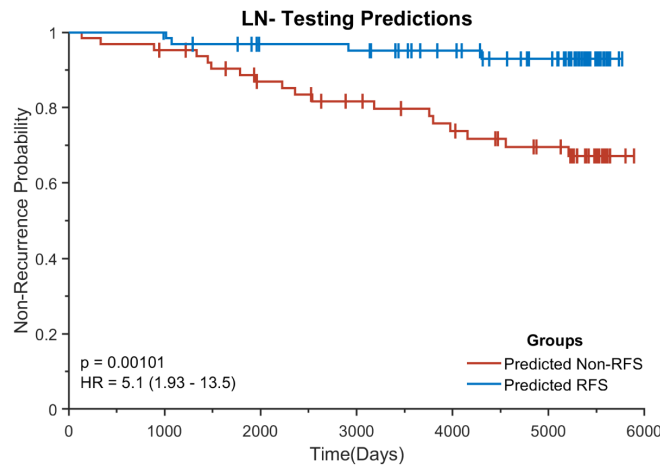


Figure 2 - 128



Conclusions: We find nuclear morphology analyzed by MIL is an independent prognostic of RFS for LN+ and LN- patients with ER+ breast cancer.

129 Prognostic Value of Androgen Receptor Expression and Molecular Alterations in Metastatic Breast Carcinomas

Tiansheng Shen¹, Anil Parwani², Zaibo Li¹

¹The Ohio State University Wexner Medical Center, Columbus, OH, ²The Ohio State University, Columbus, OH

Disclosures: Tiansheng Shen: None; Anil Parwani: None; Zaibo Li: None

Background: Metastatic breast carcinomas (BCs) with phenotypes of either triple negative (ER-/PR-/HER2-) or low hormonal receptor levels (ER and/or PR less than 10% and HER2-) are mainly treated with cytotoxic chemotherapy. A subset of these tumors eventually develop resistance urgently requiring novel therapeutic options. Targeting androgen receptor (AR) pathway may represent a potential new therapeutic strategy in breast cancer. In this report, we evaluated the prognostic value of AR expression and the molecular alterations in this subgroup of metastatic BCs.

Design: The cohort consisted of 114 metastatic BCs with phenotypes of either triple negative or low hormonal receptor levels diagnosed from 2014 to 2019 at our institution. Patient demographics, tumor pathologic characteristics (histologic type, size, lymph node status, and metastatic sites), and tumor marker profile (ER, PR and HER2) were evaluated. Assessments of AR expression by immunohistochemistry and molecular studies were performed on whole tissue sections. AR was graded as positive when at least 1% of tumor cells had nuclear immunoreactivity. Figure 1 shows representative images of AR expression in metastatic BCs.

Results: Of the 114 metastatic BCs, 37 (32.5%) cases showed AR expression and 77 (67.5%) were lack of AR expression. Statistical analysis revealed that AR expression was associated with older age, lobular carcinoma, positive ER and positive PR in primary tumors, and positive lymph nodes, but not with HER2 status in primary tumors, ER/PR/HER2 status in metastatic tumors, neoadjuvant therapy, residual tumor, and mismatch repair (MMR) proteins. In addition, patients with AR expression metastatic tumors had significantly lower rates of brain metastasis ($p = 0.025$), longer metastatic intervals ($p = 0.001$), and lower rates of death ($p = 0.036$). Moreover, compared to tumors without AR expression, tumors with AR expression had significantly higher rate of PI3CA mutation ($p < 0.001$).

Figure 1 - 129

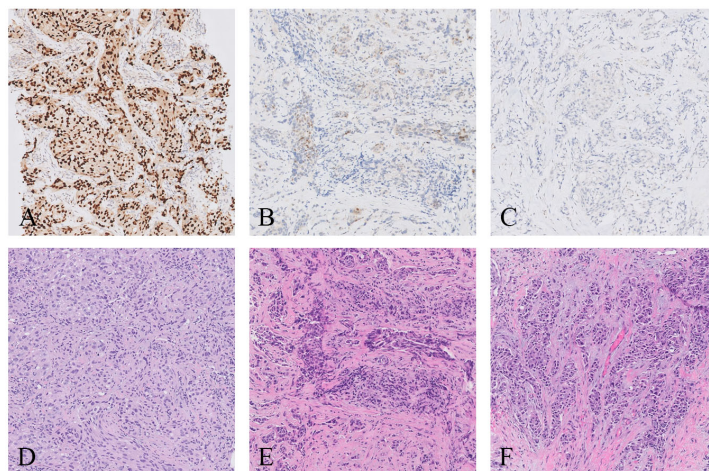


Figure 1: Illustration of high level (A), low level (B), and no expression (C) of AR in metastatic breast carcinomas, respectively. Images D, E, and F represent corresponding H&E images.

Conclusions: Our results demonstrated that AR expression has prognostic value in this subgroup of metastatic BCs and tumors with AR expression had different molecular alterations compared to those without AR expression. Our findings add to the knowledge of the molecular mechanisms that drive the different BCs and raise the interesting possibility that new treatment strategies such as targeting the AR therapy may show benefit against a subgroup of metastatic BCs.

130 Standardization of Breast Sentinel Lymph Node Evaluation at Intraoperative Consultation Decreases Discrepancies Between Frozen and Final Diagnosis

Lynelle Smith¹, Gretchen Ahrendt¹, Sharon Sams²

¹University of Colorado Anschutz Medical Campus, Aurora, CO, ²University of Colorado Denver, Aurora, CO

Disclosures: Lynelle Smith: None; Gretchen Ahrendt: None; Sharon Sams: None

Background: Intraoperative consultation of breast sentinel lymph nodes (BSN) is an invaluable tool to reduce morbidity associated with unnecessary axillary dissection. However, these specimens can be a diagnostic challenge, particularly in the setting of neoadjuvant treatment. Our aim was to evaluate reduction of discordance rates between frozen section diagnosis and final diagnosis of BSN at our institution via standardization of intraoperative consultation protocol.

Design: We implemented an intraoperative BSN evaluation protocol consisting of a standardized grossing protocol (serial sectioning at 2 mm with frozen evaluation of all sections) and a required second consult, preferentially from a pathologist with breast expertise. Comparison of discordance rate and etiology of discordant cases was performed to nonstandardized cases that were retrospectively identified from the two-years prior. Additional comparison within the protocol group was performed on specimens that were evaluated with and without a second pathologist.

Results: The non-protocol group consisted of 57 patients and 127 specimens retrospectively collected from 2017-2019. The protocol group contained 52 patients and 173 specimens prospectively collected from 2019-2020. Discordance rate significantly decreased to 5% from 12% following implementation of the standard protocol (p-value = 0.037, chi-square). The rate of review by a second pathologist increased from 8% to 57%. Four causes of discordance were identified: gross sampling, block sampling, micro-metastasis/isolated tumor cells (ITCs) and cognitive error (misdiagnosis) (TABLE). All specimens in the protocol group were grossed via standardized protocol however 99 (57%) were seconded of which 6 (16.5%) were discordant and 74 (43%) were not seconded of which 3 (12.5%) were discordant.

	Non-protocol group (127)	Protocol group (173)
Total discordant specimens *	15 (12%)	9 (5%)
Specimens seconded	10 (8%)	99 (57%)
Discordant and Seconded	2	6
Cause of discordance		
Gross sampling error	4 (27%)	1 (11%)
Block sampling error	7 (47%)	3 (33%)
Micro metastasis/ITCs	3 (20%)	5 (56%)
Misdiagnosis	1 (6%)	0
Received neoadjuvant treatment	106 (83%)	171 (99%)
Neoadjuvant + discordant	15 (100%)	8 (89%)

*p-value <.05, as calculated by chi-square analysis

Conclusions: The implementation of a standardized BSN grossing protocol significantly decreased the rate of discordance between frozen section and final diagnosis, attributed to a decrease in error in gross sampling and block sampling. In contrast, review by a second pathologist had little impact on rate of discordance. The majority of specimens in both groups received neoadjuvant therapy and therefore the impact on discrepancy rate could not be evaluated.

131 Triple Negative Breast Cancers with Low Ki-67 Proliferation Index: Clinical Pathologic Characteristics and Response to Neoadjuvant Chemotherapy

Pooja Srivastava¹, Tiannan Wang², Gloria Carter³, Beth Clark³, Jing Yu⁴, Jeffrey Fine⁴, Tatiana Villatoro¹, Rohit Bhargava³

¹University of Pittsburgh Medical Center, Pittsburgh, PA, ²University of Southern California, Keck School of Medicine of USC, LAC+USC Medical Center, Los Angeles, CA, ³Magee-Womens Hospital, Pittsburgh, PA, ⁴University of Pittsburgh, Pittsburgh, PA

Disclosures: Pooja Srivastava: None; Tiannan Wang: None; Gloria Carter: None; Beth Clark: None; Jing Yu: None; Jeffrey Fine: *Stock Ownership*, Splintellx, Inc.; Tatiana Villatoro: None; Rohit Bhargava: *Advisory Board Member*, Eli Lilly & Company

Background: Triple negative breast cancers (TNBC) are the most aggressive type of breast cancers with high tumor cell proliferation. Most TNBCs show Ki-67 proliferation index of over 50%. When treated with neoadjuvant chemotherapy (NACT), pathologic complete response (pCR) is observed in 30-40% of cases. Although patients with pCR are often considered “cured”, morbidity and mortality remains high due to recurrence in cases with residual disease (triple negative paradox). In contrast, the incidence of TNBC with lower cell proliferation index, their clinical features, particularly response to NACT remains unknown.

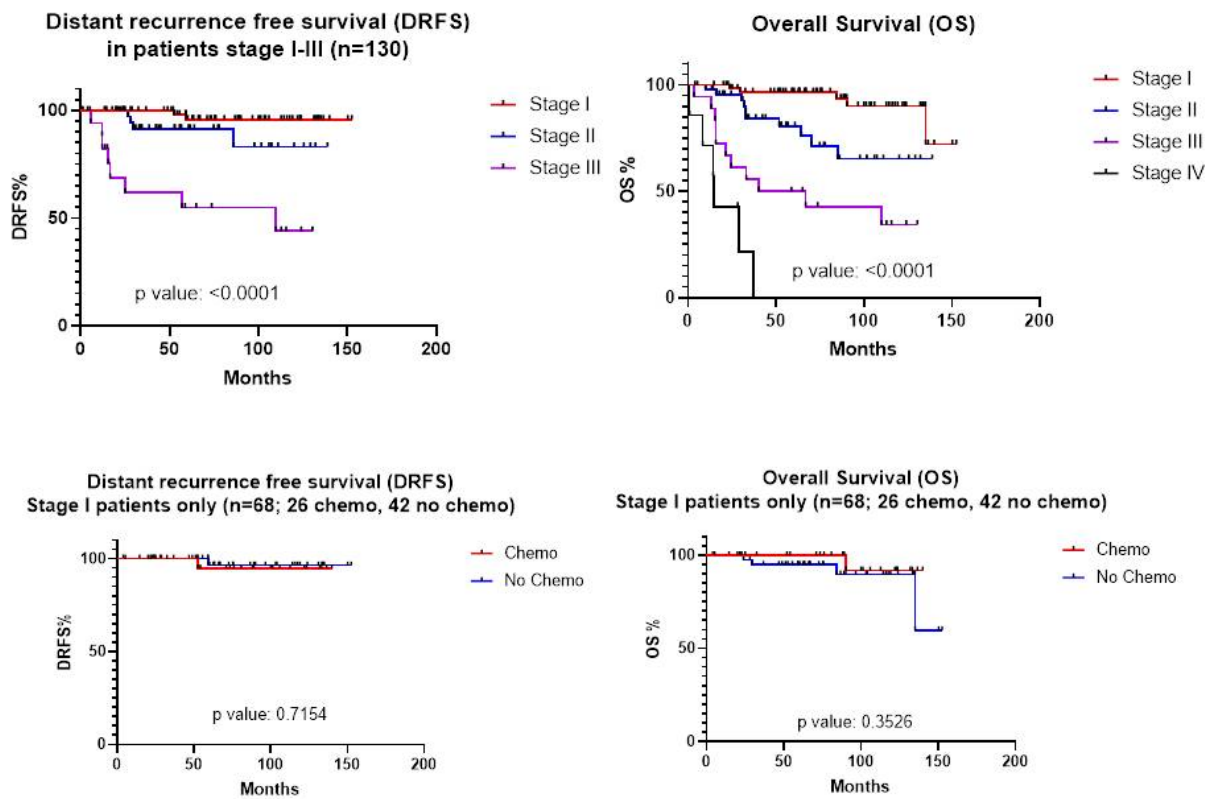
Design: We queried our institutional database (10 year) for TNBC with Ki-67 proliferation index of 30% or lower (TNlowKi). The search yielded 137 cases. The clinical features of these 137 cases are reported. Although we suspect special subtype breast cancers, basal luminal AR type, etc. to be represented in this cohort, a formal Pathology slide review is currently pending. Of the 137 cases, 31 (excludes stage IV patients) were treated with NACT. Analysis of response to NACT is also reported.

Results: TNlowKi tumors represent <2% of all breast cancers and ~10% of TNBC. Please see Table 1 for patient and tumor characteristics. In contrast to what is expected with usual TNBC, the patients with TNlowKi are slightly older, have smaller tumor size, and lower tumor grade. With average follow up of 67 months, the distant recurrence free survival was 85%, overall survival of 77% and breast cancer specific survival of 86%. Tumor stage was prognostic (see Figure 1). Overall, 57% of the patients received chemotherapy with increasing chemotherapy use in higher stage patients. Among 68 stage I patients, only 26 (38%) received chemotherapy, but this did not impact distant recurrence free and overall survival (see Figure 1). Of the 31 stage I-III patients treated with NACT, 3 (10%) showed pCR, 1 (3%) residual cancer burden (RCB) class I, 17 (55%) RCB-II, and 10 (32%) RCB-III. Three pCR and one RCB-1 patients were pre-therapy clinical stage II, had Ki-67 index of 20% or lower, did not recur, and were alive at last follow up.

Patient and Tumor characteristics	
PATIENT AND TUMOR CHARACTERISTICS	RESULTS
Age (years)	
Mean	69
Median	69
Tumor size (cm)	
Mean	2.4
Median	1.7
Grade (n=99, excludes Stage IV and neoadjuvant chemotherapy cases)	
I	10 (10%)
II	49 (50%)
III	21 (21%)
Unknown	19 (19%)
Lymph Node	
Negative (pN0)	86 (63%)
Positive (pN1)	22 (16%)
Positive (pN2)	8 (6%)
Positive (pN3)	4 (3%)

Unknown	17 (12%)
Ki-67 proliferation index	
1-10%	43 (31%)
11-20%	42 (31%)
21-30%	52 (38%)
HER2 IHC and FISH	
IHC 0	33 (24%)
IHC 1+	44 (32%)
IHC 2+, FISH HER2 copies <4/cell	54 (40%)
IHC 2+, FISH HER2 copies 4 to <6/cell	6 (4%)
Tumor Stage	
Stage I	68 (50%)
Stage II	44 (32%)
Stage III	18 (13%)
Stage IV	7 (5%)
Surgery	
Breast conserving surgery	64 (47%)
Total mastectomy	43 (31%)
Modified radical mastectomy	15 (11%)
Unknown	15 (11%)
Additional therapy	
Chemotherapy (adjuvant or neoadjuvant)	78 (57%)
Radiation therapy	82 (60%)

Figure 1 - 131



Conclusions: Despite low Ki-67 proliferation index, some patients do respond completely to NACT and have excellent prognosis. Due to overall good prognosis of stage I patients and lack of clear benefit in early stage disease, chemotherapy can be safely withheld in select stage I triple negative tumors with low Ki-67 proliferation index.

132 MYB Expression by Immunohistochemistry is Highly Specific and Sensitive for Detection of Solid Variant of Adenoid Cystic Carcinoma of the Breast, Amidst all Triple Negative Breast Cancers

Priya Subash Chandra Bose¹, Xiaoyang Ding², Harsh Batra¹, Hui Chen¹, Yun Wu¹, Maria Gabriela Raso¹, Aysegul Sahin¹, Ignacio Wistuba¹, Qingqing Ding¹, Fei Yang¹

¹The University of Texas MD Anderson Cancer Center, Houston, TX, ²Rice University, Houston, TX

Disclosures: Priya Subash Chandra Bose: None; Xiaoyang Ding: None; Harsh Batra: None; Hui Chen: None; Yun Wu: None; Maria Gabriela Raso: None; Aysegul Sahin: None; Ignacio Wistuba: None; Qingqing Ding: None; Fei Yang: None

Background: Adenoid cystic carcinoma (ACC) is rare, comprising 0.1-1% of breast carcinomas, which are ER, PR, HER2 negative. The solid variant with striking basaloid features is difficult to distinguish morphologically from some triple negative breast cancers (TNBCs) with basaloid features. This distinction is critical because, in contrast to other TNBCs with worse prognosis and outcome, ACC is a low-grade malignant tumor cured by simple mastectomy and most cases have excellent survival. Similar to salivary gland ACC, breast ACC exhibit recurrent translocation t (6:9) (q22-23; p23-24), resulting in MYB and NFIB gene fusion. MYB protein overexpression can be detected by immunohistochemistry and is useful adjunct to the diagnosis of ACC. We aimed at comparing the expression of MYB in ACC with that of other TNBCs with special reference to those with solid/ basaloid morphology.

Design: On paraffin fixed formalin embedded tissues, Immunohistochemical staining for MYB was performed on 157 cases, including ACC (n=17), TNBC (n= 140) in automated Leica system, utilizing Anti-c-Myb antibody (clone EP769Y) from Abcam. Evaluation for MYB expression by assessment of nuclear staining intensity (0, 1+, 2+, 3+) was performed, by two independent pathologists. Categorization of cases was done as follows: with strong staining (3+) as Positive; with moderate (2+) or weak staining (1+) (either focal or diffuse), as Low Positive; and those with no staining (0) as Negative.

Results: Of the 17 ACC cases (15 were of solid/ basaloid and 2 had mixed cribriform/ solid morphology), all 17 ACC cases (100%) were positive for MYB expression and exhibited strong nuclear staining. Out of 140 TNBC cases (11 had solid/ basaloid morphology and rest 129 had varied morphology), none of the TNBC were positive for MYB (0%), 37 cases exhibited low positivity (26.4%) and 103 cases were negative (73.6%). Out of 11 cases of TNBC with solid/basaloid morphology, only one (9.1%) had low positive expression and 10 cases (90.9%) were negative for MYB expression.

Figure 1 - 132

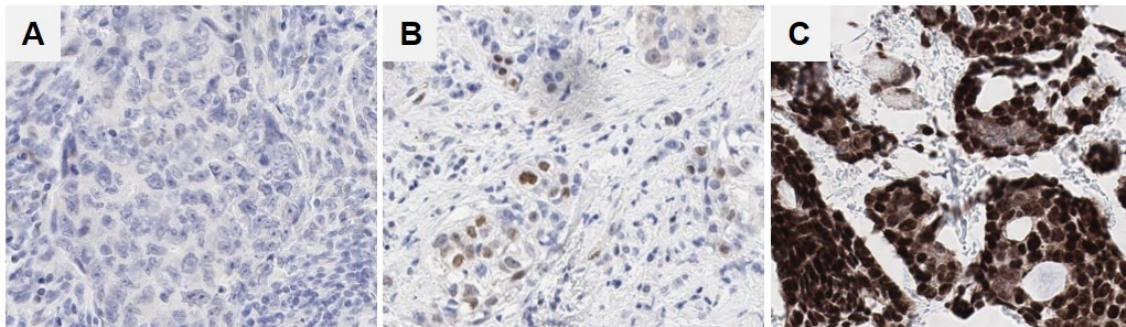


Figure 1. Representative images of MYB IHC on breast cancer, including negative staining in TNBC (A), low expression in TNBC (B) and positive staining in ACC (C).

Conclusions: Our study revealed strong nuclear staining for MYB in all ACC cases and in none of other TNBC cases, indicating that strong MYB staining by immunohistochemistry is a sensitive and specific marker for diagnosis of Adenoid cystic carcinoma of breast. Thus, we recommend routine staining for MYB antibody in all TNBCs with a solid/ basaloid morphology, to diagnose cases of ACC.

133 Expression of EMT Marker SNAIL1 Across Molecular Subtypes of Breast Carcinoma and its Clinicopathological Correlation

Sandhya Sundaram¹, Mahalakshmi Ramadoss¹, Krishnakumar Ramanathan¹, Devarajan Karunagaran²
¹Sri Ramachandra Institute of Higher Education and Research, Chennai, India, ²Indian Institute of Technology, Chennai, India

Disclosures: Sandhya Sundaram: None; Mahalakshmi Ramadoss: None; Krishnakumar Ramanathan: None; Devarajan Karunagaran: None

Background: SNAIL1 is a zinc finger transcription factor that regulates epithelial to mesenchymal transition (EMT) of tumor cells and has been associated with poor prognosis. The expression pattern of SNAIL1 across molecular subtypes of Breast carcinoma has been studied in patients reporting to a South Indian multispecialty tertiary care hospital.

Design: SNAIL 1 expression was assessed by immunohistochemical studies on 200 breast carcinoma tissue samples of different molecular subtypes including Luminal A, Luminal B, Her2Neu and triple negative breast cancer. Nuclear staining of SNAIL1 in more than 5 % of tumor cells was considered positive (**Figure1**). Cytoplasmic staining of SNAIL 1 was considered negative (**Figure2**). A correlation was drawn with detailed clinicopathological annotation and outcome to analyze influence of SNAIL 1 on clinicopathological parameters.

Results: SNAIL 1 expression varied significantly in the different intrinsic subtypes of breast carcinoma. We observed strong SNAIL1 expression in Triple Negative and Her2 subtypes of Breast Cancer among other subtypes. In the 200 breast carcinoma tissue samples analyzed triple negatives and Her2Neu were found to show increased expression of SNAIL1 than the subtypes luminal A and B (p=0.000). Differential expression was also established with different grades of breast carcinoma. A significant association of SNAIL1 expression with increasing grade was observed in the study (p=0.000). Higher tumour grade (II and III) was significantly associated with increased SNAIL1 expression. A strong and significant association of SNAIL1 expression was seen with pTNM stage of breast cancer, T (p=0.030), N (p=0.000) and M (p = 0.001) (**Table 1**). Parameters like age and family history of the subjects did not show any direct relation with SNAIL1 expression.

Table1: Comparison of tumor characteristics with the immunostaining for SNAIL 1

	SNAIL 1 >5%	SNAIL1 <5%	p value
Age			
>50 yrs	76(57.1%)	57(42.8%)	0.812
<50 yrs	40(59.7%)	27(40.3%)	
Family H/O			
Yes	7(58.3%)	5(41.7%)	0.981
No	109(58%)	79(42%)	
Tumor Subtype			
Luminal A	11(19.6%)	45(80.4%)	0.000
Luminal B	23(57.5%)	17(42.5%)	
Triple negative	46(80.7%)	11(19.3%)	
Her Neu	36(76.6%)	11(23.4%)	

Grade			
I	8(22.2%)	28(77.8%)	0.000
II	75(65.2%)	40(34.8%)	
III	33(67.3%)	16(32.7%)	
Stage(T)			
0	0	1(100%)	0.030
1	14(38.9%)	22(61.1%)	
2	70(59.3%)	48(40.7%)	
3	23(67.6%)	11(32.4%)	
4	9(81.8%)	2(18.2%)	
Stage (N)			
0	42(42.9%)	56(57.1%)	0.000
1	30(62.5%)	18(37.5%)	
2	24(77.4%)	7(22.6%)	
3	20(87.0%)	3(13.0%)	
Stage (M)			
Yes	22(88.0%)	3(12.0%)	0.001
No	94(53.7%)	81(46.3%)	

Chi square test was done and the p value < 0.05 is considered statistically significant

Figure 1 - 133

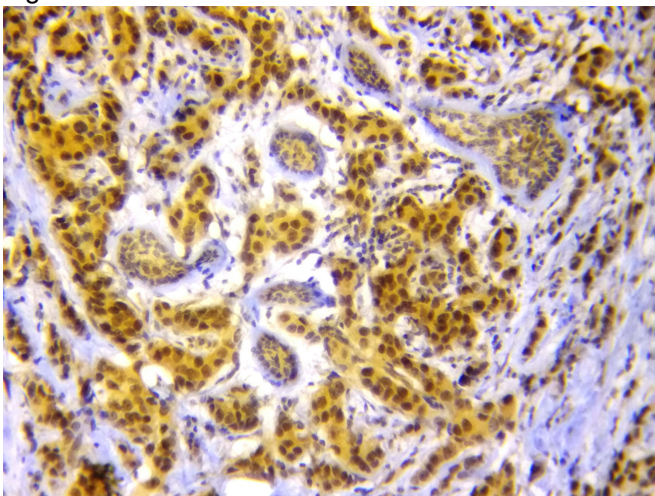
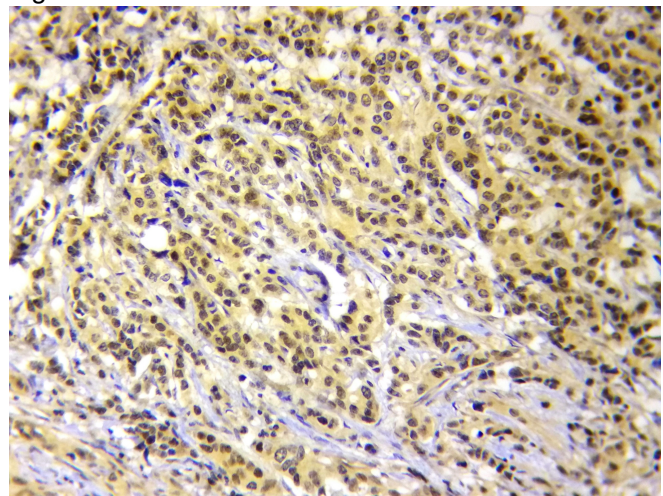


Figure 2 - 133



Conclusions: The differential expression of SNAIL 1 among intrinsic subtypes of breast cancer and correlation of SNAIL 1 expression with high grade breast carcinoma shown in the study has important implications in understanding role of SNAIL 1 and might form basis for developing targeted therapies against EMT in breast cancer in future.

134 Immunohistochemical Evaluation of 5-hydroxymethylcytosine (5-hmC) in Breast Phyllodes Tumors

Jasmine Vickery¹, Lisa Han², Stephen Dzul³, Wei Zhang⁴, Zhou Zhang⁵, Razvan Lapadat⁶, Paul DiMaggio⁷, Husain Sattar², Jeffrey Mueller⁸, Thomas Krausz⁹, Anna Biernacka²

¹University of Chicago Pritzker School of Medicine, Chicago, IL, ²University of Chicago, Chicago, IL, ³Barbara Ann Karmanos Center and Wayne State University School of Medicine, Detroit, MI, ⁴Feinberg School of Medicine/Northwestern University, Chicago, IL, ⁵Northwestern Medicine, Chicago, IL, ⁶North Shore Pathologists, SC, Milwaukee, WI, ⁷Genesis Healthcare System, Davenport, IA, ⁸University of Chicago Medical Center, Chicago, IL, ⁹University of Chicago Medicine, Chicago, IL

Disclosures: Jasmine Vickery: None; Lisa Han: None; Stephen Dzul: None; Razvan Lapadat: None; Paul DiMaggio: None; Husain Sattar: None; Jeffrey Mueller: None; Thomas Krausz: None; Anna Biernacka: None

Background: Phyllodes tumors (PTs) pose a significant diagnostic challenge in breast pathology as histological criteria and cutoffs for grading are complex and arbitrary. Nevertheless, the clinical behavior of PTs varies widely and correlates, in part, with the histological grade. Methylation signatures have gained interest as diagnostic and prognostic tools in a variety of neoplasms. In particular, 5-hydroxymethylcytosine (5-hmC) has been found to be a useful biomarker. Herein, we examine 5-hmC levels in PTs by immunohistochemistry (IHC) in relation to the clinicopathologic characteristics. Since cellular fibroadenoma (cFA) is a differential diagnosis of benign Phyllodes, it is also included in the study.

Design: A representative section of 30 benign, 11 borderline, and 10 malignant PTs, and 15 cFA was immunostained with anti-5-hmC antibody (Active Motif, Inc., Carlsbad, CA). The intensity and percent positivity of stromal cell nuclei were assessed by three pathologists blinded to the diagnosis. A final score was calculated by multiplying the intensity (1=weak, 2=moderate, 3=strong) and proportion (1=0-25%, 2=26-50%, 3=51-75%, 4=76-100%) scores. Linear regression, Fisher's exact test, and ROC curve were used for statistical analysis (Microsoft Inc, Redmond, CA).

Results: Mean nuclear expression of 5-hmC did not differ significantly between cFA and benign PT stroma, whereas it showed a gradual reduction as PT grade increased ($p < 0.001$, Table 1, Figure 1). In addition, 5-hmC levels significantly decreased with adverse histologic features, including large tumor size, infiltrative margin, marked stromal cellularity, marked stromal cell atypia, increased stromal mitoses, as well as the presence of stromal overgrowth and heterologous elements. Defining borderline PT by an IHC score of ≥ 9 (170), 5hmC showed a sensitivity of 90.5% and specificity of 91.1%; for malignant PT defined as score ≥ 3 (70), 5-hmC IHC achieved a sensitivity of 90% and specificity of 96.4%.

Figure 1 - 134

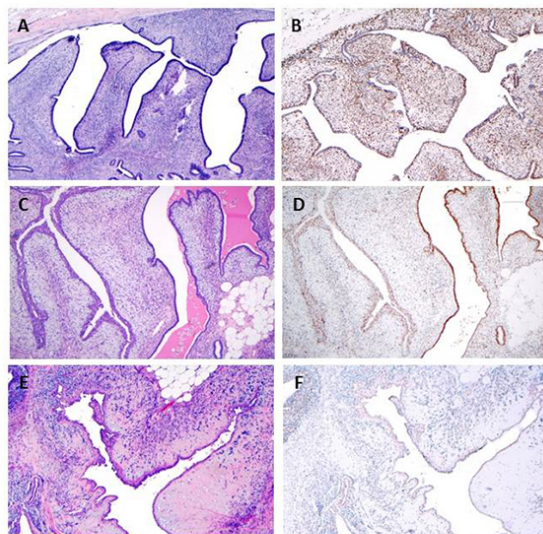


Figure 1. Representative images of the histomorphology and 5hmC immunostaining in the benign (A, B), borderline (C, D), and malignant (E, F) phyllodes tumor (40x).

Figure 2 - 134

Table 1. 5hmC expression and tumor characteristics.

Parameters	Cellular FA, N=15	Phyllodes tumors, N=51			5hmC (mean ± SD)	p-value
		Benign, N=30 (58.8%)	Borderline, N=11 (21.6%)	Malignant, N=10 (19.6%)		
Tumor size (cm, mean ± SD)	2.4±1.3	2.7±1.7	4.8±3.0	9.5±8.5	9.2±4.0	0.001
5hmC IHC score (mean ± SD)	11.6±1.5	11.4±1.6	6.3±3.5	2.3±2.1		
Tumor margin	Circumscribed	15	29	5	1	10.7±2.9
	Infiltrative		1 (focal)	6 (focal)	9	4.7±3.9
Architecture	Intracanalicular	3	17	7	7	8.6±4.3
	Pericanalicular	10	6	2	1	10.2±3.2
	Mixed	2	7	2	2	9.4±4.7
Prominent leaf-like fronds	Absent	15	15	5	4	10.1±3.6
	Present		15	6	6	8.0±4.4
Gland-to-stroma ratio	Uniform	13	8	3	1	10.3±3.3
	Variable	2	22	8	9	8.5±4.4
Stromal cellularity	Mild	5	21	1		11.5±1.5
	Moderate	10	9	10	1	9.2±3.7
	Marked				9	2.3±2.2
Stromal cell distribution	Uniform	11	6		1	10.9±2.8
	Variable	4	24	11	9	8.6±4.3
Stromal cell atypia	No/Mild	14	26	1		11.4±1.8
	Moderate	1	4	10	1	7.4±3.8
	Marked				9	2.3±2.2
Stromal mitosis/10 HPFs	0 to 4	13	29	3		11.0±2.4
	5 to 9	1	1	5	1	7.8±4.2
	≥10	1		3	9	3.7±3.4
Stromal overgrowth	Absent	15	30	7	4	10.0±3.5
	Present			4 (focal)	6	5.0±4.5
Heterologous elements	Absent	15	30	11	6	9.7±3.6
	Present				4	1.3±0.5

Conclusions: In PTs, the stromal expression of 5-hmC decreases with increasing histologic grade and correlates with morphologic predictors of adverse behavior. Benign PT and cFA show comparably high levels of 5-hmC, supporting previous studies on similarities between the two neoplasms. The reduced nuclear 5-hmC expression shows promise as a sensitive and specific marker for borderline and malignant PT, especially in distinguishing these tumors from benign fibroepithelial lesions.

135 Rate of Diagnosis Upgrade to Carcinoma in Patients with Core Biopsy Diagnosis of Intraductal Papilloma: A Single Institution Experience

Anjanaa Vijayanarayanan¹, Kevin Ginnebaugh¹, Laura Favazza², Sanam Husain², Nilesh Gupta¹, Oudai Hassan¹, Ghassan Allo², Wamidh Alkhoory¹
¹Henry Ford Health System, Detroit, MI, ²Henry Ford Hospital, Detroit, MI

Disclosures: Anjanaa Vijayanarayanan: None; Kevin Ginnebaugh: None; Laura Favazza: None; Sanam Husain: None; Nilesh Gupta: None; Oudai Hassan: None; Ghassan Allo: *Employee*, Tempus labs; Wamidh Alkhoory: None

Background: Management of intraductal papilloma (IDP) diagnosed on core needle biopsy is controversial. It has been recommended that all IDPs, especially when symptomatic, to be excised. We sought to examine the rate of upgrade to carcinoma of cases diagnosed as IDP without atypia on core needle biopsy (CNB) and compare it to cases with diagnosis of IDP with atypia.

Design: The study was approved by our institution review board (IRB). All consecutive cases with the biopsy diagnosis of intraductal papilloma between January 2010- December 2015 were included (n=437). Patients who did not undergo resection (256, 58.6%) and those with simultaneous biopsy diagnosis of ductal carcinoma in situ (DCIS) or invasive carcinoma (IC) with IDP (30, 6.9%) were excluded. Clinical features were reviewed and pathological findings were collected from the pathology reports. Pathology upgrade is defined as the presence of DCIS or IC in the subsequent resection specimen.

Results: Of the 151 IDP cases, 110 (77.8%) had biopsy diagnosis of IDP with no atypia, two of which (1.8%) had diagnosis upgrade to malignancy on subsequent resection (IC, 1; DCIS, 1). The remainder 41 cases of IDP with atypia (31 within papilloma, 9 outside papilloma, and one case with atypia within and outside the IDP), of which 14 (41.1%) demonstrated pathology upgrade to carcinoma on resection (DCIS, 12; IC, 2). Features associated with upgrade to malignancy diagnosis on subsequent resection include patient age (P= 0.0009) and presence of atypia in association with IDP (P< 0.0001). Table summarizes the relation between patient's demographic, clinical and pathology data (atypia versus no atypia) and the upgrade rate.

		IDP with no upgrade on resection	IDP with upgrade on resection	P-value	OR [95%CI]	test
n		136	15			Wilcoxon rank-sum test
Age median (range) years		57 (20-91)	71 (50-82)	0.0009		
Atypia on biopsy				<0.0001	28.0 [5.99-130.67]	Chi Square
	absent	108 (98.2%)	2 (1.8%)			
	present	27 (65.9%)	14 (34.1%)			
Screening detected				0.543	1.6 [0.3-15.5]	Chi Square
	yes	99 (89.2%)	12 (10.8%)			
	no	27 (93.1 %)	2 (6.9%)			
	unknown	10 (90.9%)	1			
Clinical presentation				0.938	1.1 [0.29-3.84]	Chi Square
	asymptomatic/unknown	101 (90.2%)	11 (9.8%)			
	nipple discharge	19 (86.4%)	3 (13.6%)			
	nipple mass	13 (92.9%)	1 (7.1%)			
	pain	2 (100%)	0 (0%)			
	combination	1 (100%)	0 (0%)			
Radiologic findings				0.277		Fisher's exact
	mass	97 (91.5%)	9 (8.5%)			
	calcifications	23 (92.0%)	2 (8.0%)			
	architectural distortion	10 (83.3%)	2 (16.7%)			
	combination	6 (75%)	2 (25%)			
BiRADS				0.889		Fisher's exact
	3	1 (100%)	0 (0%)			
	4	5 (83.3%)	1 (16.7%)			
	4a	21 (91.3%)	2 (8.7%)			
	4b	26 (81.3%)	6 (18.8%)			
	4c	7 (87.5%)	1 (12.5%)			
	5	2 (100%)	0 (0%)			

Conclusions: The findings of our study support the recommendation of resecting all IDPs with atypia. While the risk of immediate upgrade is low in IDPs without atypia, further studies are needed to address short- and long-term progression risk in this group to tailor treatment accordingly.

136 Mammprint: Update on Histo-Pathologic Associations, Comparison to Magee Equations and Utility in Neoadjuvant Setting

Tatiana Villatoro¹, Stephanie David², Beth Clark³, Jing Yu⁴, Gloria Carter³, Jeffrey Fine⁴, Adam Brufsky⁴, Shannon Huggins-Puhalla¹, Vikram Gorantla¹, Rohit Bhargava³

¹University of Pittsburgh Medical Center, Pittsburgh, PA, ²Diagnostic Pathology Services, Chattanooga, TN, ³UPMC Magee-Womens Hospital, Pittsburgh, PA, ⁴University of Pittsburgh, Pittsburgh, PA

Disclosures: Tatiana Villatoro: None; Stephanie David: None; Beth Clark: None; Jing Yu: None; Gloria Carter: None; Jeffrey Fine: *Stock Ownership*, Splintellx, Inc.; Adam Brufsky: *Consultant*, Agendia; *Consultant*, Biotheranostics; *Consultant*, Myriad; Shannon Huggins-Puhalla: *Grant or Research Support*, Pfizer; *Grant or Research Support*, Astra Zeneca; *Advisory Board Member*, Abbvie; Vikram Gorantla: None; Rohit Bhargava: *Advisory Board Member*, Eli Lilly & Company

Background: Mammprint (MP) is an FDA cleared multi-gene assay indicated for prognostic use in early stage breast cancer, regardless of ER status. However, similar to other multigene assays, it is often used for making chemotherapy decisions (predictive use) in ER+ breast cancers in routine practice. The various test results are not interchangeable and there is a considerable difference in risk assignment between different tests at the individual tumor level. Alternatively, multivariable models such as Magee Equations (MEs) can also be used either definitively or in triage for selecting cases for molecular testing. ME3 score has been shown to have chemo-predictive value - rare pathologic complete response (pCR) to chemotherapy with score 25 or below, up to 14% pCR rate with scores >25 to <31 and 40% pCR rate in patients with score 31 or higher (Farrugia DJ et al. *Mod Pathol.* 2017. PMID: 28548119 and Bhargava R et al. *Mod Pathol.* 2020. PMID: 32661297).

Design: The current study analyzed the clinical requests for MP testing at our institution from the last 4 years. MP testing was performed on 367 cases in the adjuvant setting. Additional 18 treated with neoadjuvant chemotherapy [NACT] were assessed for response with respect to MP result and ME3 scores. All Magee equations were calculated on 365 of 367 non-neoadjuvant cases but only ME3 was calculated on neoadjuvant cases. The associations between MP results with average ME scores and other variables are described. Responses to NACT on 18 cases were compared between MP results and ME3 scores.

Results: Associations between MP results and pathological variables is shown in Table 1. All 18 cases except one treated with neoadjuvant chemotherapy showed high MP result, but none achieved pCR, only one showed residual cancer burden (RCB)-1, 11 RCB-II, and 6 RCB-III. In contrast, only one case showed ME3 score >31 and this case showed RCB-1. The ME3 scores ranged from 13.8 to 32.7 with mean and median ME3 scores of 23.4 and 21.9 respectively. None of the 9 neoadjuvant cases with positive pre-therapy lymph node core biopsy had negative node on resection.

Table 1: Associations between MP results and pathological variables

Variables	MP high (n=163)	MP low (n=204)	p-value
Age (years)	55	55	0.9949
Nottingham Score ^a	58	156	<0.0001*
4-6	104	47	
7-9			
Nottingham Grade ^a	4	35	Ref
I	91	152	0.0005
II	67	16	<0.0001*
III			
ER H-score	241	245	0.4669
PR H-score	130	170	0.0003*
HER2 Status	145	193	0.0526
Negative	18	11	
Equivocal			
Ki-67 Proliferation Index (%)	29	17	<0.0001*
Tumor size	2.6	2.8	0.4665
LN status	7	7	0.7375 (neg vs pos)
ITC	96	117	
Negative	56	75	
Positive	4	5	
Unknown			
Tumor type	139	156	<0.0001* (ductal vs lob)
Ductal	17	56	
Lobular	7	12	
Mixed			
Average ME score	34	99	Ref
Less than 18	90	93	<0.0001*
18 to 25	31	10	<0.0001*
>25 to <31	7	1	0.0007*
31 or higher			

^aNottingham score/grade/ME score available on 365 cases. *Statistically significant. MP: Mammaprint; ME: Magee Equations. HER2 equivocal defined as HER2 IHC score of 2+ and HER2 copies/cell of 4 to <6

Conclusions: High MP results are associated with high Nottingham grade, low PR H-score, and high Ki-67 proliferation index. Increasing ME scores predicted for high MP results. Results on 18 cases subjected to NACT shows that MP-high doesn't always predict for chemotherapy benefit. MP is FDA cleared for prognostic use only and caution is advised in using MP results for selecting cases for neoadjuvant chemotherapy.

137 PTEN Alteration in ER+ Breast Cancer: Correlative Study of Immunohistochemistry and Next Generation Sequencing

Jing Wang¹, Constance Albarracin¹, Lei Huo¹, Qingqing Ding¹, Yun Wu¹, Sinchita Roy-Chowdhuri¹, Keyur Patel¹, Mark Routbort¹, Rajyalakshmi Luthra¹, Hui Chen¹

¹The University of Texas MD Anderson Cancer Center, Houston, TX

Disclosures: Jing Wang: None; Constance Albarracin: None; Lei Huo: None; Qingqing Ding: None; Yun Wu: None; Sinchita Roy-Chowdhuri: None; Keyur Patel: None; Mark Routbort: None; Rajyalakshmi Luthra: None; Hui Chen: None

Background: While PTEN loss in HER2+ and triple-negative breast cancers (BC) is associated with worse disease free survival and overall survival, it is not well studied in ER+ BC, even though there is known association with tamoxifen resistance. One of the major limitations is that PTEN assessment lacks consistency and reproducibility. Concordance between immunohistochemistry (IHC) and next generation sequencing (NGS) is not well established. This study is to compare PTEN expression by IHC and *PTEN* gene alteration by NGS in ER+ BC.

Design: We reviewed 372 ER+ advanced BC tested by NGS Oncomine v3 (Thermo Fisher) from 2018 to 2020 to assess *PTEN* mutation and copy number aberration. 48 cases were selected to perform IHC with a monoclonal antibody to human PTEN (6H2.1, Dako). PTEN IHC interpreted as retained (>5% cytoplasmic and/or nuclear stain in tumor cells), loss (<1%, with retained stain in adjacent benign cells), and equivocal (focal/weak stain or heterogeneous stain). Consensus was reached between 4 pathologists.

Results: In 372 ER+ BC cases tested by NGS, 23 (6.2%) had *PTEN* mutations, 10 (2.7%) had deletion. In the 48 cases wherein both NGS and IHC were tested, IHC showed loss in 7 (15%), equivocal in 5, and retained in 36 tumors (Table 1). NGS showed *PTEN* alteration in 15 (31%) including deletion in 8, point mutation in 4, in-frame indel in 1, nonsense in 1, and splice-site mutation in 1 tumor. All tumors with PTEN loss had either *PTEN* deletion or splice-site and nonsense mutations. 89% (32/26) tumors with retained PTEN had no *PTEN* alteration detected by NGS. 4 equivocal cases showed focal/weak stain, with 1 deletion, 1 in-frame indel, 1 point mutation, and 1 no detected alteration. The other equivocal case showed heterogeneous PTEN staining and partial *PTEN* deletion.

PTEN Protein by IHC	PTEN Gene Alteration by NGS			
	Deletion (n = 8)	Splice site/ Nonsense Mutation (n = 2)	In-frame Indel/ Point Mutation (n = 5)	Not Detected (n = 33)
Loss (n = 7)	5	2	0	0
Equivocal (n = 5)	2	0	2	1
Retained (n = 36)	1	0	3	32

Conclusions: *PTEN* gene alterations are present in 8.9% of advanced ER+ BC by NGS. PTEN loss by IHC correlates with *PTEN* deletion, splice-site or nonsense mutations. Equivocal PTEN expression warrants further reflex test by alternative assay. Our data support complementary testing by IHC and NGS to accurately assess *PTEN* status in ER+ BC.

138 Pathological Response to Neoadjuvant Chemotherapy in HER2-positive Breast Cancer Patients Stratified by Detection Method According to the 2018 CAP/ASCO Guideline Update

Lin Wang¹, Jaya Asirvatham², Yanlin Ma³, Emily Reisenbichler⁴, Julie Jorns¹

¹Medical College of Wisconsin, Milwaukee, WI, ²Baylor Scott & White Health/Texas A & M Health Science Center College of Medicine, Temple, TX, ³University of Virginia, Charlottesville, VA, ⁴Yale University, New Haven, CT

Disclosures: Lin Wang: None; Jaya Asirvatham: None; Yanlin Ma: None; Emily Reisenbichler: None; Julie Jorns: None

Background: HER2, a routine breast cancer marker, is associated with worse prognosis but increased sensitivity to targeted chemotherapeutics such as trastuzumab and pertuzumab that are frequently used in the neoadjuvant setting. The purpose of this study was to compare pathological outcomes in HER2-positive patients treated with HER2-targeted neoadjuvant chemotherapy (NAC) following guideline updates set by CAP/ASCO in 2018.

Design: 99 HER2-positive patients, as defined by the 2018 CAP/ASCO updated guidelines, from three institutions were identified. All institutions used primary immunohistochemistry (IHC) and reflexed fluorescence in situ hybridization (FISH) if IHC (2+) equivocal. Clinicopathologic features, HER2 positivity method (IHC or FISH), and post-NAC tumor response were reviewed. Biomarker status was dichotomized as HER2 if estrogen receptor (ER) and/or progesterone receptor (PR) were negative or low positive (1-10%) and luminal-HER2 (LUMHER2) if ER/PR positive (>10%). Response was measured by three prognostic markers— pathologic complete response (pCR), Residual Cancer Burden (RCB), and downstaging.

Results: Most (97%) were female with mean age of 54 yrs. 54 were LUMHER2 and 45 HER2. 71 were IHC positive and 28 FISH positive. Of those that were FISH positive, mean HER2/CEP17 ratio was 3.28 (range 1.57-8.1) and mean average HER2 signals/cell was 7.47 (range 3.55-14.4), with 25 group 1 (HER2/CEP17≥2 and average HER2/cell≥4), 1 group 2 (HER2/CEP17≥2 but average HER2/cell<4) and 1 group 3 (HER2/CEP17<2 but average HER2/cell≥6). Most (94%) underwent NAC plus trastuzumab and pertuzumab, with the remainder receiving NAC plus trastuzumab.

On univariate analysis, pCR was associated with HER2 (vs LUMHER2) biomarker status and HER2 positivity detection method of IHC (vs FISH), with features of higher biopsy grade (p=.06) and clinical stage (p=.07) approaching significance. Multivariate analysis showed pCR and RCB to be associated with HER2 biomarker status and IHC detection method. Downstaging also showed variable significant associations with HER2 biomarker status and IHC method (Table 1).

Table 1. Multivariate analysis

Outcome/variable	Odds ratio [95% CI]	P-value
pCR		
FISH vs. IHC	0.37 [0.14, 0.96]	0.05
HER2 vs. LUMHER2	3.41 [1.45, 8.30]	0.003
RCB		
FISH vs. IHC	3.64 [1.54, 8.81]	0.004
HER2 vs. LUMHER2	0.34 [0.15, 0.77]	0.007
ΔT Stage		
FISH vs. IHC	2.67 [0.94, 7.90]	0.08
HER2 vs. LUMHER2	0.26 [0.10, 0.63]	0.002
ΔN Stage		
FISH vs. IHC	0.24 [0.06, 0.86]	0.03
HER2 vs. LUMHER2	1.33 [0.42, 4.28]	0.62

Conclusions: Overall biomarker status and HER2 detection method allow for further prognostic stratification of HER2-positive patients when 2018 ASCO/CAP guideline updates are applied.

139 The Clinical, Pathological and Molecular Features of Breast Cancer with Pathogenic Germline Variants Other Than BRCA1/2

Xi Wang¹, Kimberly Cole², Malini Harigopal², Karin Finberg², Zenta Walther², Minghao Zhong²
¹Yale School of Medicine, Yale New Haven Hospital, New Haven, CT, ²Yale School of Medicine, New Haven, CT

Disclosures: Xi Wang: None; Kimberly Cole: None; Malini Harigopal: None; Karin Finberg: None; Zenta Walther: None; Minghao Zhong: None

Background: There has been considerable progress in our understanding of *BRCA1* and *BRCA2* mutations, which account for approximately 5% of all breast cancers (BC). *BRCA1* mutation is associated with high histologic grade, ER/PR/HER2 triple negative breast cancer and *BRCA2* mutation is usually high-grade, ER+/HER2-. While the characteristics of *BRCA*-mutant BC have been well established, the features of BC with other pathogenic germline variants (PGV) are less well studied. We aimed to characterize the clinical, pathological and molecular features of BC with PGV other than *BRCA1/2*.

Design: Breast cancer patients' samples as well as germline control specimens were submitted for molecular profiling using OncoPrint Comprehensive Assay panel (OCP; Thermo Fisher Scientific) to identify alterations in up to 143 cancer related genes by targeted next generation sequencing (NGS). We searched our data base for BC with non-*BRCA1/2* PGV and analyzed their clinical, pathological and molecular features.

Results: 8 breast carcinoma patients with PGV other than *BRCA1/2* were identified. 3 patients (37.5%) carried *ATM* mutations; each of the others harbored a mutation in one of the following genes: *CHEK2*, *TP53*, *NBN*, *ERCC2* and *BAP1*. Besides the germline mutations, tumors also had somatic variants in genes such as *ESR1*, *PI3KCA*, *TP53*, and a few gene amplifications including *MYC* and *MDM2*. The average onset age was 48.3 years old (+/-4.7 years) and no patient had a personal history of other malignancy. 7 patients had significant family histories of cancer, and 1 reported Ashkenazi Jewish ancestry. Carcinomas from patients with PGV other than *BRCA1/2* were associated with intermediate to high grade (at least grade 2) histology. 7 patients had infiltrative ductal carcinoma and 1 patient (with a *TP53* PGV) had infiltrative lobular carcinoma. The biomarker tumor profile by IHC revealed 7 (87.5%) ER+/PR+/HER2- and only 1 (12.5%) ER-/PR-/HER2-.

Patient	Germline mutation	Somatic variants	Clinical features (onset age/ family history)	Breast pathology (grading, morphology, phenotype)
1	<i>ERCC2</i>	<i>ESR1/MAX/PALB2</i>	48/ breast and colon cancer, melanoma	Grade 2, ductal carcinoma, ER+/PR+/HER2-
2	<i>BAP1</i>	<i>PIK3CA/CCND3</i>	51/ prostate cancer	Grade 3, ductal carcinoma, ER+/PR+/HER2-
3	<i>CHEK2</i>	<i>TP53/PIK3CA/SMARCA4</i> <i>FGFR2/ATRX/NTRK3/</i> <i>RAD51C/BRCA2</i>	52/anal and bladder cancer	Grade 2, ductal carcinoma, ER+/PR+/HER2-
4	<i>TP53</i>	<i>PI3K3CA</i>	57/no pertinent	Grade 2, lobular carcinoma, ER+/PR+/HER2-
5	<i>ATM</i>	<i>ESR1/SF3B1</i>	46/ovarian and breast cancer	Grade 3, ductal carcinoma, ER+/PR+/HER2-
6	<i>ATM</i>	<i>ESR1</i>	39/colon and prostate cancer	Grade 2, ductal carcinoma, ER+/PR+/HER2-
7	<i>NBN</i>	<i>TP53/FANCD2</i>	47/lung cancer	Grade 3, ductal carcinoma, ER-/PR-/HER2-
8	<i>ATM</i>	<i>PIK3CA/BRCA2</i>	46/breast cancer	Grade 2, ductal carcinoma, ER+/PR+/HER2-

Conclusions: Most of the non-*BRCA* PGV in our study are DNA damage response (DDR) genes including ATM, CHEK2, ERCC2 and NBN. The patients with those PGV in DDR genes may be eligible for certain clinical trials, such as PARP inhibitor. Patients with PGV other than *BRCA1/2* presented with breast cancer at young age, had at least grade 2 infiltrative carcinoma and were strongly associated with ER+/PR+/HER2- immunophenotype. Although a small series, our data suggests the distinct characteristics of non-*BRCA* mutations in breast cancer patients and highlights the value of multi-gene panel testing.

140 Utilization of Commercial SP142 PD-L1 Testing of Breast Carcinomas at a Large Academic Cancer Center

Serena Wong¹, Emily Reisenbichler²

¹Yale New Haven Hospital, New Haven, ²Yale University, New Haven, CT

Disclosures: Serena Wong: None; Emily Reisenbichler: None

Background: Triple negative (TN) breast cancer, defined as hormone receptor and HER2 negative, is an aggressive tumor subtype with poor clinical outcome. The IMpassion130 trial showed that patients with locally advanced or metastatic TN carcinoma demonstrating at least 1% immune cell (IC) staining with the PD-L1 assay SP142 had improved survival with the addition of Atezolizumab to Nab-Paclitaxel. As a result, in March 2019, the FDA approved the SP142 PD-L1 assay as a companion diagnostic test to determine eligibility for immunotherapy in these patients. Due to the availability of numerous PD-L1 assays and the complexity of various scoring methods required for tumors of different organ systems, many institutions are choosing to use commercial labs for the performance and interpretation of this assay. We review the utilization and results of commercial PD-L1 testing at our institution.

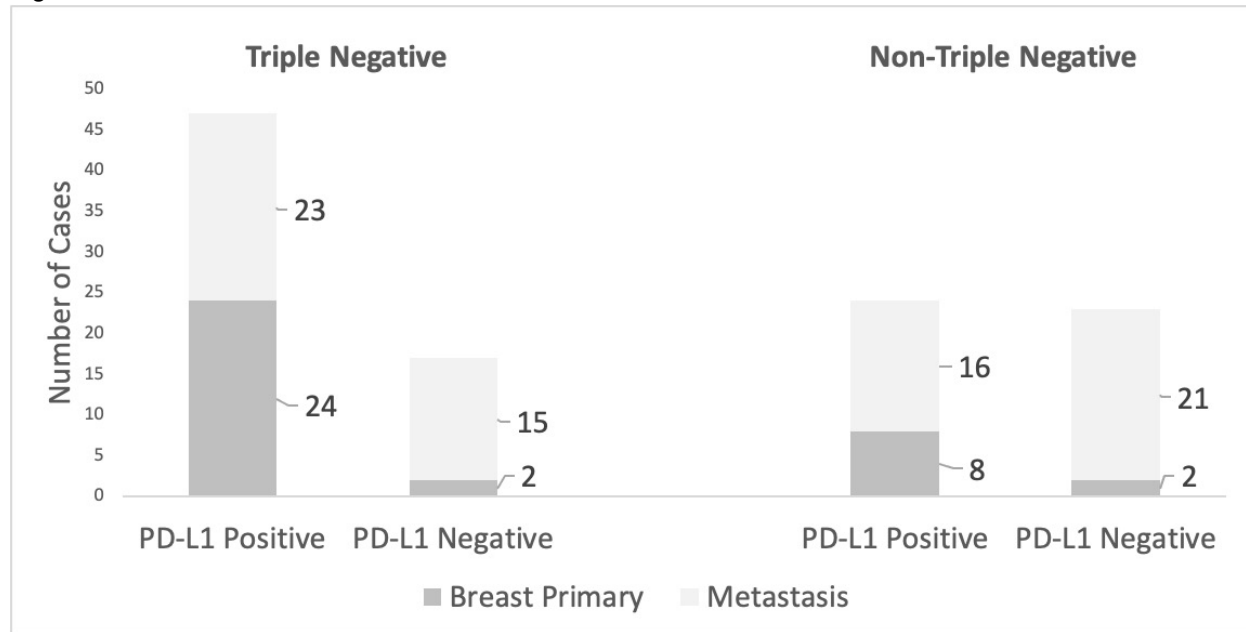
Design: Retrospective review of send out SP142 testing was collected from 3/2019 to 8/2020. Clinical and pathologic information was collected from pathology reports and medical record review, including receptor profile of primary and metastatic tumors (if present). PD-L1 results were obtained from commercial lab reports with percentage (%) and intensity of IC staining. Cases with low or negative hormone receptor and negative HER2 were classified as TN. Cases with hormone receptor and/or HER2 positivity in both primary and metastatic tumors were classified as non-TN. PD-L1 results were defined as negative (IC<1% staining) or positive (IC³ 1% staining).

Results: 118 samples (50 non-TN tumors, 60 TN tumors, and 8 non-TN breast primaries with TN metastases) from 111 patients were tested for PD-L1 SP142. 36 samples were from breast primaries and 82 were from metastases. 7 samples were deemed quantity not sufficient (QNS) or indeterminant for PD-L1 assessment. More than one sample was sent for testing in 5 patients, 3 of which were repeats for initial QNS results. 2 patients had testing from multiple metastatic sites, all of which were PD-L1 positive. Of the 111 total cases with results, 40 were PD-L1 negative and 71 were PD-L1 positive. All PD-L1 negative cases were reported with 0% staining (none with <1%IC). PD-L1 was positive in a significantly higher percentage of TN cases than non-TN cases (Table 1 and Figure 1). Staining in all positive cases ranged from 1-80% (mean 3.9) with only 10 cases (8%) showing >5% IC staining. Although higher % IC staining was seen in TN than non-TN tumors, it was not statistically significant.

	Triple Negative* (n=64)	Non-Triple Negative (n=47)	p-value
Number of PD-L1 positive cases (%)	47 (73)	24 (51)	0.018
Mean % staining in positive cases (range)	7.87 (1-80)	2.63 (1-20)	0.172
Mean intensity staining in positive cases (range)	2.64 (1-3)	2.21 (1-3)	0.015

* Includes cases with hormone receptor or HER2 positive primary tumors that developed triple negative metastases

Figure 1 - 140



Conclusions: Most PD-L1 testing from our center was performed in TN tumors on metastases and showed a higher rate of positivity than in the IMpassion130 trial. Although not currently FDA approved in this tumor type, non-TN breast tumors showed a significantly lower rate of PD-L1 positive cases.

141 WT1 is Selectively Expressed in Breast Carcinoma with >90% Mucinous Components

Xiaoli Xu¹, Rui Bi², Ruohong Shui¹, Bao-Hua Yu¹, Yufan Cheng¹, Xiaoyu Tu¹, Wentao Yang¹
¹Fudan University Shanghai Cancer Center, Shanghai, China, ²Fudan University Shanghai Cancer Center, Shanghai Medical College, Fudan University, Shanghai, China

Disclosures: Xiaoli Xu: None; Rui Bi: None; Ruohong Shui: None; Bao-Hua Yu: None; Yufan Cheng: None; Xiaoyu Tu: None; Wentao Yang: None

Background: Mucinous production can be found in different types of invasive breast carcinoma. Mucinous carcinoma is defined as invasive carcinoma with >90% mucinous component, but not all invasive carcinomas with >90% mucinous component can be diagnosed as mucinous carcinoma. This study aimed to investigate the characteristics of immunohistochemical WT1 expression in invasive breast carcinoma with >90% mucinous components and the clinicopathological significance.

Design: One hundred specimens of invasive breast carcinoma with >90% mucinous component were collected. All haematoxylin and eosin (H&E)-stained slides were reviewed, and the clinicopathological data, including sex, age, tumour size, nuclear grade, histological grade, growth pattern, and lymph node (LN) status, were collected. Immunohistochemistry (IHC) of WT1 (Wilm’s tumour 1), oestrogen receptor (ER), progesterone receptor (PR), human epidermal growth factor receptor 2 (HER2) and Ki-67 was performed. Fluorescence in situ hybridization (FISH) was used to verify the amplification of the HER2 gene in cases with an IHC score of 2+. The relationship between WT1 expression and clinicopathological features was analysed statistically.

Results: WT1 expression was detected in 67% (67/100) of invasive carcinomas with >90% mucinous components, and most (93%) of the positive staining was diffuse and strong. WT1 expression was significantly associated with low-intermediate nuclear grade/histological grade, ER and/or PR positivity, negative HER2 status, Ki-67 proliferation index <30% and no lymph node metastasis (all P<0.001). Micropapillary architecture was observed in 80% of cases. WT1 expression was not significantly correlated with different percentages of micropapillary components (P=0.422). None of the histological grade 3 tumours, tumours with HER2 overexpression/amplification and triple-negative specimens showed WT1 expression.

Conclusions: WT1 expression was significantly correlated with low-intermediate nuclear/histological grade, ER positivity, HER2 negativity, a lower Ki-67 proliferation index and no lymph node metastasis in invasive breast carcinoma with >90% mucinous component. The micropapillary growth pattern in this type of tumour did not show a specific relationship with WT1 expression.

142 Clinicopathologic and Immunohistochemical Features of Breast Angiosarcoma and Atypical Vascular Proliferation: A Single Institutional Cohort

Mingfei Yan¹, Hannah Gilmore², Philip Bomeisl³, Aparna Harbhajanka⁴

¹Case Western Reserve University/University Hospitals Cleveland Medical Center, OH, ²University Hospitals Case Medical Center, Case Western Reserve University, Cleveland, OH, ³University Hospitals Cleveland Medical Center, Cleveland, OH, ⁴Case Western Reserve University/University Hospitals Cleveland Medical Center, Cleveland, OH

Disclosures: Mingfei Yan: None; Hannah Gilmore: None; Philip Bomeisl: *Consultant*, Path AI; Aparna Harbhajanka: None

Background: Breast angiosarcoma (AS) is a rare malignancy which can either be primary or secondary to breast cancer treatment. Pathologically, breast AS has a wide spectrum of morphologic presentations, and its diagnosis can be challenging based on morphologic evaluation.

Design: We identified 7 patients with radiation-associated AS (RA-AS) and 3 patients with primary AS (P-AS). Four cases of atypical vascular proliferation (AVP), the most common differential diagnosis for AS, were also collected. All cases were reviewed by experienced breast pathologists. Relevant clinical information and patient's prognosis were collected from electrical medical records according to institutional review board guidelines. c-MYC immunostains were performed for all cases. D2-40 immunostains were also performed for a subset of cases to determine their lymphatic differentiation.

Results: The latency between radiotherapy and AS was 8.1 years. RA-AS mostly occurred in breast dermis, while all primary AS involved breast parenchyma. All the 10 AS cases were high grade, and local recurrence or distant metastasis were only seen in 4 cases with epithelioid morphology. High-grade P-AS showed a mixture of both low- and high-grade lesions (Figure 1A, 1B). Identification of hemorrhage, necrosis or confluent growth classified them as high-grade lesions (Figure 1B), though such findings may be present focally. Besides, P-AS did not show prominent vesicular nuclei and conspicuous nucleoli (Figure 1C) as seen in RA-AS (Figure 1D). Epithelioid AS showed great morphologic overlap with breast carcinoma (Figure 2A). Two epithelioid AS cases showed distinct morphology of discohesive cells sloughing off at periphery of vascular cores (Figure 2B), and both of which showed lymphatic differentiation by D2-40 positivity. P-AS was either negative for c-MYC or showed rare weak positivity in high-grade areas. In comparison, RA-AS were consistently positive for c-MYC (Figure 2C). Besides, epithelioid AS, especially cases with lymphatic differentiation, tended to show stronger or more diffuse c-MYC positivity than other AS cases (Figure 2D). Morphologically, AVP could show atypical nuclear features with prominent nucleoli, making it important to differentiate from low grade AS. However, all cases of AVP were either negative for c-MYC or showed only rare weak positivity.

Case	Age (yr)	Gender	Diagnosis	Side	Treatment	Diagnosis	Latency after prior treatment (yr)	Side	Prior breast cancer			Breast vascular lesion		
									Size (cm)	Breast skin involvement	Breast parenchyma involvement	Treatment	Recurrence or metastasis	c-MYC IHC
1	63	F	IDC	L	MAS	Angiosarcoma, high grade	18	R	7.5	Yes	Yes	MAS	None	Focal weak positivity
2	73	F	ILC	L	LUM, ALND, CHEM, RAD, TAM	Angiosarcoma, high grade	8	L	2.5	Yes	No	Paclitaxel	None	Partially positive
3	93	F	IDC	R	LUM, RAD	Angiosarcoma, high grade	6	R	5	Yes	No	MAS	None	Partially positive
4	57	F	IDC	R	RAD, TAM	Epithelioid angiosarcoma	7	R	0.4	No	Yes	Paclitaxel, MAS, RAD	Chest wall recurrence	Diffusely positive
5	67	F	IDC	R	LUM, ALND, CHEM, RAD, TAM	Epithelioid angiosarcoma	10	R	2.5	Yes	No	MAS, RAD	Chest wall recurrence, then metastasis to spleen, contralateral breast and brain	Partially positive
6	80	F	IDC	R	MAS, RAD	Epithelioid angiosarcoma	8	R	3	Yes	No	Paclitaxel, Bevacizumab	Axillary metastasis	Diffusely positive
7	54	F	None	N/A	N/A	Angiosarcoma, high grade	N/A	L	6	No	Yes	MAS	None	Focally positive
8	67	F	IDC	R	LUM, CHEM, RAD	Epithelioid angiosarcoma	10	R	2.5	Yes	Yes	Paclitaxel, Cisplatin, MAS, RAD	Chest wall recurrence	Diffusely positive
9	69	F	IDC	L	LUM, ALND, CHEM, RAD	Angiosarcoma, high grade	8	L	7.8	Yes	No	Paclitaxel, MAS	None	Partially positive
10	75	F	None	N/A	N/A	Angiosarcoma, high grade	N/A	L	17	No	Yes	MAS, RAD	None	Negative

Note: F: Female. R: Right. L: Left. IDC: Invasive ductal carcinoma. ILC: Invasive lobular carcinoma. IHC: Immunohistochemistry. DCIS: Ductal carcinoma in situ. LUM: Lumpectomy. ALND: Axillary lymph node dissection. CHEM: Chemotherapy. RAD: Radiation. TAM: Tamoxifen. MAS: Mastectomy. SLND: Sentinel lymph node dissection. TRANS: Transtuzumab. N/A: Not available.

Figure 1 - 142

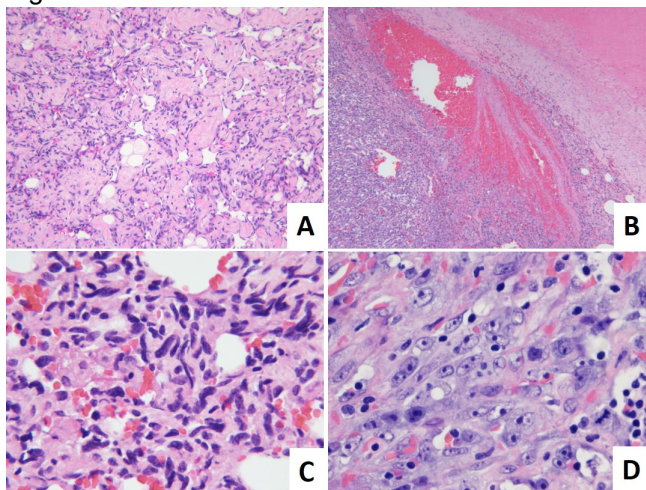
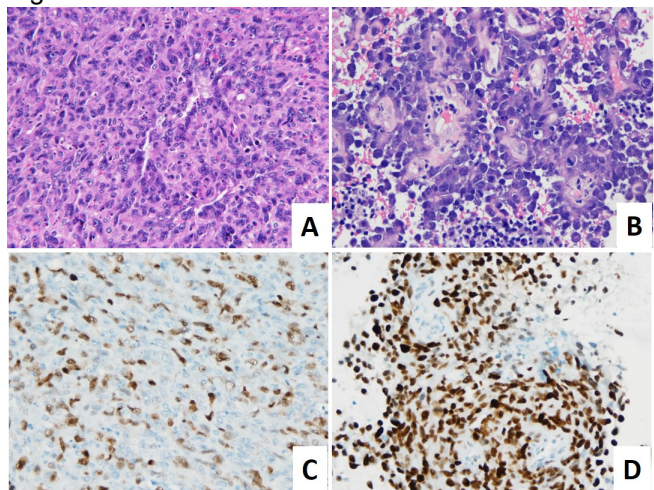


Figure 2 - 142



Conclusions: Correct diagnosis and grading of breast AS require thorough sampling of the specimen as well as careful pathologic examination. In this cohort, breast RA-AS were distinct from P-AS in terms of breast dermal

involvement, presence of vesicular nuclei and conspicuous nucleoli, and c-MYC immunoreactivity. Breast AS with epithelioid morphology was associated with worse prognosis, and cases with lymphatic differentiation showed distinct histologic morphology and tend to have strong or diffuse c-MYC immunoreactivity. c-MYC immunostain is helpful in differentiating RA-AS from AVP.

143 Primary and Secondary Angiosarcoma of Breast Represent Distinct Entities

Natalia Yanchenko¹, Andrew Rosenberg², Jaylou Velez Torres³, Elizabeth Montgomery³, Carmen Gomez-Fernandez³

¹University of Miami, Miami, FL, ²University of Miami Health System, Miami, FL, ³University of Miami Miller School of Medicine, Miami, FL

Disclosures: Natalia Yanchenko: None; Andrew Rosenberg: None; Jaylou Velez Torres: None; Elizabeth Montgomery: None; Carmen Gomez-Fernandez: None

Background: Breast angiosarcomas are uncommon, diagnostically challenging, and difficult to treat. New targeted biotherapy treatments require predictive criteria for disease response. In this study we provide additional evidence that suggests that primary (PBAS) and secondary (radiation induced) (SBAS) angiosarcomas of breast are distinct diseases with different clinicopathologic characteristics, genomic alterations, responses to therapy, and patient outcomes.

Design: The pathology databases of the participating institutions were searched for angiosarcoma of breast from 2004 - 2020. Only cases for which histological materials and follow-up information were available were included in the study. Clinicopathological information was obtained from the medical records. Statistical analysis was performed using Chi-square or t-tests. NGS CARIS was used for genomic analysis.

Results: 12 cases of PBAS and 12 cases of SBAS fulfilled the study criteria. Clinical, pathologic, and genetic features of PBAS and SBAS are summarized in Table 1. Genetic information was available in 4 PBAS and 4 SBAS.

Important findings include: PBAS and SBAS have statistically significant differences in age at presentation, ethnicity, histological grade, hormonal status, response to biotherapy, and outcomes. PBAS and SBAS have different mutation profiles.

Table 1. Clinicopathological features and outcomes

	Primary	Secondary	P value	<0.05
Number of cases	12	12		
Age of onset, years (all data: mean ± SD)	41.6±13.1	68.3±8.8	p < 0.0001	YES
– after radiation, years	–	5.9±2.7	–	–
Ethnicity:				
Hispanic;	7	3	p=0.031	YES
Non-Hispanic White;	2	9		
Non-Hispanic Black	1	0		
Hormonal status				
Postmenopausal	4	12	p=0.006	YES
Associated with pregnancy	4	0		
Family history				
Number of 1-2 nd degree relatives with malignancy	3.2±2.2	1.6±1.7	p=0.0587	-
– with breast cancer	1.3±1.8	0.4±1.1	p=0.1536	-
Follow-up time (since symptoms onset), months	41.7±30.5	33.9±24.1	p=0.4943	-
Delay in diagnosis, months	8.5±5.7	5.0±3.7	p=0.0882	-

At diagnosis were localized : multifocal	6 : 2	11 : 0	p= 0.3193	-
Recurrence:				
Local recurrence	0	4		
Distant metastasis	8	1	p=0.0012	YES
No recurrence	0	4		
Time before recurrence, months	19.4±16.1	17.0±21.3	p=0.7584	-
In disease with outcomes:				
• Unfavorable Outcomes (Death, Loss of follow-up with terminal disease and chemoradiation failure)	6	1		
	1	1	p=0.0230	YES
• Stable, with disease	0	7		
• Disease free (before or after recurrence)				
Biotherapy treatment	5	3		
Response (even with PD-L1 negative)	0	3	p=0.0380	YES
Tumor size (in resection specimen), cm	6.6±2.1	6.3±6.5	p=0.8805	-
Tumor grade (before treatment):				
Low, 1/3	7	1		
Intermediate, 2/3	4	7	p=0.0431	YES
High, 3/3	0	3		

Table 2. Genetic alterations in 4 PBSA and 4 SBCA.

	Primary	Secondary
Seen more than once:	<i>PIK3CA, KDR (VEGFR2)</i>	<i>c-MYC</i> amplification; <i>BRCA1</i> pathologic variants
Genes involved in VEGFR signaling	<i>KDR (VEGFR2)</i>	<i>FLT4 (VEGFR3)</i>
Other genes	<i>TGFBR2, MAPK3K6, HIST1H1D</i> <i>BRIP1; MECOM-EIF5A2</i> fusion; <i>MTOR, PPP2R1A, RASA1, TERT</i> translocation	<i>ABL, SMO, ALK</i>
Microsatellite instability	no	no
Tumor mutation burden:	low or cannot be determined	intermediate or low

Conclusions: PBAS and SBAS have different important characteristics indicating that they are biologically distinct diseases requiring different forms of therapy. PBAS occur in younger women, often associated with changes in hormonal status, are histologically lower grade, but, paradoxically have worse outcomes; mutations in *PIK3CA* and *KDR* are common. In contrast, SBCA develop in older women who are status post breast cancer and radiation, are histologically high grade, respond to biotherapeutics, have amplification of *c-MYC* and mutations in *BRCA1*, and have better outcomes. Additional forms of therapy are needed for patients with breast angiosarcoma. Given the distinct clinicopathologic differences between PBAS and SBAS, management strategies will need to be specifically tailored for these distinct entities.

144 Cystic Neutrophilic Granulomatous Mastitis: Clinicopathological Correlation with 16S Ribosomal RNA Gene Sequencing for Corynebacterium

Ellen Yang¹, Rob Kozak², Sharon Nofech-Mozes³, Ekaterina Olkhov-Mitsel², Elzbieta Slodkowska³, Anna Plotkin¹, Fang-I Lu³

¹University of Toronto, Toronto, Canada, ²Sunnybrook Health Sciences Centre, Toronto, Canada, ³University of Toronto, Sunnybrook Health Sciences Centre, Toronto, Canada

Disclosures: Ellen Yang: None; Rob Kozak: None; Sharon Nofech-Mozes: None; Ekaterina Olkhov-Mitsel: None; Elzbieta Slodkowska: None; Anna Plotkin: None; Fang-I Lu: None

Background: Cystic neutrophilic granulomatous mastitis (CNGM) is a rare cause of mastitis characterized by neutrophilic and granulomatous inflammation surrounding cystic spaces, occasionally filled by clusters of gram-positive *Corynebacterium* spp. It has been associated with breastfeeding in which the bacterium is postulated to gain entry via lactiferous ducts during lactation. CNGM is resistant to medical treatments and can recur even after breast resection. We set out to review the clinicopathologic features of CNGM in our institution.

Design: A retrospective search of breast specimens with a diagnosis of granulomatous inflammation identified 82 cases from 2010-2020. 77 cases with available H&E slides were reviewed by one resident and two staff breast pathologists to reach consensus on the histologically-diagnosed CNGM cohort. Formalin-fixed, paraffin-embedded (FFPE) tissue blocks were used for PCR-based identification of *Corynebacterium* by 16S ribosomal RNA (16S rRNA) gene sequencing. Clinical and radiological features, and microbiology workup results were retrieved from the electronic patient records.

Results: 34 CNGM cases were identified, all in female patients. The median age was 38.5 years. Most patients were multiparous (82%) and had breastfeeding history (65%). Most presented with a unilateral breast mass (97%) with size ranging from 1.6 – 8 cm, associated with pain (82%), spontaneous discharge (56%), and skin irritation (85%). Culture of tissue aspirate were done on 22 (64.7%) cases and PCR of FFPE tissue were done on all cases. 5 (14.7%) CNGM cases demonstrated positive microbiology studies (see Table 1), with 3 cases positive for *Corynebacterium*, 1 case positive for *Mycobacterium abscessus* and 1 case positive for *Staphylococcus lugdunensis*. On histological examination, 7 cases (21%) demonstrated gram-positive organisms, including all cases positive for *Corynebacterium*. 24 patients (71%) received antibiotic treatment, and 6 patients (18%) also received concurrent corticosteroid treatment. Therapeutic drainage was performed in 6 cases (18%), while 1 case (3%) underwent resection. Complete resolution was achieved in 21 cases (62%), taking on average 4.6 months. However, 3 patients had recurrence in ipsilateral or contralateral breast, with a mean time-to-recurrence of 13 months. Cases positive for *Corynebacterium* were more likely to persist and to recur than cases negative for *Corynebacterium* (p=0.062).

Conclusions: CNGM presents as a painful unilateral breast mass in women of reproductive age

Case	1	2	3	4	5
Clinical features					
Age (years)	40	33	44	37	49
Gravida	G2P1	G3P1	G3P3	G1P1	G5P3
Breastfeeding	Unknown	Y	Y	Y	Y
Mass	Y (Unifocal)	Y (Unifocal)	Y (Multifocal)	Y (Unifocal)	Y (Multifocal)
Size (cm)	6.5	7.7	4	10	3
Painful	Y	Y	Y	Y	Y
Drainage/ Rupture	Y	Y	Y	Y	Y
Skin irritation	N	Y	Y	Y	Y
Microbiology					
Gram stain	+ (Cocci)	+ (Cocci)	Not done	-	-
16S rRNA	-	+	+	-	-
Culture	+ <i>Corynebacterium</i>	+ <i>Corynebacterium</i>	-	+ <i>Mycobacterium abscessus</i>	+ <i>Staphylococcus lugdunensis</i>
Treatments					

Antibiotic	Clavulin, Doxycycline	Keflex	N	Keflex, Clindamycin, Vancomycin, Doxycycline	Keflex , Cloxacillin
Corticosteroid	N	N	N	N	N
Drainage	Y	N	N	N	Y
Excision	N	N	N	N	N
Outcomes					
Resolution	Y	Y	N	Y	Unknown
Recurrence	Y (Contralateral)	Y (Ipsilateral)	N	N	N
Culture	+ <i>Corynebacterium</i>	-	Not done	Not done	Not done

with a history of pregnancy and breastfeeding. 14.7% of CNGM cases in our study demonstrated a positive culture or PCR, with *Corynebacterium* being the most common pathogen. Recognition of the characteristic histological patterns of CNGM and microbiology studies on tissue aspirate and FFPE tissue blocks are recommended to direct appropriate therapy.

145 **Breast Cancer Harboring KRAS Mutations: A Data Analysis Of 7283 Patients From cBioPortal**

Qiqi Ye¹, Minghao Zhong²

¹Westchester Medical Center, Valhalla, NY, ²Yale School of Medicine, New Haven, CT

Disclosures: Qiqi Ye: None; Minghao Zhong: None

Background: *KRAS* mutations are highly recurrent in specific common cancers, such as lung and colon, where they have important therapeutic implications. The frequency and clinical significance of *KRAS* mutations in breast cancer are still largely unknown. Here we sought to explore the frequency of *KRAS* mutations and co-occurrence of other alterations in invasive breast cancers in cBioportal database.

Design: All data analysis was performed using <https://www.cbioportal.org>, which includes 7,283 breast cancers from 14 studies. Breast cancers with *KRAS* mutations were identified and classified into hotspots or non-hotspot mutations. Additional clinico-pathologic information, including hormone receptor and HER2 status and other concurrent genetic alterations, was retrieved for each individual case.

Results: *KRAS* hotspot mutations were identified in 42 breast cancers (<1%) from 7,283 patients. Of these, 28% samples contains G12V mutation while 17% with G12A, 11% with G12D, 9% with G12C, 9% with G12S, 4% with G12R, 4% with G13D (4%), and 2% with Q61H (2%). 34 (81%) were estrogen receptor (ER)-positive and HER2-negative, 6 (14%) were ER/HER2-negative, 2 (5%) were ER /HER2-positive. A statistically significant co-occurrence of *PIK3CA* and *KRAS* mutations was observed, with 34 (81%) of *KRAS*-mutant tumors harboring *PIK3CA* mutations.

Conclusions: Less than 1% of invasive breast cancers harbor *KRAS* hotspot mutations. The majority (81%) of *KRAS*-mutant breast cancers also harbor *PIK3CA* mutations, which can be targeted with an FDA-approved PI3K inhibitor (alpelisib). Further studies to assess the effect of the presence of *KRAS* hotspot mutations on PI3K pathway activation and response to alpelisib in *PIK3CA*-mutant breast cancer are warranted.

146 **Pathological Response in Mucinous Carcinoma of Breast After Neoadjuvant Therapy - A Multi-Institutional Study**

Haiying Zhan¹, Susan Fineberg², Yihong Wang³, Malini Harigopal⁴, Kamaljeet Singh⁵

¹Yale New Haven Hospital, Yale School of Medicine, New Haven, CT, ²Montefiore Medical Center, Bronx, NY, ³Brown University, Rhode Island Hospital, Providence, RI, ⁴Yale School of Medicine, New Haven, CT, ⁵Women and Infants Hospital, Providence, RI

Disclosures: Haiying Zhan: None; Susan Fineberg: None; Yihong Wang: None; Malini Harigopal: None; Kamaljeet Singh: None

Background: Although mucinous carcinoma (MC) is considered to be a favorable histologic subtype of invasive breast cancer (BC) a subset of MC (high stage, HER2+) is managed with neoadjuvant therapy (NAT). The clinical and pathologic features of MC following NAT are not well known. The aim of this study is to characterize pathologic response in MC treated with NAT, including neoadjuvant chemotherapy (NAC) and neoadjuvant endocrine therapy (NET).

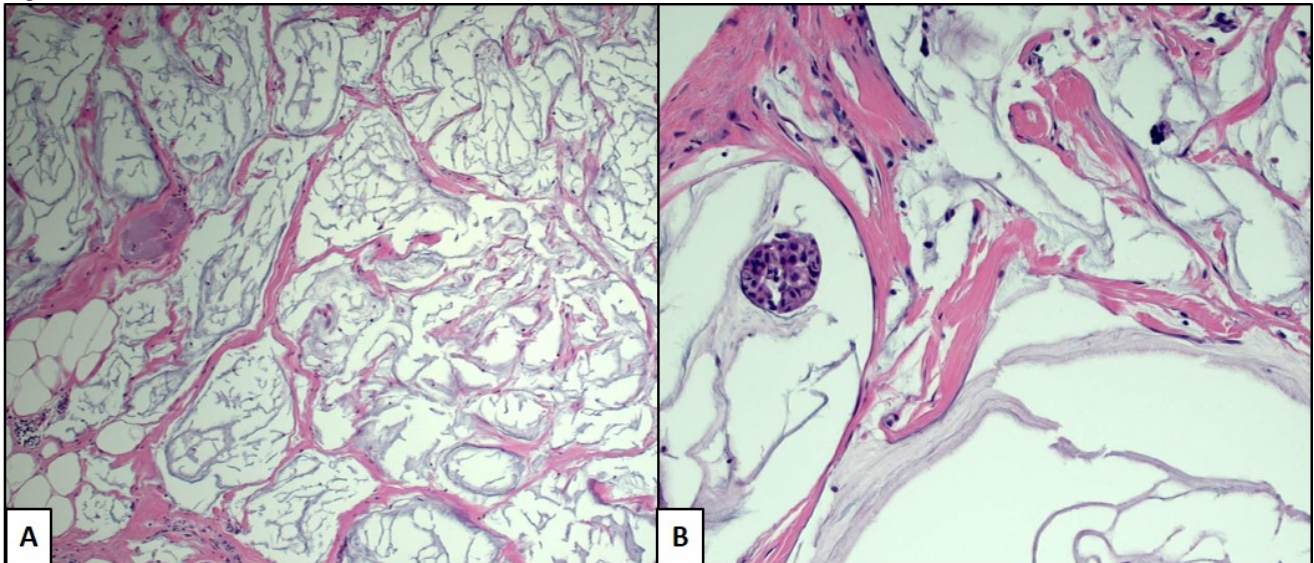
Design: Our multi-institutional study included 28 MC treated with NAT followed by resection between 2010 and 2020. We conducted a pathologic review of the post NAT resection specimens including tumor grading, staging, tumor size, residual tumor cellularity, estrogen receptor (ER), and HER2 status. Residual Cancer Burden (RCB) was calculated in all cases. Clinical data including age, specific neoadjuvant therapy, and imaging findings were reviewed.

Results: All 28 MC were estrogen receptor (ER)+ ductal carcinoma, of which 11 were HER2+. Nine (32%) ER+/HER2- MC received NET, 8(29%) ER+/HER2- MC were treated with NAC only, and 11(39%) HER2+ MC received HER2-targeted NAC (H-NAC). The HER2+ MC patients were younger (45 vs. 64 years; $p=0.006$). The HER2+ MC were of higher grade ($p=.03$) and more likely to be multifocal ($p=0.008$). Only 2 of 28(7%) MC (both HER2+) showed complete pathologic response with residual acellular mucin pools (Figure 1A). Persistent mass-forming mucin pools were present in 26(93%) cases. The residual tumor cellularity was markedly reduced ($\leq 5\%$) in H-NAC treated MC (11/11, 100%), followed by NET group (6/9, 67%) (Figure 1B) and NAC only group (4/8, 50%) ($p=0.011$). Similarly, a higher rate of pathologic response (pCR/RCB-I) was observed in H-NAC (7/11, 64%), followed by NET group (5/9, 56%), and NAC only group (1/7, 13%) ($p=0.053$). Post-therapy, all HER2+ MC were smaller than 2 cm and ypT size was significantly smaller in H-NAC group (11/11, 100%) versus combined NET (5/9, 55%) and NAC only groups (4/8, 50%) ($p=0.029$).

	Endocrine Therapy (%)	HER2 -targeted NAC (%)	NAC only (%)	
Number of cases	9(32%)	11 (39%)	8 (29%)	
Age	76	45	50	$P<.0001$
Histology	8(89)	9 (82)	6 (75)	$P=0.756$
Mucinous	1(11)	2 (18)	2 (25)	
Micropapillary				
Focality	3 (33)	0	4 (57)	$P=0.66$
Single	6 (67)	8 (100)	3 (43)	
Multifocal				
Grade	4 (44)	1 (9)	1 (14)	$P=0.066$
1	5 (56)	7 (64)	6 (86)	
2	0	3 (27)	0	
3				
Progesterone receptor	8 (89)	6 (55)	6 (75)	$P=0.216$
Positive	1 (11)	5 (45)	2 (25)	
Negative				
DCIS Present	4 (50)	6 (60)	4 (50)	$P=0.88$
Absent	4 (50)	4 (40)	4 (50)	
ypT	0	2 (18)	0	$P=.099$
0	2 (22)	3 (27)	0	

1mi	3 (33)	6 (55)	4 (50)	
1a-1c	3 (33)	0	4 (50)	
2	1 (12)	0	0	
3				
ypN	5 (83%)	8(80%)	4 (50)	P=.395
N0 and ITC	0	1 (10)	2 (25)	
N1mi	1 (17)	0	1(13)	
N1	0	1(10)	1(12)	
N3				
Tumor Cellularity	6 (67)	11 (100)	4 (50)	P=0.011
≤5%	3 (33)	0	4 (50)	
>5%				
RCB Score	5 (56)	7 (64)	1 (13)	P=0.053
Low (0, 1)	4 (44)	5 (36)	8 (88)	
High (2, 3)				

Figure 1 - 146



Conclusions: Mucinous carcinomas of the breast show variable response to neoadjuvant therapy. Best response is noted to HER2 targeted therapy (in HER2+ MC), followed by NET only, with least response to non-HER2 targeted NAC. We also report that MC after NET demonstrate marked reduction in cellularity, which is in contrast to the therapy response to NET in non-mucinous tumors. These findings need to be confirmed in a larger cohort study of mucinous and non-mucinous carcinomas of the breast.

147 Clinicopathological and Molecular Features of 39 Breast Squamous Cell Carcinomas

Siyuan Zhong¹, Shuling Zhou¹, Ming Li¹, Hong Lv¹, Shaoxian Tang, Xiaoli Xu¹, Ruohong Shui¹, Wentao Yang¹

¹Fudan University Shanghai Cancer Center, Shanghai, China

Disclosures: Siyuan Zhong: None; Ming Li: None; Hong Lv: None; Shaoxian Tang: None; Xiaoli Xu: None; Ruohong Shui: None; Wentao Yang: None

Background: Squamous cell carcinoma (SCC) is a subtype of metaplastic breast carcinoma. Its clinicopathological features and prognostic factors are not well recognized due to its rarity. There is no unified histological grading system of SCC and the response of neoadjuvant treatment is still unclear. To improve the understanding of this group of tumors, 39 cases were analyzed.

Design: 25 pure SCC and 14 mixed SCC from 2007–2020 in our center were analyzed. In mixed cases, the proportion of SCC was more than 50%. A three-tiered grading system for esophageal SCC was applied for histological grading. Seven patients received neoadjuvant chemotherapy and the histological response was assessed according to Miller-Payne grading (MPG) system. Ten pure cases were sequenced by DIAN (Hangzhou Lab) using a 324-gene platform (Foundation One CDx) with licensed technologies. Survival analysis was performed using SPSS version 16.0 software.

Results: All cases were female ranging from 33 to 83 years (median 53 years). The mean diameter of tumor was 32.5 (10-70) mm and the median disease-free survival (DFS) was 22 (2-139) months. At the time of diagnosis, half of the patients (18/39, 46.2%) reached stage IIA and ten patients (10/39, 25.6%) had lymph node metastasis. Recurrence and/or distant metastasis occurred in eight patients (8/39, 20.5%) after 4-46 months' (median 18.5 months) follow-up. The most common site of recurrence was chest wall and the most common metastatic site was lung and bone respectively. According to our assessment, most of cases (30/39, 76.9%) were grade 2 (moderately differentiated) and nine cases (9/39, 23.1%) were classified as grade 3 (poorly differentiated). In both univariate and multivariate analysis, poor differentiation was associated significantly with reduced DFS (P = 0.008, P = 0.017<0.05). Age, laterality, tumor size, axillary lymph node metastasis, stage and treatment had no significant effect in our analysis (P>0.05). None of the seven patients who received neoadjuvant chemotherapy achieved pathological complete remission and all of them underwent modified radical mastectomy. According to the MPG system, two cases achieved grade 1, four cases achieved grade 2 and one case achieved grade 3. Most SCC were triple negative, but four (4/39, 10.3%) in our series showed HER2 amplification, the significance of HER2-targeted treatment in HER2-positive SCC was still unclear due to the limitation of cases and follow-up time. High frequency pathogenic mutations of *TP53* (8/10, 80%) and *PIK3CA* (7/10, 70%) in SCC were observed which might have potential implication for targeted therapy.

Table1. Univariate analysis of prognostic factors for DFS

Variable	No. of patients (%)	No. of patients with recurrence or metastasis	Disease free survival (DFS)	P value
			median (95%CI) , months	
Differentiation				0.008
Moderate	30(76.9)	4	33.5 (103.0-152.2)	
Poor	9(23.1)	4	15 (11.0-77.6)	

Figure 1 - 147

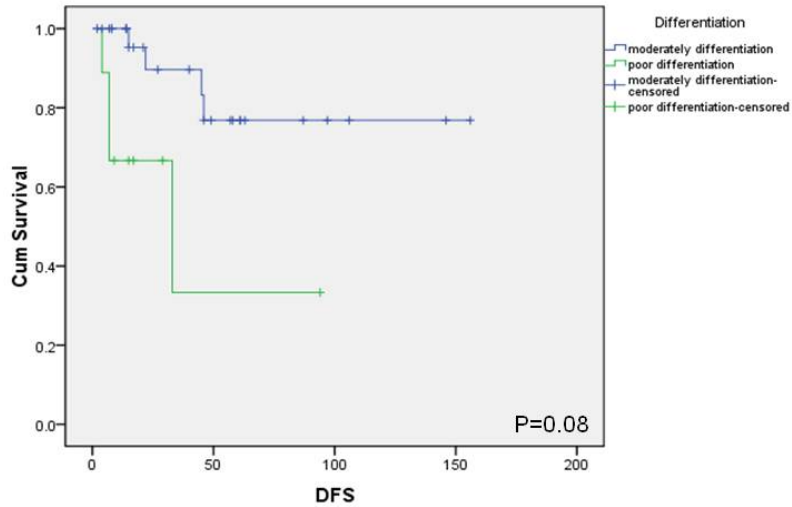


Figure 2. Patient's survival curves of moderately and poorly differentiated SCC. Patients with poorly differentiated SCC demonstrated shortened DFS.

Figure 2 - 147

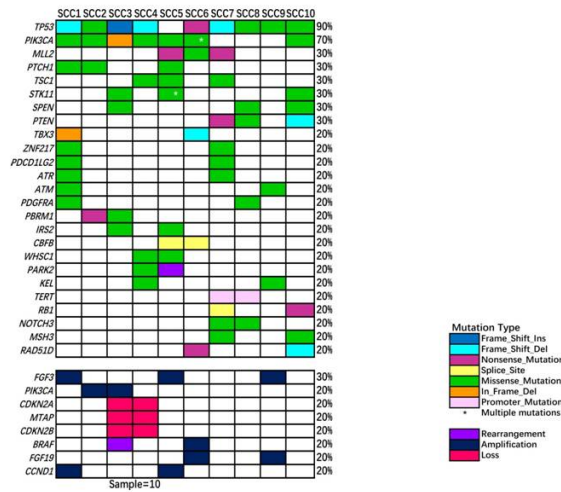


Figure 3. Genomic aberrations of ten pure SCC. Pathogenic mutations include all *TP53* and *PIK3CA* mutations except *SCC9*'s uncertain significant *TP53* mutation.

Conclusions: According to our research, the degree of differentiation is an independent prognostic factor of SCC. Neoadjuvant therapy should not be given priority in initial treatment decisions. The high frequency of *PIK3CA* mutation suggests the role of *PIK3CA* inhibitors in SCC.